Delft University of Technology

FACULTY MECHANICAL, MARITIME AND MATERIALS ENGINEERING
Department Marine and Transport Technology

Mekelweg 2
2628 CD Delft
the Netherlands
Phone +31 (0)15-2782889
Fax +31 (0)15-2781397
www.mtt.tudelft.nl

Specialization:	Transport Engineering and Logistics
Report number:	2011.TEL.7549
Title:	**Analysis of snag loads in a ship-to-shore crane**
Author:	B.J. de Vette

Title (in Dutch) Analyse van snag belastingen in containerkranen

Assignment:	Master Thesis
Confidential:	yes (until June 2013)
Initiator (university):	prof.ir. J.C. Rijsenbrij
Initiator (company):	ir. R.J.G. Kleiss
Supervisor (company):	ir. C.A. Angevaren
Supervisor (university):	ir. W. Van den Bos
Date:	June 22, 2011

Delft University of Technology

FACULTY MECHANICAL, MARITIME AND MATERIALS ENGINEERING
Department Marine and Transport Technology

Mekelweg 2
2628 CD Delft
the Netherlands
Phone +31 (0)15-2782889
Fax +31 (0)15-2781397
www.mtt.tudelft.nl

Student:	B.J. de Vette	Assignment type:	Master project
Supervisor (TUD):	Ir. W. van den Bos	Creditpoints (EC):	36
Supervisor (Company):	Ir. C.A. Angevaren	Specialization:	TEL
		Report number:	2011.TEL.7549
		Confidential:	Yes
			until: June 2013

Subject: **Analysis of snag loads in a ship-to-shore crane**

One of the design issues in a container crane is to deal with the effect of a snag load in the hoist system. A snag load being the sudden stop of the spreader (for instance as it gets stuck inside the cells of a container vessel) while the drive-line is still running at full speed. This results in high forces in wire ropes, high torque peaks in the components of the hoist winch and important forces in the steel structure of the crane.

In the past, with limited speeds of the load, cranes were not equipped with special equipment to limit the loads resulting from such a snag situation, but with increasing load on the ropes and with increasing speeds (thus higher inertia's in the winch) the loads from a snag increased and special anti-snag systems were developed and implemented.

These anti-snag systems lead to increased cost of the container crane and can be a new source of failures in the crane. Therefore Kalmar is looking again for a smart redesign of the hoist system, taking into account the dynamic effects of the hoisted load, the wire rope reeving, the winch inertia and the control of the hoist winch, all of this to the background of the stiffness of the total crane.

In your assignment, you should study at least the following issues:

- History and development of hoist speeds and winch inertia with resulting loads on the crane during a snag situation
- Theoretical analysis of the snag situation
- Determination of design parameters to quickly check the resulting forces from a snag situation on the crane and it's components
- Study of today's state of the art drive-line components and control systems to limit the effect of snag load
- Development of a calculation tool for Kalmar to prove to their customers and inspectors of external parties that with the right choice of components an anti-snag-load system can be left out

The professor,

Prof.ir. J.C. Rijsenbrij

Preface

The last step in becoming a master of science is the completion of the master thesis. This is the report of the master thesis of Bart de Vette, master student at the department of Transportation Engineering, specialization Transportation Engineering & Logistics. This department is part of the faculty of Mechanical Engineering at the TU Delft.

First I would like to thank the company Cargotec (Kalmar) for the opportunity to do this research, and their support during the process. I would like to thank my supervisors at Cargotec Cock Angevaren and René Kleiss for their helpful remarks and knowledge. I would also like to thank the supervisors from the TU Delft, Wouter van den Bos and Professor Rijsenbrij, for their remarks, and inspiration during the meetings.

Bart de Vette

June 1st, 2011

Summary

Ever since the start of containerisation ship sizes kept increasing, and still are to this day. Because of the demands on short cycle times for the cranes, port operators required faster hoisting speeds to keep up with the increased hoisting height. These increased hoisting speeds (up to 180 m/min for an empty spreader), introduced a new problem to STS cranes: snag loads.

Snag loads are the shock loads which are exerted on the crane when the load of the crane snags behind an object during hoisting. It's also possible for the container to jam inside the ship cell due to skewing. These shock loads can greatly exceed the normal operating loads of the crane, causing damage to the crane. This damage ranges from minor damage like bent rope sheaves mounting, to an entire boom collapsing.

Through time, a number of devices were installed on STS cranes to absorb or reduce the snag load. These mechanisms proved to be expensive, and required maintenance. It is therefore favourable to reduce the snag loads to a level where the crane is strong enough to withstand it without a snag protection device. The purpose of this thesis is to construct a method to calculate the snag loads on the STS crane and improve the hoisting winch so that snag loads are reduced to an acceptable level.

During a snag the load of the crane is suddenly stopped, while the inertia of the winch prevents it from stopping. When a snag is detected by means of rope tension monitoring or through detection of motor overload, an emergency stop can be performed. During such a stop, motor torque is reversed, and all brakes are applied. To be able to operate without a snag protection device, this stop should be performed as fast as possible, so that the rope tension will not increase beyond the limits of the crane.

Eccentric snag:

2-rope snag

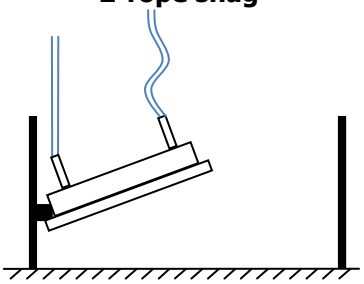

Centric snag:

4-rope snag

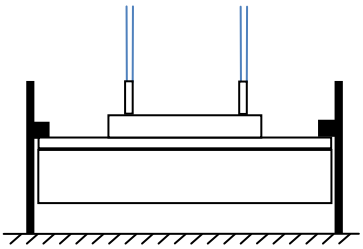

The worst case scenario for a snag occurs at minimum outreach, where crane deflection is minimal. A 4-rope snag, where all four hoisting ropes are stretched, results in the highest total load on the crane. A 2-rope snag will result in higher rope tension and is therefore more dangerous for individual components of the crane, for example the wire rope.

The snag load is dependent on a number of parameters. The hoisting speed of the crane determines the required size of the motors, and their rotational speed. This determines the amount of kinetic energy that is stored in the hoisting winch. This energy will have to either be absorbed by the hoisting ropes, or dissipated through the brakes installed in the hoisting winch.

The stiffness of the hoisting ropes determines the speed at which the rope tension rises during a snag. It is therefore critical to have elastic hoisting ropes. This allows the hoisting winch enough time to stop.
STS cranes with the hoisting winch installed on the trolley have very short hoisting ropes, thus having a high rope stiffness. This type of STS crane are therefore subjected to high snag loads when hoisting at the high hoisting speeds required nowadays. Therefore these cranes will always require some sort of snag protection device.
The response time of the control system has to be minimized, to be sure that the brakes dissipate as much energy as possible. The response time can be improved by implementing a variable load limit which depends on the hoisted load.
By selecting smaller AC motors which are overloaded, the inertia of the winch is reduced. This allows for faster stopping of the winch.

The maximum allowable snag load is determined at the maximum load at which snag is not governing for the design of the crane. This limit is found analyzing four existing cranes, and calculating their maximum strength.
This limit is found to be at 219 kN of rope tension for a 4-rope snag, and 250 kN of rope tension for a 2-rope snag. Besides the rope tension, the torque on the components in the driveline is analyzed. The motor couplings proved to be critical for the snag load, since these are heavily loaded during the emergency stop.
Using a case study on an STS crane currently in production, it is found that it is not safe to hoist at 180 m/min without a snag protection device installed. Even with the improvements found in this thesis, the rope tension still exceeds the limits.
When the maximum hoisting speed is limited at 160 m/min inside the ship cell (where there is danger of snagging), a snag protection device is no longer required. However the operating brake should not be applied during a snag. It only adds a large shock load to the driveline, while it does not significantly contribute to a faster stop, because of its slow response time.
This reduction in speed will increase the cycle times of the crane by 1%.

Summary (Dutch)

Al sinds het begin van de containerisatie zijn de afmetingen van container schepen blijven groeien, en dat doen ze nog steeds. Vanwege de vraag naar korte laad- en lostijden, eisen de exploitanten van havens snellere hijssnelheden, om de grotere hijshoogte te compenseren. Door deze toegenomen hijssnelheden (tot 180 m/min voor een lege spreader), is er een nieuw probleem ontstaan bij STS kranen: Snag belasting.

De snag belasting is de schok belasting die op de kraan wordt uitgeoefend als de hijslast van de kraan achter een obstakel blijft hangen tijdens het hijsen. Ook kan het gebeuren dat de container zich verklemt in het scheepsruim d.m.v. een schrankbeweging. De schokbelasting die ontstaat kan veel groter zijn dan de belasting tijdens normaal bedrijf en kan de kraan beschadigen. Deze schade varieert van kleine schade zoals een verbogen ophanging van een kabelschijf, tot het afbreken van een complete klap.

De afgelopen jaren zijn er verschillende apparaten geinstalleerd op STS kranen om de snag belasting te absorberen of te verminderen. Deze mechanismes bleken duur en vereisten veel onderhoud. Daarom is het wenselijk om de snag belasting te verminderen tot een niveau wat de kraan wel kan verdragen zonder een anti-snag systeem geinstalleerd. Het doel van deze afstudeeropdracht is om een manier te ontwikkelen om de snag belasting uit te rekenen en de hijslier te verbeteren zodat de snag belasting verminderd wordt tot een acceptabel niveau.

Tijdens een snag wordt de hijslast plotseling gestopt tijdens het hijsen, terwijl de traagheid van de hijslier ervoor zorgt dat de lier nog door draait. Op het moment dat de snag wordt gedetecteerd, ofwel door de lastbeveiliging van de hijskabels of vanwege overbelasting van de motoren, wordt er een noodstop uitgevoerd. Tijdens zo'n stop wordt het motorkoppel omgedraaid, en alle remmen van de lier sluiten. Om te kunnen functioneren zonder anti-snag systeem moet zo'n noodstop zo snel mogelijk uitgevoerd worden, zodat de kabelkracht niet de limieten van de kraan overschrijdt.

Eccentrische snag:

Snag van 2 hijskabels

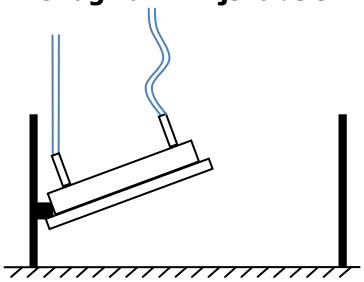

Centrische snag:

Snag van 4 hijskabels

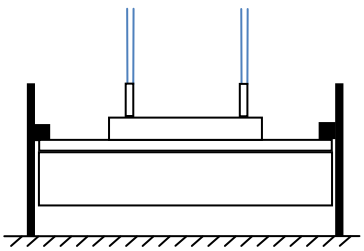

De ergste snag treedt op bij minimale outreach, waar de kraan doorbuiging het minst is. Bij een centrische snag, waarbij alle vier de hijskabels worden uitgerekt, zal de totale belasting op de kraan het hoogst zijn. Een eccentrische snag resulteert in hogere kabelkrachten en is daarom gevaarlijker voor individuele componenten van de kraan, zoals de hijskabel.

De snag belasting hangt af van een aantal parameters. De hijssnelheid en maximale last van de kraan bepalen de vereiste grootte van de motoren en hun draaisnelheid. Die bepalen de hoeveelheid kinetische energie die opgeslagen is in de hijslier tijdens het hijsen. Deze energie moet tijdens een snag worden opgenomen door de hijskabels, of gedissipeerd door de remmen van de hijslier.
De stijfheid van de hijskabels bepaalt de snelheid waarmee de kabelkracht toeneemt tijdens een snag. Het is daarom erg belangrijk om elastische hijskables te hebben, zodat de hijslier genoeg tijd heeft om te stoppen.
STS kranen met de hijslier op de kat hebben erg korte hijskabels, die daarom een hoge kabelstijfheid hebben. Dit type STS kranen worden daardoor belast door grote snag belastingen als ze hijsen met de hoge hijssnelheden van tegenwoordig. Deze kranen zullen daarom altijd een soort ant-snag systeem nodig hebben.
De reactietijd van het meetsysteem moet geminimaliseerd worden, zodat de remmen zoveel mogelijk energie dissiperen. De reactie tijd kan verbeterd worden door een variabele last limiet te gebruiken, die afhangt van hijslast op dat moment.
Door kleinere, zwaar overbelaste wisselstroommotoren te gebruiken, wordt de traagheid van de hijslier verminderd. Hierdoor kan de hijslier eerder gestopt worden.

De maximaal toelaatbare snag belasting wordt bepaald als de maximale belasting waarbij snag niet maatgevend zal zijn voor het ontwerp van de kraan. Deze limiet wordt gevonden door vier bestaande kranen te analyseren en hun maximale sterkte uit te rekenen.
De limiet voor een centrische snag is 219 kN kabelkracht, en 250 kN kabelkracht een eccentrische snag. Naast de kabelkracht wordt er ook rekening gehouden met het koppel op de componenten van de hijslier. De motorkoppelingen blijken bepalend voor de snag belasting, omdat deze zwaar belast worden tijdens een noodstop.
Als de maximale hijssnelheid gelimiteerd wordt op 160 m/min in het scheepsruim (waar gevaar is op snag), is een anti-snag systeem niet langer vereist. Deze verlaging van de hijssnelheid lijdt tot een toename van de cyclustijd van 1%.

List of symbols

Below is a list of symbols used in this thesis.

A	=	Cross-sectional area
E	=	Young's modulus
F	=	Force
f_a	=	Motor overload factor
g	=	Gravitational acceleration
k	=	Stiffness
m	=	Mass
M	=	Moment
n	=	Quantity (i.e. $n_{snagged\ ropes}$ = number of snagged ropes).
u	=	Elongation
v	=	Translational speed
η	=	Efficiency
ω	=	Rotational speed
ω_n	=	Natural frequency

List of abbreviations

AC	=	Alternating Current
DC	=	Direct Current
FEM	=	Finite Element method
FEM1.001	=	A European design standard for crane builders
LS	=	Landside
MBL	=	Minimum breaking load
MOT	=	Machinery On Trolley
PLC	=	Programmable Logic Controller
PS	=	Portside
SB	=	Starboard
STS	=	Ship-To-Shore
TEU	=	Twenty-feet Equivalent Unit (size of a 20'-container)
WS	=	Waterside

Remark

In this thesis tension is used as a measurement of tensile force rather than tensile stress.

Contents

PREFACE **3**

SUMMARY **4**

SUMMARY (IN DUTCH) **6**

LIST OF SYMBOLS **8**

LIST OF ABBREVIATIONS **8**

CONTENTS **9**

1. INTRODUCTION **12**

1.1 GENERAL INTRODUCTION 12
1.2 GOAL OF THE RESEARCH 16
1.3 STRUCTURE OF THE REPORT 16

2. LITERATURE STUDY **17**

2.1 RESEARCH AND PUBLICATIONS 17
2.2 DESIGN STANDARDS 18
2.3 CONTAINER CRANE SPECIFICATION REQUIREMENTS 19

3. THE HOISTING OPERATION **20**

3.1 MECHANICAL SYSTEM 20
3.2 CONTROL SYSTEM 26
3.3 TIMELINE OF A SNAG EVENT 27

4. MOVEMENT OF THE LOAD DURING A SNAG **29**

4.1 TYPES OF SNAG 29
4.2 THE MODEL 30
4.3 RESULTS 33
4.4 CONCLUSIONS 37
4.5 IMPLEMENTATION OF RESULTS INTO SNAG CALCULATION 37

5. THE CALCULATION MODEL **39**

5.1 MODELLING OF THE MECHANICAL SYSTEM 39
5.2 MODELLING OF THE CONTROL SYSTEM 40
5.3 INFLUENCES ON SNAG LOAD 43

6. CALCULATION OF SNAG LOADS **56**

6.1 SIMPLIFIED CALCULATION 56
6.2 SIMULINK MODEL 59

6.3 VERIFICATION AND VALIDATION 62

7. HISTORY AND DEVELOPMENT OF THE STS CRANE DRIVELINE 66

7.1 EVALUATED CRANES 66
7.2 RESULTS 67
7.3 CONCLUSIONS 72

8. DESIGN IMPROVEMENTS TO REDUCE SNAG LOADS 73

8.1 MONITORING METHOD 73
8.2 SELECTION OF ELECTRIC MOTORS 79
8.3 WINCH INERTIA 84
8.4 BRAKE RESPONSE TIME 86
8.5 BRAKING TORQUE 87
8.6 WIRE ROPE STIFFNESS 88
8.7 CONCLUSIONS 89

9. MAXIMUM ALLOWABLE SNAG LOAD 90

9.1 WIRE ROPE 90
9.2 CRANE STRUCTURE AND RELATED MECHANISMS 90
9.3 MECHANICAL COMPONENTS OF THE REEVING AND WINCH 93
9.4 HOISTING TOOLS 96
9.5 CONCLUSION 98

10. CASE: 180 M/MIN WITHOUT AN ANTI-SNAG DEVICE 99

10.1 IMPLEMENTED IMPROVEMENTS 99
10.2 RESULTS 102
10.3 CONCLUSION 104

11. CONCLUSIONS 106

11.1 ANALYSIS OF SNAG LOADS 106
11.2 DESIGN IMPROVEMENTS TO THE HOISTING SYSTEM 107
11.3 RECOMMENDATIONS 108

12. REFERENCES 110

APPENDIX A SCIENTIFIC RESEARCH PAPER 112

APPENDIX B EXISTING ANTI-SNAG SYSTEMS 113

B.1 HYDRAULIC SYSTEMS 113
B.2 MECHANICAL SYSTEMS 115

APPENDIX C VARIABLE SPEED AC MOTOR CHARACTERISTICS 120

APPENDIX D IDEAS FOR ANTI-SNAG SOLUTIONS 122

D.1 ADDITION OF WIRE ROPE FALLS 122
D.2 MASS TO LIMIT THE MAXIMUM ROPE TENSION 124
D.3 SPRING BASED ROPE BUFFER 126
D.4 CONCLUSION 129

APPENDIX E SIMULINK MODEL AND CODE 130

E.1 GLOBAL MODEL 130
E.2 INPUT SHAFT + MOTORS & BRAKES 131
E.3 BRAKES & MOTORS 132
E.4 AC-MOTOR 133
E.5 SHAFT DECELERATIONS 134
E.6 ROPES 135
E.7 CODE 136
E.8 MODEL USED FOR CONTAINER MOVEMENT 144

APPENDIX F DATA OF EXISTING CRANES 149

1. Introduction

In this chapter a short introduction to container shipping is given, together with an introduction to STS cranes and the problem of snag loads. In the last section, the goal of the research will be discussed.

1.1 General introduction

1.1.1 Container shipping

Up to the 1950's, the handling of ship cargo was a slow and labour-intensive job. Each pallet or bag had to be moved separately, causing ships to spend more time in the harbour than at sea. As the ships grew larger, the time and labour required to handle a single ship kept increasing. During the second half of the 1950's, the container box started its life, revolutionizing shipping, as the cargo could be moved on and off the ship much faster.

In the beginning, the containers were handled using standard luffing cranes, but these proved to be inefficient, as a single load cycle took 2-3 minutes. To reduce the cycle times the first real STS crane was constructed in 1959 (see Figure 1.1). These developments reduced the loading and unloading times into days rather than weeks. Since then, ships continue to grow larger to reduce the shipping cost per container. [1] [2]

Recently Maersk set a new ship size record, ordering 10 ships with a capacity of 18.000 TEU each, measuring 400m long and 59m (23 containers) wide. These ships are claimed to have a 50% better fuel efficiency per container, compared to the average container ship currently in use. [3]

To be able to still load and unload these large ships, STS cranes had to keep up with the growth. Together with the size of the crane the hoisting speeds increased, to keep the cycle time of the crane acceptable. Nowadays, cranes are able to hoist loads with speeds up to 180 m/min, requiring over 1000 kW of installed hoisting power.

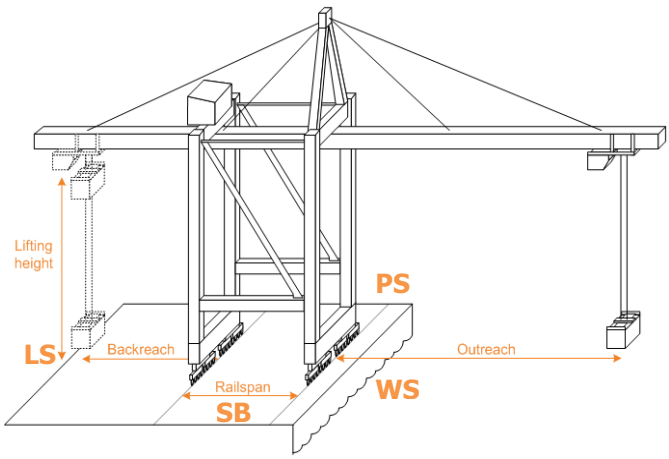

Figure 1.1: Comparison in size of the first STS crane with a Kalmar super-post panamax crane produced in 2005 (Source: Kalmar)
Figure 1.2: Main dimensions and orientation of an STS crane

1.1.2 The Ship-To-Shore crane

1.1.2.1 Main dimensions

The design of the STS crane can be characterised by a few dimensions, as shown in Figure 1.2.
The maximum width of the crane is usually equal to the width of two adjacent ship cells. This allows the port operator to use one crane on every two ship cells, allowing more cranes to operate simultaneously on a single ship. This leads to shorter berth times. The minimum width inside the portal is defined by the size of the load that has to pass between the legs.

1.1.2.2 Crane construction

Figure 1.3 shows a model of an STS crane to highlight the main components of the crane. This terminology will be used throughout the report.

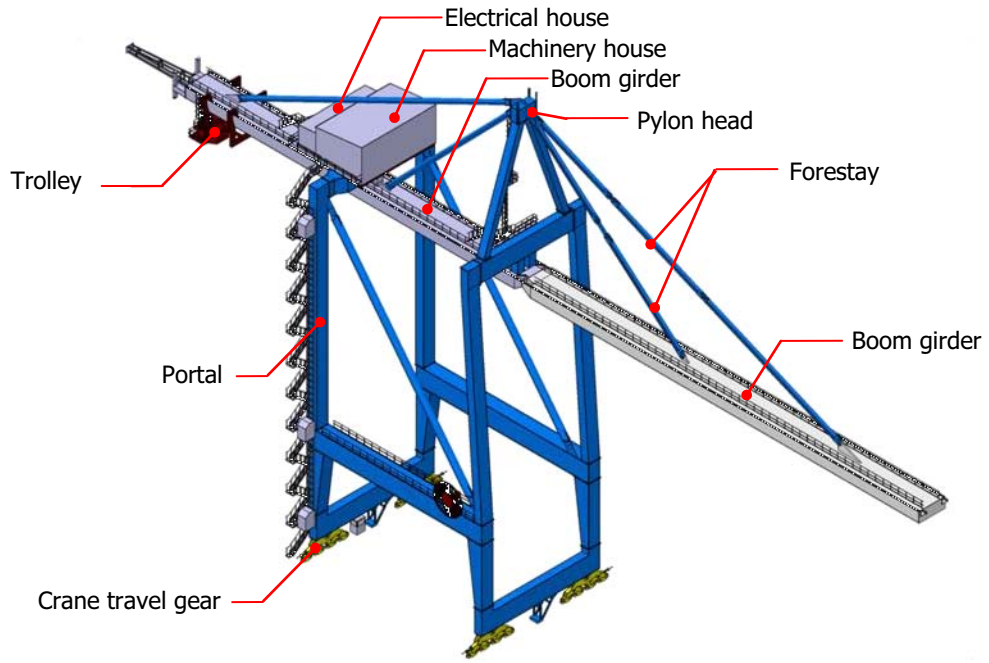

Figure 1.3: Schematic overview of an STS crane (source: Cargotec)

The crane designs can be sorted in three different types:
Monobox girder or single box girder is currently the design preferred by Cargotec due to its simple construction, reducing production costs. The disadvantage of this design is a relatively high flexibility of the boom. The girder consists of a single box section, with the rails mounted on top. The trolley is travelling below the girder.
Double box girder cranes consist of two parallel girders, with a trolley travelling in between. The construction is heavier and more complex than the Monobox. The benefit of this construction is its strength, allowing for tandem lift operations (lifting two 40' containers in a single lift)
Lattice girder cranes require the highest production costs of the three type, due to the large amount of welds in the construction. The benefits of this type are its low wind loads and low weight, allowing it to operate on older and weaker quays.

Figure 1.4: Three types of STS crane girders: (from left to right): Monobox girder, Double box girder and lattice girder

1.1.2.3 Hoisting tools

A spreader picks up a container using twistlocks to form a connection between the container and the crane. These twistlocks allow the spreader to lock onto a container in seconds, speeding up the process of loading and unloading of the ship.

Current spreaders have the possibility to switch between a 20'-mode and a 40'- or 2x20'-mode (also known as twinlift), based on the dimension of the container that needs to be picked up.

The wire ropes of the STS crane are connected to the spreader through the headblock. The headblock itself is constructed by Kalmar, while the spreader is bought from spreader manufacturers.

Figure 1.5: Headblock and spreader in twinlift mode, with an open top and a standard 20' container. All 8 container corners will be connected using twistlocks on the spreader (source: Cargotec)

1.1.3 Problem description

A snag situation occurs when the load of the STS crane is suddenly stopped during the upwards movement of the load. This stopping of the load is caused by jamming inside the ship's cell, or getting caught behind an object, i.e. the edge of the ships cell.

When the load is stopped, the driveline will continue to rotate for a short period of time, until it has been braked down. During this period, the hoisting ropes can be stretched far beyond normal operating conditions, increasing the rope tensions proportionately. The increased rope tension can

cause damage to the crane, ranging from minor damage to hoisting sheaves and wire rope (Figure 1.8) up to boom or total crane collapse.

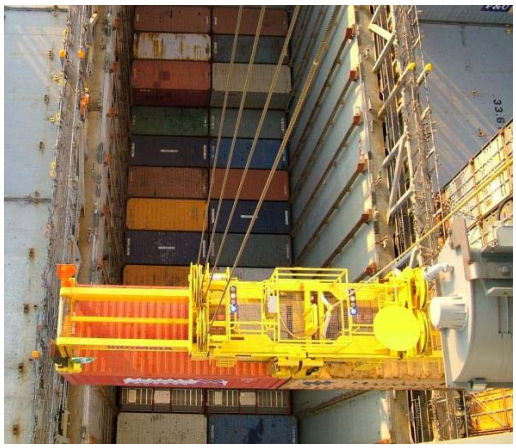

Figure 1.6 (left): Example of a snagged load caused by skewing in the ship cell, in this case two 20'-containers on a twin-lift spreader (Source: Cargotec)
Figure 1.7 (right): Top view of a ship cell, with the cell guides visible on the right side of the cell (Source: Cargotec)

During the first decades of container transportation, the hoisting speeds were too low for snag to cause a threat to STS cranes. Even when a snag did occur, the crane was strong enough to withstand the high rope tensions.

However as crane sizes increased, so did hoisting speeds and motor sizes. As was learnt by experience, the snag loads increased as well, causing damage to the cranes.

Data logging from the MSC terminal in Antwerp shows an average of 5 snags occurring per month at the terminal, which has 19 STS cranes in operation. Operators at the Euromax terminal in Rotterdam mentioned around one snag every week on the terminal, which operates with 11 STS cranes.

Figure 1.8: Example of damage caused by snag: plastic deformation of rope sheave mounting at the tip of the boom. Extreme rope tension caused by snag bent the sheaves upwards [4]

Current solutions

During the 1990's, crane designers and operators started to be aware of this problem, and a variety of equipment was developed to reduce or absorb these snag loads. A number of these mechanisms are described in Appendix B. This equipment lead to an increase in crane costs, as well as an extra source of failures in the crane. The equipment also requires to be thoroughly maintained during the lifetime of the crane. Because of these reasons, Cargotec is looking for a method to reduce snag loads in such a way, that the equipment to absorb the snag load is no longer needed.

1.2 Goal of the research

1.2.1 Main goal

The main goal of this master assignment is to redesign the hoist system in such a way, that an STS crane can withstand a snag load without the use of extra equipment to absorb a snag load, taking into account:

- Dynamic effects of the hoisted load
- Configuration of the hoisting ropes
- Inertia of the hoisting winch
- Control of the hoisting winch

Also, a calculation tool will be developed to examine the snag load on a new crane during the design phase.

1.2.2 Sub problems

To reach the main goal, the following points need to be determined:

- Occurrence of events during a snag event
- The loads on an STS crane caused by a snag event
- Possible design improvements to reduce snag loads
- Maximum allowable snag loads on an STS crane

1.3 Structure of the report

To reach the main goal, the research is split up in the following steps:

1. Introduction into STS cranes, literature research
2. Properties of the components in the crane
3. Construction of a model to analyse the snag load on a crane
4. Analysis of snag loads on STS cranes of the past 20 years
5. Design improvements to reduce snag loads
6. Determining design limit for snag load
7. Case study

2. Literature study

This chapter examines existing literature and other information regarding snag loads. First a number of publications regarding snag loads will be examined. Next a number of design standards regarding crane design are reviewed, as well as the description of snag loads in container crane inquiries and requirements.
Publications and patents regarding snag protection devices to reduce snag loads will be discussed in Appendix B.

2.1 Research and publications

There are only a few articles published on the subject of snag loads. These articles will be described in this paragraph.

2.1.1 Snag loads with DC motors

General Electric, together with Casper, Philips & Associates published two articles regarding snag loads in 1993 and 1995 [5] [6]. In the articles, snag is claimed to be the most common cause of mechanical and structural failure of STS cranes. Two types of snag are possible: either jamming in a ship cell, overloading two of the four hoisting ropes, or "two-blocking" against the underside of the trolley, overloading all 4 hoisting ropes. The latter is said to be more severe, because of the much shorter hoisting ropes.
The regular control systems are too slow to stop the rotating inertia in time, especially with the increasing hoisting speeds.
Six major factors influencing snag are identified:

- The rotating components (inertia)
- Control design (response times)
- Ropes (stiffness)
- Brakes (response times and torque)
- 2-rope vs. 4-rope snag (determines the load per cable)
- Snag protection device (absorbs part of the load)

A 2-rope snag situation with empty spreader is examined in a post-Panamax crane with 50 tons hoisting capacity and DC motors. It has a reeve-through trolley with a total cable length of 226 m. A comparison is made between load dependent snag detection and a conventional system, with a trip point set at 110% of maximum load. The load dependent system is able to react 0,22 seconds faster, resulting in a reduction of the total snag load by 18%, from 163 tons to 133 tons. A system using two different load limits is recommended. For speeds up to 125% of nominal speed, the limit is set at a constant of 110-115% of maximum lifted load. For higher speeds, the limit is set at 125% of actual load. This 25% margin is considered large enough to cope with variations in rope tension. Experiments are recommended to verify these results.

The results show that the time between snag of the load and the completed stop of the winch varies from 0.5 to 0.7 seconds.

2.1.2 J. Verschoof, Cranes – Design, Practice and Maintenance

This book, published in 2002 [7], discusses a wide variety of topics regarding crane design. Hydraulic cylinders are advised to act as wire rope buffers to reduce the snag load, especially for machinery trolleys. Two calculation examples are shown to emphasize the importance of an anti-snag device:

- A 2-rope snag for a machinery trolley hoisting at 90 m/min results in a 40 ton rope tension if no anti-snag device is present.
- For a full rope trolley, a 3 rope snag at 170 m/min results in a 25 ton rope tension without anti-snag device installed.

The results show a time between snag and the completed stop of the winch of 0.5 seconds.

2.1.3 Method for solving multi-disciplinary problems

In 2010, a new method to solve multi-disciplinary design problems was investigated as a PhD research [8]. The problem of snag loads was used as an example to implement this new method.
This research states the hydraulic anti-snag systems are not preferable, because of their high requirements on inspection and maintenance. High hoisting speeds with low loads are identified as the case which causes the highest snag loads.
After implementing the new design method with a multi-disciplinary team, a number of interesting conclusions are made. The control system is found to be the most important tool to reduce the snag loads. The same dynamic triggering limit as described in [6] was implemented in a simulation, showing "promising results". The exact results were not mentioned in the thesis.
Another idea was to decouple the moment of inertia, in this case the motors, from the rest of the system. This idea will be further developed. It should be noted that this system already exists for a few years (see paragraph B.2.1), which may not have been known by the writer of this PhD thesis.

2.1.4 Literature research on snag load protection systems

In 2007, a literature research at the TU Delft was performed regarding snag load protection systems in cranes [9]. Some of these patents are relevant for STS cranes and will be described in Appendix B. It also estimates the load peaks on a crane with a hydraulic anti-snag system, for two different response times. It concludes that a short response time is recommendable.

2.2 Design standards

Throughout the industrialized world design standards are applied. The main reasons to apply design standards are the improvement of safety of products and to improve fair competition in the market.
Currently, there is a wide variety of standards that are applied to STS-crane design, as is shown in Table 2.1.

None of the design standards mentioned in Table 2.1 mention snag load as a specific load case. In these standards, snag should be assumed as an extreme load case, with its appropriate safety factors to i.e. the yield stress.

Original area	Standard	Year of Publication
European manufacturer standard	FEM 1.001	1987
Netherlands	NEN 2018, 2019, 2020	1974
Belgium	NBN E52	1976
Germany	DIN 15018	1984
Great Britain	BS 466	1984
Europe	EN 13001	2004
Worldwide	ISO 8686-1, 8686-5	1989

Table 2.1: A number of design standards currently in use

2.3 Container crane specification requirements

Usually clients send a list of requirements to manufacturers of STS cranes. These lists contain a number of requirements on snag loads. The requirements can include a dynamic analysis of snag loads on a crane (centric and eccentric), or even demand a certain type of anti-snag system to be installed, like a hydraulic system, or the Bubenzer-Malmedie system described in paragraph B.2.1.

3. The hoisting operation

In this chapter the hoisting winch is examined. First the mechanical system and the control system of the winch are explained. The final paragraph examines the events that occur in the winch during a snag event:

1. Mechanical system
    a. Hoisting rope reeving
    b. Wire rope properties
    c. Hoisting winch components
2. Control system
    a. PLC
    b. Rope tension monitoring
    c. AC drive
3. Timeline of a snag event

3.1 Mechanical system

In this paragraph the current configuration of the main hoist will be examined, as well as the properties of its components.

3.1.1 Hoisting rope reeving

Reeve-through trolley vs. Machinery on trolley (MOT)

There are two different locations where the hoisting winch can be installed. The winch can be installed in the machinery house (reeve-through trolley), or on the trolley (Machinery on trolley), as can be seen in Figure 3.1. The choice between these two systems has a large influence on the design of the rest of the crane.

In case of a reeve-through trolley, the four hoisting ropes run along a number of hoisting sheaves, through the trolley and the headblock to the tip of the boom. Wire rope sag will occur, because the rope has to span the length of the entire girder, which can be over 100 m long. To compensate for wire rope sag, the hoisting ropes are supported using a continuous rope support system, or using catenary trolleys.

In case of a machinery on trolley (MOT) system the hoisting winch is installed on the trolley. This system results in much shorter hoisting ropes compared to the reeve-through trolley, leading to more precise load control. A disadvantage of this system is that it leads to a heavier trolley, causing higher loads on the crane structure.

The choice between these two systems depends on a number of design considerations, some of which were discussed above. It should be noted that the longer hoisting ropes of the reeve-through trolley are more elastic. This makes it easier for the crane to absorb shock loads, like the loads

caused by a snag.

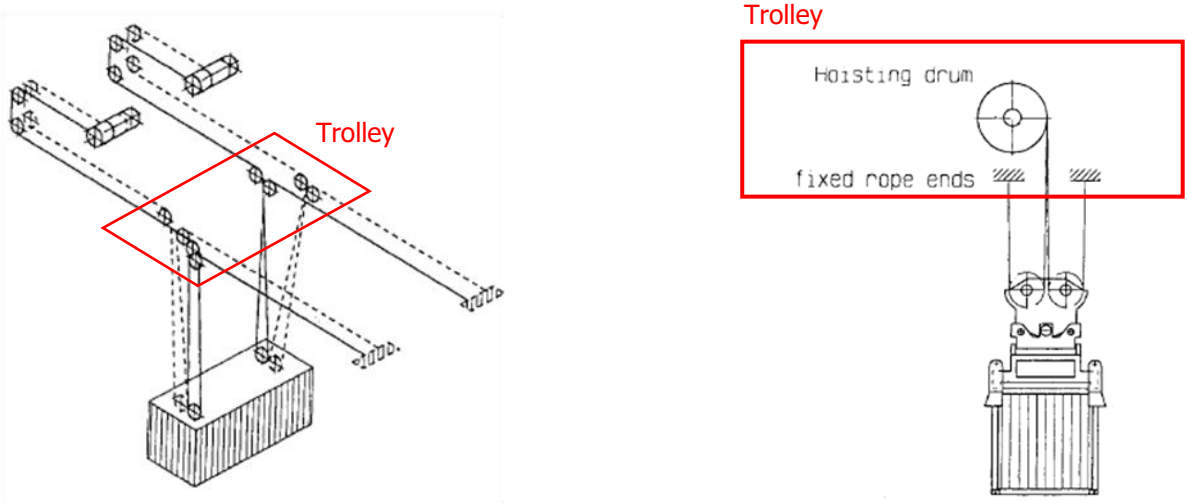

Figure 3.1: On the left the reeving on a crane with reeve-through trolley. On the right: half of the reeving of a machinery trolley [7]

Trim and list movements of the load

Figure 3.2 shows the rope reeving on an STS crane with a reeve-through trolley and without an anti-snag device. Four hoisting ropes are clamped on the two rope drums located inside the machinery house. A single hoisting rope is highlighted to indicate its path. The hoisting ropes are connected to spindles at the top of the boom, which can be used to trim and list the load of the crane by adjusting the lengths of the hoisting ropes. These movements are needed when a ship is not completely level, or the container is eccentrically loaded.

Figure 3.3 shows the reeving for an STS crane with anti-snag device. This system contains hydraulic cylinders for snag protection. These cylinders can be used for trim and list manoeuvres as well.

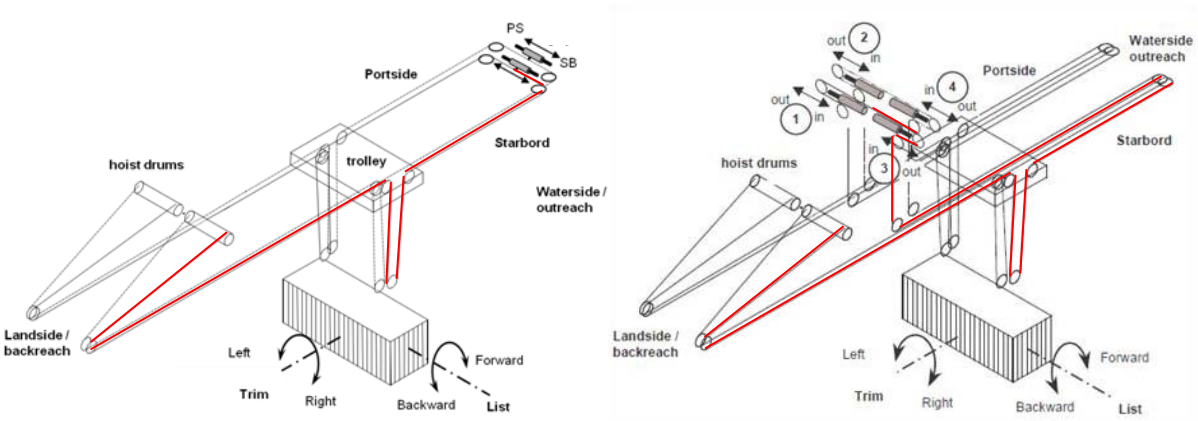

Figure 3.2 (left): Rope reeving of a reeve-through trolley without anti-snag device (source: Cargotec)
Figure 3.3 (right): Rope reeving of a reeve-through trolley with hydraulic anti-snag device inside machinery house (source: Cargotec)

3.1.2 Wire rope properties

Wire rope is constructed from cold drawn wires, which are wound to strands that are used to construct the total wire rope, as is shown in Figure 3.4. The properties of wire rope depend on the materials used, as well as the methods and layout of the construction. [10]

The most important properties for wire rope regarding a snag load are the minimum breaking load and the stiffness. The minimum breaking load is the tension which the rope is guaranteed to be able to sustain without breaking.

The elastic limit of wire rope is approximately 55-65% of the minimum breaking load. During a snag the tension varies between 10 and 50% of the minimum breaking load. In this range the stiffness of the rope is close to constant, as can also be seen in Figure 3.5.

The Young's modulus for wire rope varies between $0.85 \cdot 10^5$ N/mm^2 and $1.25 \cdot 10^5$ N/mm^2, depending on the wire rope construction. For the ropes used in STS cranes, the Young's modulus is $1.05 \cdot 10^5$ N/mm^2. [11]

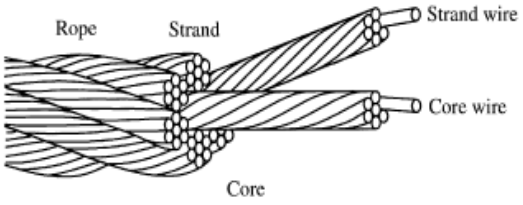

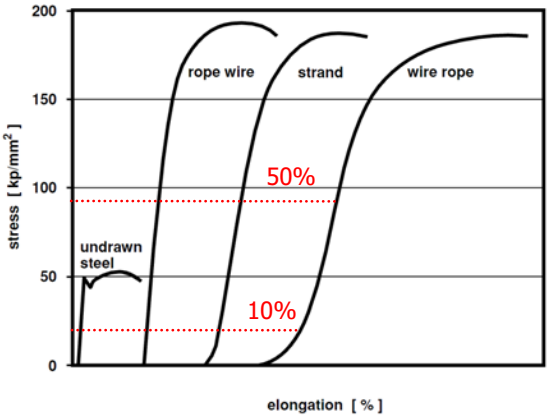

Figure 3.4 (left): Drawing of the construction of a wire rope [10]
Figure 3.5 (right): Stress-strain relation for wire rope and its components [12]

During the lifetime of a crane, the hoisting rope is replaced a number of times. The wire ropes have a limited number of moves they can perform before its fatigue life is reached. Sometimes the hoisting ropes are damaged due to collisions with for example a ship cell, and are replaced pre-emptively.

3.1.3 Hoisting winch components

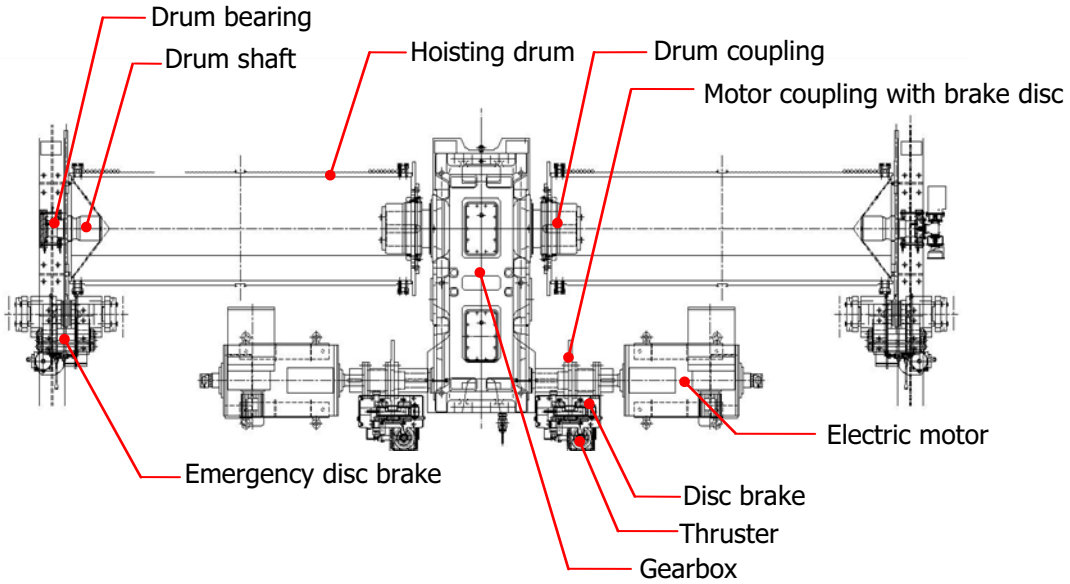

Figure 3.6: Top view of a typical main hoist configuration (source: Cargotec)

A typical main hoist consists of one or two electric motors on the input shaft, which are connected through a helical gearbox to two rope drums on the output shaft. Frequency controllers are used to control the speed of these asynchronous AC motors.

Two operational brakes, usually disc brakes, are installed on the input shaft, which are used during normal operation of the crane. These brakes will close when the input shaft has been stopped by regenerative braking of the motors. The brakes will then hold the load, until hoisting or lowering of the load is needed. When the motors are repowered and producing enough torque to hold the load, the brakes are released again.

An emergency disc brake is mounted on the outside flange of each of the rope drums. In case of an emergency stop, these brakes are applied together with the operating brakes, but the emergency brakes respond faster. An emergency stop is initiated when an extreme failure is detected, or when an emergency button is pressed.

All the brakes are hydraulically opened, spring closed brakes. This causes the brakes to close in case of a power failure, preventing the load of the crane to fall.

Figure 3.7: Overview of the machinery room of an STS-crane with an anti-snag device as shown in Figure 3.3. In the center the anti-snag device is visible, on the right the main hoisting winch (source: Cargotec)

3.1.3.1 Frequency controlled asynchronous AC motor

The typical motor used for hoisting winches is the three-phase asynchronous AC motor. The AC motor is connected with the AC drive, which can vary the supply frequency and current of the motor, controlling the produced torque and speed, using vector control. The AC motor has a separate motor used to power the cooling fan. This enables the motor to produce its maximum torque at low speeds, without risk of overheating the motor.

This section will explain the behaviour of the combination of the drive and motor. A more detailed explanation of the operating principles of AC motor and drive can be found in Appendix C.

Duty cycle

The duty cycle is a method to define the way in which an electric motor is used. An S1 duty cycle indicates that the motor produces torque for a continuous period of time, so that thermal equilibrium is reached in the motor.

Hoisting motors only have to provide torque for a small part of a single hoisting cycle. During trolley travel the motors are switched off, which allows the motors to cool down after each lift. This type of duty cycle is called S3. The ratio between the operating time and the total cycle time is called the

cyclic duration factor, usually 60% for hoisting motors. This factor influences the power at which the motor is rated. [13]

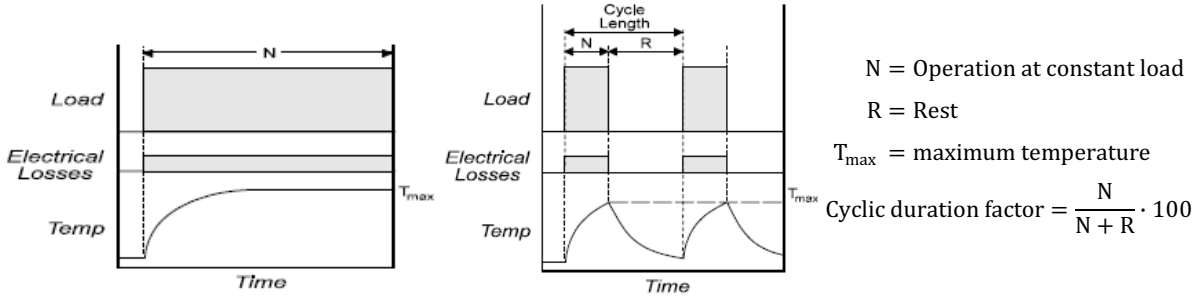

Figure 3.8: Characteristics of a S1 duty cycle (left) and S3-40% duty cycle (right) [13]

Produced torque

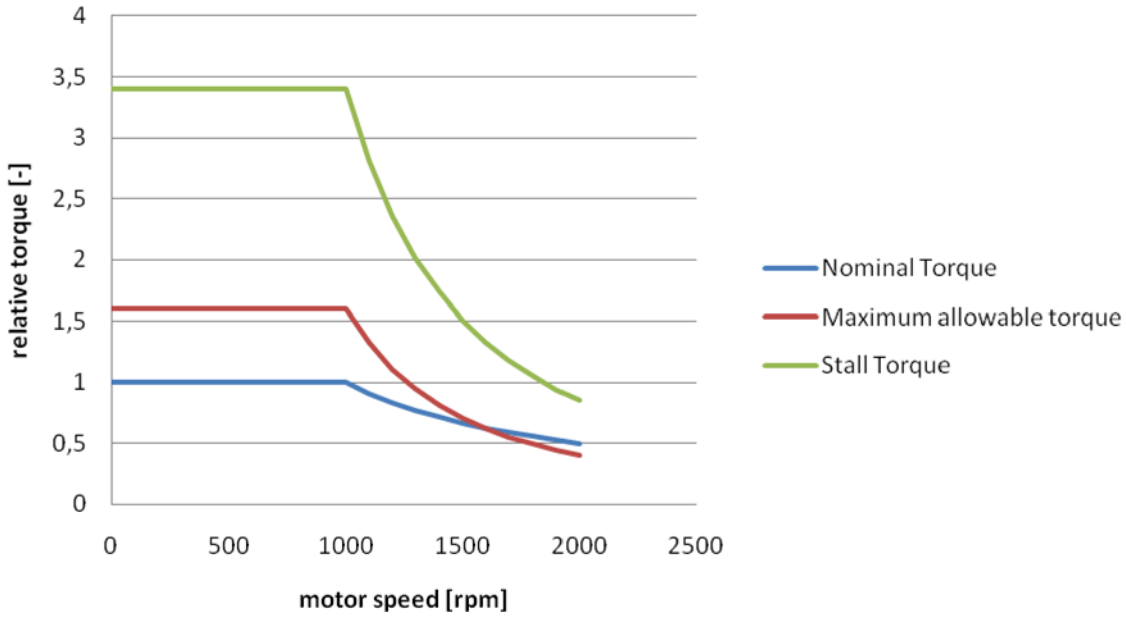

Figure 3.9: Speed torque characteristic of a 6-pole AC motor with variable speed drive

Figure 3.9 shows the speed-torque diagram of a variable speed drive, for a motor with an overload factor of 1.6 and a stall torque of 340% of nominal torque.

Nominal torque: The torque which corresponds to the rated power of the motor, at the duty cycle at which it's used.

Stall torque: The stall torque of the motor is the maximum torque the motor can produce at a certain speed. If the load of the motor exceeds this limit, the motor can no longer support the load and will stall. In case of a hoisting motor, this will cause the load to drop, and must therefore be avoided at all times.

The stall torque scales down quadratically when the speed is increased. [14]

Maximum allowable torque: The torque at which the motor is limited by the drive, to prevent the motor from reaching stall torque. The maximum allowable torque is greater than the nominal torque, allowing the motor to produce more torque during accelerations of the load. The ratio between nominal torque and maximum allowable torque is defined as the overload factor f_a. Figure 3.9 shows an overload factor of 1.6. When the motor exceeds this limit, the AC drive will shut down the motor,

after which it will signal the PLC that this has happened. The response times of the AC drives range between 25 and 50 ms, depending on the type of feedback used. [8] [13] [15]

For this particular example, the maximum allowable torque will be normative for the amount of torque the motor will produce at speeds over 1600 rpm. This is caused by the stall torque, which scales down quadratically to the speed. The maximum allowable torque scales in the same manner, to maintain a constant safety factor to the stall torque.

Regenerative braking

When lowering a load or performing an emergency stop the electric motor can operate as a generator, braking the load and generating electric energy. This energy can be fed back to the power supply, or stored in a storage system such as a battery or a flywheel. The maximum braking torque of the motor at a certain speed is equal to the maximum allowable torque at that speed.

3.1.3.2 Operational brakes

The operational brakes located on the input shaft are disc brakes, operated by hydraulically opened spring closed thrusters. The closing time of the brakes is dependent on the response time of the thrusters. The response time of a typical thruster for the crane brakes is shown in Figure 3.10.

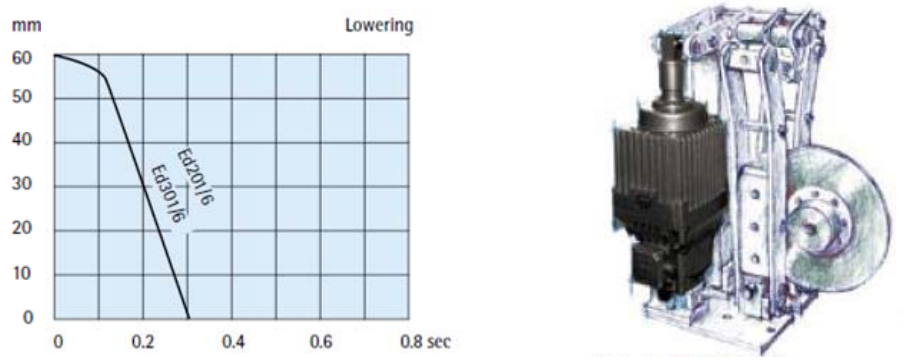

Figure 3.10: Closing time of a typical thruster for the operational brakes [16]

3.1.3.3 Emergency brakes

The emergency brakes consist of one or more braking callipers located on the rope drums. They are kept open by hydraulic pressure. When the brakes need to close, a valve is opened, releasing the hydraulic oil, and a set of cup springs will close the brake. Due to its construction, the emergency brakes have a closing time of approximately 200 ms.

In contrast to operating brakes, the emergency brakes are not installed on all cranes. The decision of installing emergency brakes is based on client requirements, as well as regulations and laws of the country where the crane will be installed.

3.2 Control system

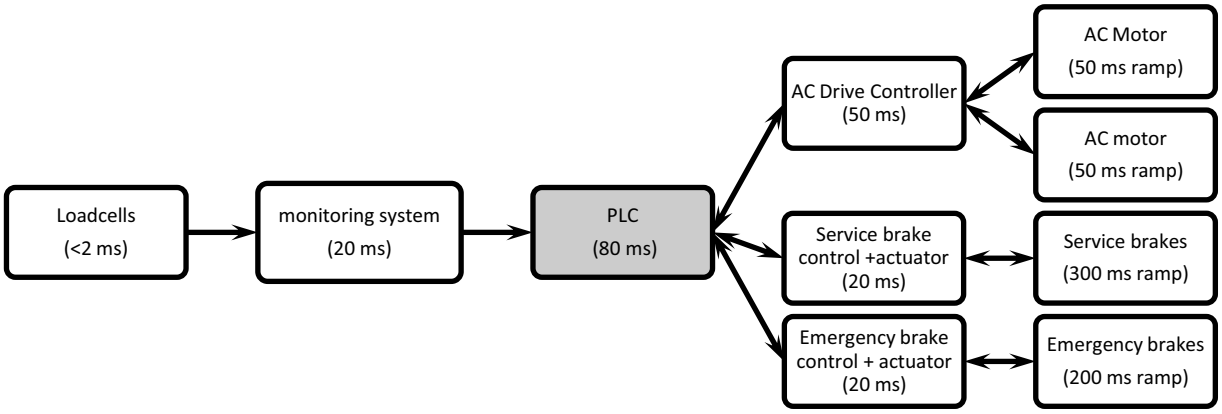

Figure 3.11: Schematic overview of the control system of the winch

During a snag situation, the control system needs to detect the snag, and perform an emergency stop. An emergency stop comprises of closing of all brakes, and reversing motor torque to stop the hoisting winch as fast as possible.

Figure 3.11 shows the layout of the control system as it is currently being installed in an STS crane. The PLC is the central controller of the crane, which controls all the actuators, depending on input from sensors and the crane driver.

A snag situation can be detected in three different ways:

- Crane driver
- Rope tension monitoring
- AC motor overload

The crane driver will always respond slower to a snag than the other two possibilities, and will therefore not be examined any further. First of all it is hard to spot a snag from the driver's cabin of the crane. Even when the driver sees or feels the snag happening, a human will have a response time between 0.2 and 0.5 seconds.

3.2.1 PLC

Currently the PLC used is a Siemens 319F, which is a so called safety PLC. This type of PLC has two separate programs, one for general control, and one for safety (the F-part). The emergency stop is included in the F-part, which has a typical response time of 100 to 200 ms. Because the PLC in the current STS cranes has a very short program in the F-part of the PLC, its response time is around 80 ms, according to the electrical engineer at Cargotec.

3.2.2 Rope tension monitoring

Rope tension monitoring is currently performed by a load pin on which the hoisting sheave are mounted. A load pin sends out a signal, of which the voltage varies depending on the load acting on the pin. The four load pins are connected to a central monitoring PLC, which calculates and monitors a number of loads:

- rope tension

- total load
- underload
- eccentric loads (portside vs. starboard load, waterside vs. landside load)

When the rope tension exceeds the load limit, the monitoring system will send the PLC, after which the PLC will initiate an emergency stop.
The system currently installed in the Kalmar STS cranes is the Hirschmann/Pat-Kruger system: DS120 PSA 3/1, which is claimed to have a response time of 20ms. [17]

3.2.3 AC Drive

As was explained in section 3.1.3.1, the AC-drive powers and monitors the motor.
It's possible for the motor to overload before the rope tension exceeds the load limit. When the motor reaches overload torque, it will be shut down by the drive and a signal will be send to the PLC. The PLC will then perform an emergency stop. Calculations regarding the response time of the control system to a snag situation are performed in paragraph 5.2.

3.3 Timeline of a snag event

As was discussed previously, the snag can be detected by either the rope tension monitoring or the AC drive. The order of events during a snag depends on the type of detection, as will be illustrated in this paragraph.

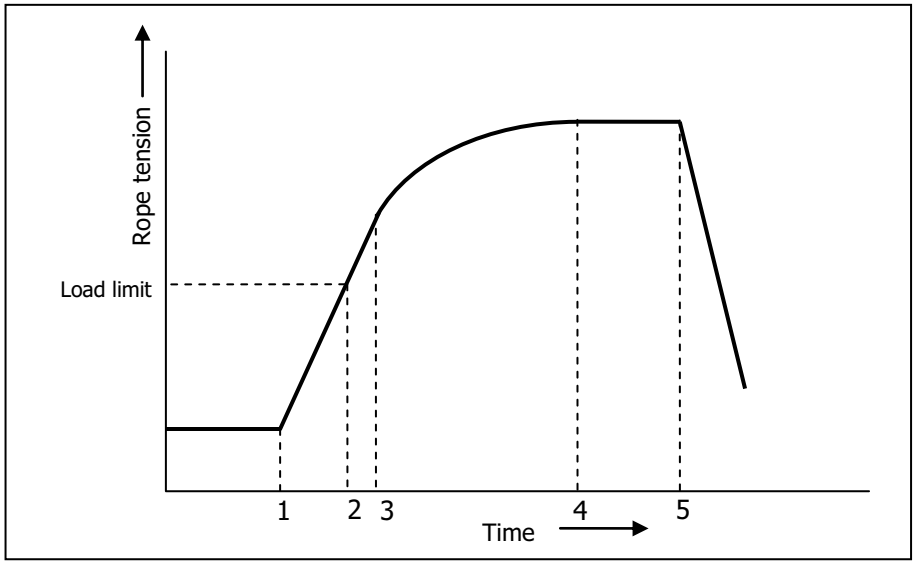

Figure 3.12: The development of rope tension during a snag event through time

The events during a snag of a container inside a ship cell are described below. The numbers correspond to the figure above.

3.3.1 Detection by rope tension monitoring

1. Container jams in cell guide
    - The winch continues to rotate, causing the ropes to stretch, increasing rope tension
    - Voltage of load cells (analogue signal) mounted in the shaft of rope sheaves rises

- The torque and current of the hoist motors rise

2. Rope tension monitoring detects an overload situation. A digital signal is sent to the PLC controlling the crane to transmit the overload.
3. The PLC determines an emergency stop has to be made.
   The PLC sends signal to the AC drive to start reversing torque. The PLC also switches a relay which will break the electric circuit of the brakes. This will cause the spring applied brakes to activate.
4. Emergency brakes and service brakes together with reversed motor torque stop the winch.
5. Motors are repowered, after which brakes are released to decrease the rope tension.

3.3.2 Detection by AC drive

1. Container jams in cell guide
   - The winch continues to rotate, causing the ropes to stretch, increasing rope tension
   - Voltage of load cells (analogue signal) mounted in the shaft of rope sheaves rises
   - The torque and current of the hoist motors rise
2. An overload situation is detected by AC Drive. The motor is unpowered, to prevent it from stalling. A digital signal is sent to the PLC controlling the crane to transmit the overload.
3. The PLC determines an emergency stop has to be made
   The PLC sends signal to the AC drive to start reversing torque. The PLC also switches a relay which will break the electric circuit of the brakes. This will cause the spring applied brakes to activate.
4. Emergency brakes and service brakes together with reversed motor torque stop the winch.
5. Motors are repowered, after which brakes are released to decrease the rope tension.

4. Movement of the load during a snag

To calculate the snag load on the crane, it is necessary to analyze the load movement and the corresponding rope tension through time. This will therefore be investigated in this chapter.
The load movement depends on the way in which the load jams. These movements will determine the speed at which rope tension rises, and the number of ropes that are stretched during a snag load. The problem will be approached in the following order:

1. Determine types of snag
2. Construct dynamic model
3. Solve the model
4. Determine the worst possible load cases
5. Implementation of the results in the snag calculations

4.1 Types of snag

A sudden stop of the load can be caused by:

- Jamming in the ship cell by skewing of the container
- Getting caught behind part of the ship construction (i.e. edge of the ship cell)
- Failure of limit switches, causing the headblock to run into the trolley
- Obstruction of the vertical path of the load by an object, i.e. another container (which is possible with poorly placed 45'-containers)

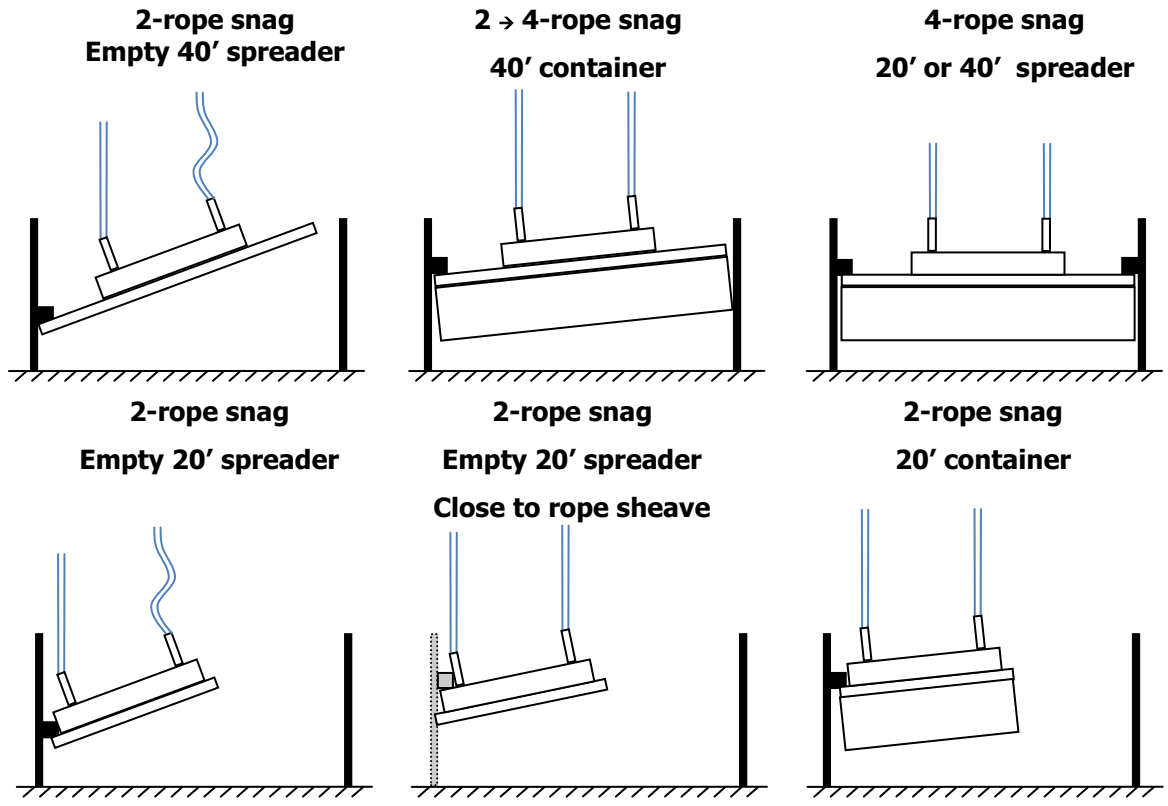

Figure 4.1: Different ways in which a load can snag. A 4-rope snag is possible for 20' as well as 40' spreaders. Only the 4-rope snag of a 40' spreader is illustrated

As is shown above, the way the load snags influences the increase in rope tension.

4-rope snag

During a 4-rope snag, indicated in the top right of Figure 4.1, all 4 hoisting ropes are immediately stretched by the hoisting winch, all at the same speed.

2-rope snag

During a 2-rope snag, the spreader will rotate around the point at which it snags, while the portside and starboard ropes are taken in by the winch at the same speed. Therefore the tension in the portside ropes will differ. It's possible for the free ropes to slack due to container rotation, depending on the parameters of the system. Examples of these parameters are the distance between rope sheaves and the load of the container.

To analyze this behaviour of the ropes during a 2-rope snag, a dynamic model of the load will be constructed in the next paragraph.

4.2 The model

The snagged load is modeled as if it is suspended by two linear-elastic springs, which are pulled upwards by the winch at the hoisting speed. The stiffness of these springs is dependent on the stiffness of the wire rope reeving.

4.2.1 Wire rope reeving stiffness

$$F_{rope} = k_{rope} \cdot u_{rope} \tag{4.1}$$

Due to the mechanical advantage of the wire rope reeving, the following equations hold:

$$F_{rope} = \frac{F_{reeving}}{2} \tag{4.2}$$

$$u_{rope} = 2 \cdot u_{reeving} \tag{4.3}$$

$$\frac{F_{reeving}}{2} = k_{rope} \cdot 2 \cdot u_{reeving} \tag{4.4}$$

$$F_{reeving} = 4 \cdot k_{rope} \cdot u_{reeving} \tag{4.5}$$

$$k_{reeving} = 4 \cdot k_{rope} \tag{4.6}$$

The stiffness of the springs can be calculated at:

$$k_{1,2} = k = 2\,ropes \cdot 4 \cdot k_{rope} = 2 \cdot 4 \cdot 145 = 1160\,kN/m \tag{4.7}$$

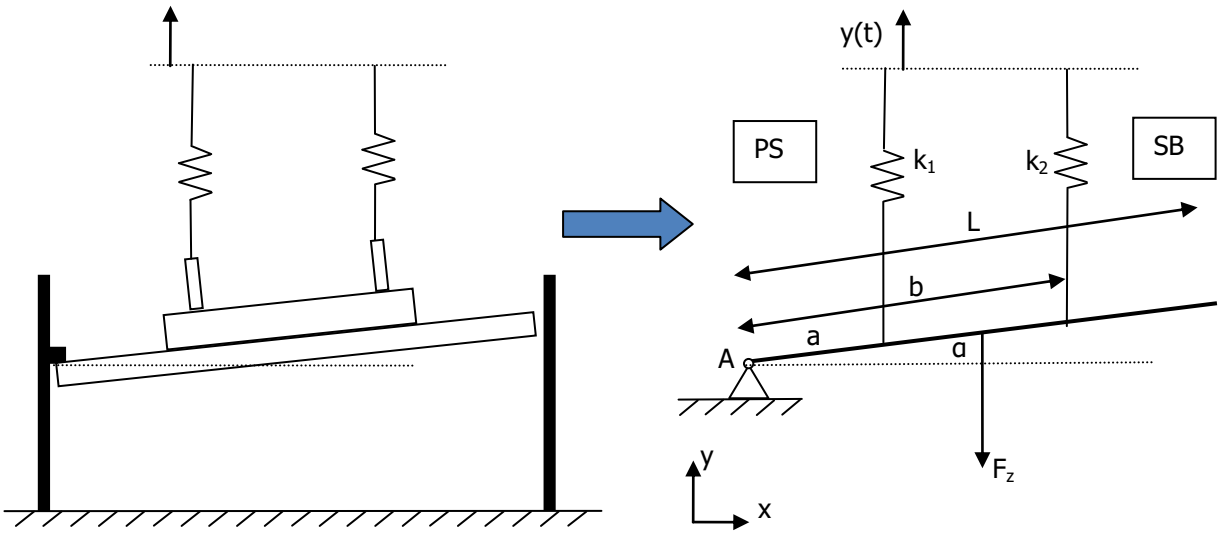

Figure 4.2: The model used to analyze the tension in the ropes during a 2-rope snag

k = stiffness of wire rope reeving

u = elongation of wire rope reeving

F_z = weight

The point of rotation is assumed to be at the edge of the spreader. The dimensions are taken from the construction drawings of the components available at Kalmar.

The elongation of both springs can be described

$$u_1 = u_{static} + u_{snag} = \frac{F_z}{2k} + y(t) - a \cdot \sin(\alpha) \tag{4.8}$$

$$u_2 = u_{static} + u_{snag} = \frac{F_z}{2k} + y(t) - b \cdot \sin(\alpha) \tag{4.9}$$

With:

$$y(t) = v_{hoist} \cdot t \tag{4.10}$$

$$F_z = m \cdot g \tag{4.11}$$

If a rope elongation is negative the resulting rope tension will be zero, since the ropes cannot transfer a compression force.

The angle of rotation is determined in the following paragraph using differential equations.

4.2.2 Equation of motion

The movement of the spreader during a snag can be described by solving the Euler equation around its point of rotation A:

$$\sum M_A = I \cdot \ddot{\alpha}(t) \rightarrow F_1 \cdot a + F_2 \cdot b - F_z \cdot \frac{L}{2} = I \cdot \ddot{\alpha}(t) \tag{4.12}$$

$$\boldsymbol{\sum M_A = I \cdot \ddot{\alpha}(t) \rightarrow u_1 \cdot k \cdot a + u_2 \cdot k \cdot b - F_z \cdot \frac{L}{2} = I \cdot \ddot{\alpha}(t)} \tag{4.13}$$

4.2.2.1 Initial conditions

The starting condition for the rotational angle is defined as: $\alpha(0) = 0\,rad$. The starting condition for the rotational speed will now be determined by analysing the conservation of momentum at the moment of impact.

The law of conservation of momentum will be applied around rotation point A. Zero deformation of the object blocking the spreader is assumed:

$$m \cdot v_0 \cdot \frac{L}{2} + I \cdot \omega_0 = m \cdot v_1 \cdot \frac{L}{2} + I \cdot \omega_1 \tag{4.14}$$

The rotational inertia of a prismatic beam around its corner is defined as:

$$I = \frac{m \cdot L^2}{3} \tag{4.15}$$

The rotational speed before impact ω_0 is zero:

$$m \cdot v_0 \cdot \frac{L}{2} = m \cdot v_1 \cdot \frac{L}{2} + I \cdot \omega_1 \tag{4.16}$$

v_0 is equal to the hoisting speed. The two unknowns are:

v_1 = vertical speed after impact

ω_1 = rotational speed after impact

These two variables are related through the kinematic relation of:

$$u = \frac{L}{2} \cdot \sin(\alpha(t)) \tag{4.17}$$

$$\frac{du}{dt} = v = \frac{L}{2} \cdot \cos(\alpha(t)) \cdot \frac{d\alpha}{dt} \tag{4.18}$$

At the time of impact, t=0, the angle of rotation is 0. Therefore the relation between the rotation and translation is defined as:

$$v = \frac{L}{2} \cdot \cos(0) \cdot \omega = \omega \cdot \frac{L}{2} \tag{4.19}$$

Inserting (4.19) into (4.16) returns:

$$m \cdot v_0 \cdot \frac{L}{2} = m \cdot \omega_1 \cdot \frac{L}{2} \cdot \frac{L}{2} + I \cdot \omega_1 \tag{4.20}$$

Simplifying:

$$v_0 = \omega_1 \cdot \frac{L}{2} + \frac{L}{1.5} \cdot \omega_1 \tag{4.21}$$

Rewriting for the rotational speed after impact ω_1:

$$\omega_1 = \frac{v_0}{\frac{L}{2} + \frac{L}{1.5}} \tag{4.22}$$

This equation is implemented in the model. For example, an 80 ton load returns a rotational speed at t=0 of 0.11 rad/s.

4.2.2.2 Solving the equation of motion

The differential equation (4.13) describing the motion of the container cannot be solved analytically due to a non-linearity introduced by the constraint of the hoisting ropes, which are not capable of transferring compression forces.

A Simulink model will therefore be constructed to solve the differential equation (4.13). The model can then be used to evaluate the load combinations described in the next section.

Matlab/Simulink is a tool for simulating dynamic systems. These systems can be a combination of different types of systems, like electronic, mechanical, thermal, etc.

The Simulink model and the Matlab code can be found in Appendix E.

4.2.3 Loads to be analyzed

Three different types of 2-rope snag will be analyzed:

Spreader mode	Mass [tons]	L [m]	a [m]	b [m]
40' (single lift) or 2 x 20' (twinlift)	17 to 80	12.2	3.55	8.65
20' (single lift)	17 to 47.5	6.1	0.4	5.6
Empty 20' spreader, impact close to sheaves	17	6.1	0.1	5.6

Table 4.1: Load cases and corresponding parameters for 2-rope snag

The 2 → 4 rope snag will not be analysed, since its result will be somewhere in between the results for a 2-rope snag and a 4-rope snag. The exact result would be dependent on deformations of the ship structure and friction of the cell guides.

The speed of the container will be determined by linear interpolation between the following two duty points:

- Nominal load: 80 tons, 90 m/min
- Empty spreader: 17 tons, 180 m/min

The calculation assumes the hoisting speed remains constant, even when load limits are exceeded. The model is stopped when the angle of rotation has reached 90°.

4.3 Results

Now that the model is explained, the results can be examined. First the result of a single load case will be examined to explain the events occurring during a snag. Next all load cases will be examined in detail to see what the consequences are of the different load cases.

4.3.1 Explanation of results

Figure 4.3 shows the rotation of the container and the development of the portside and starboard rope tension through time.

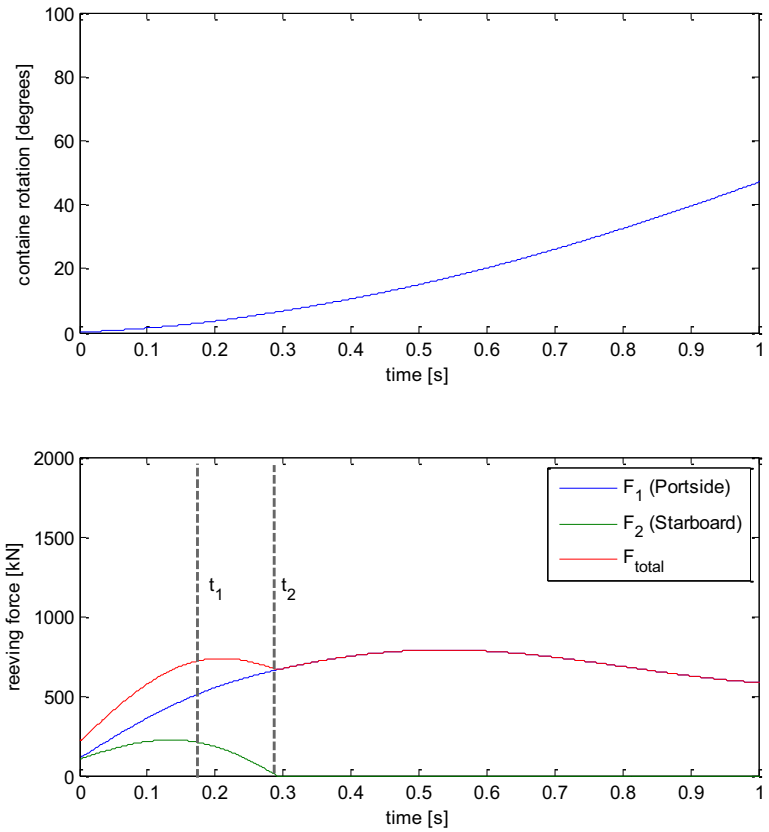

Figure 4.3: Top figure shows the rotation of the container through time. Bottom figure shows the development of rope tension through time for a snag of an empty 40' spreader at 180 m/min

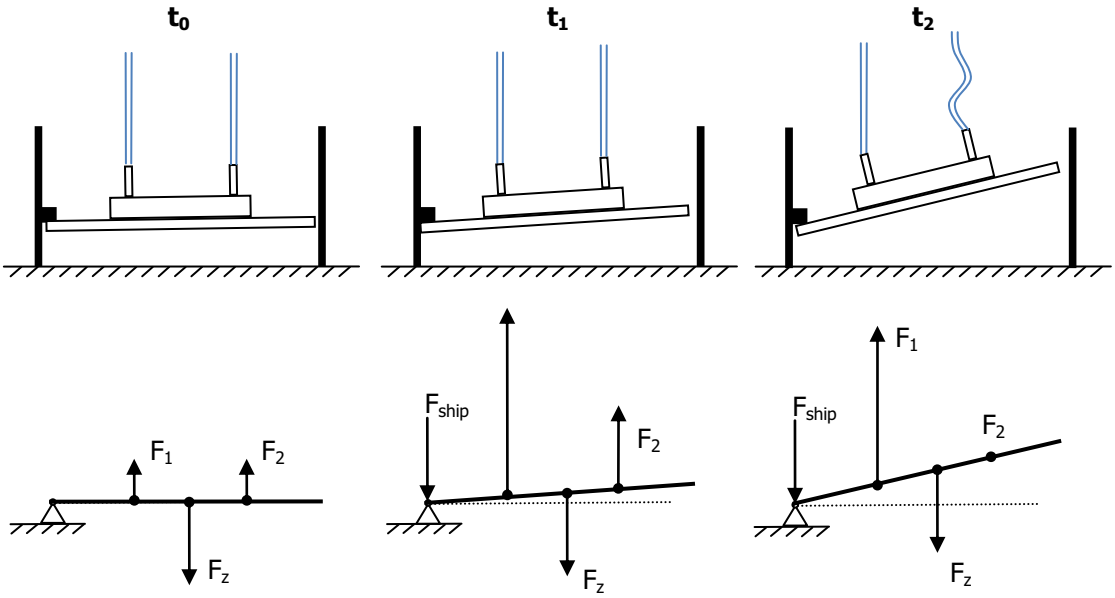

Figure 4.4: Illustrations corresponding to the events occurring in Figure 4.3

t_0: At the moment of impact the weight of the spreader is evenly distributed over the hoisting ropes. After impact, the spreader will have a rotational speed as calculated in section 4.2.2.1.

t_1: The hoisting winch is taking in the ropes at a higher speed than the hoisting sheaves move in vertical direction on the spreader. Therefore the wire rope is stretched, causing the rope tension to rise.

t_2: The spreaders rotation speed increases due to the increased rope tension. The starboard rope sheaves soon slack, due to the hoisting sheaves vertical displacement.

4.3.2 Results for all four load cases

In the following figures the rotation of the container and the forces in the wire rope reeving are shown for both spreader modes, for the corresponding maximum and minimum load. A snag event typically lasts less than one second. Therefore only the first second is shown.

40'-spreader, 90 m/min

The rope tension in both the portside and starboard ropes will rise at first, due to the inertia of the load. When the rotational speed of the spreader accelerates, the rope tension decreases again. After 0.75 s, the starboard ropes have slacked. Due to rotation of the spreader the tension in the portside ropes rises very slowly. The rotation causes a vertical displacement of the hoisting sheaves.

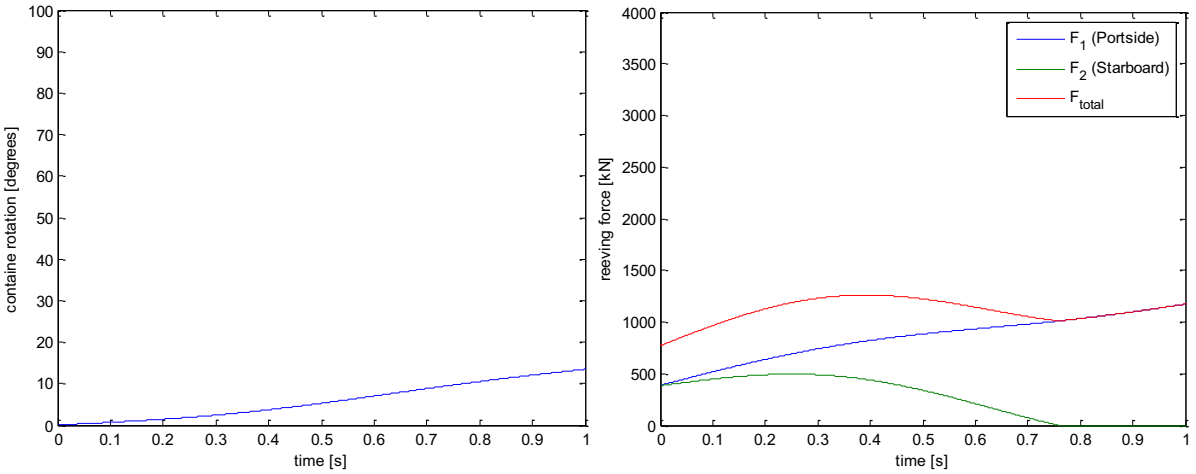

Figure 4.5: Rotation of the container and forces in starboard and portside reeving for a 2-rope snag of a 40-foot spreader, with an 80 ton load at 90 m/min

40'-spreader, 180 m/min

The behaviour of the empty 40'-spreader is roughly the same as the fully loaded spreader described previously. The only difference between these two load cases is the speed at which the event occurs, due to the higher hoisting speed and the smaller inertia of the load.

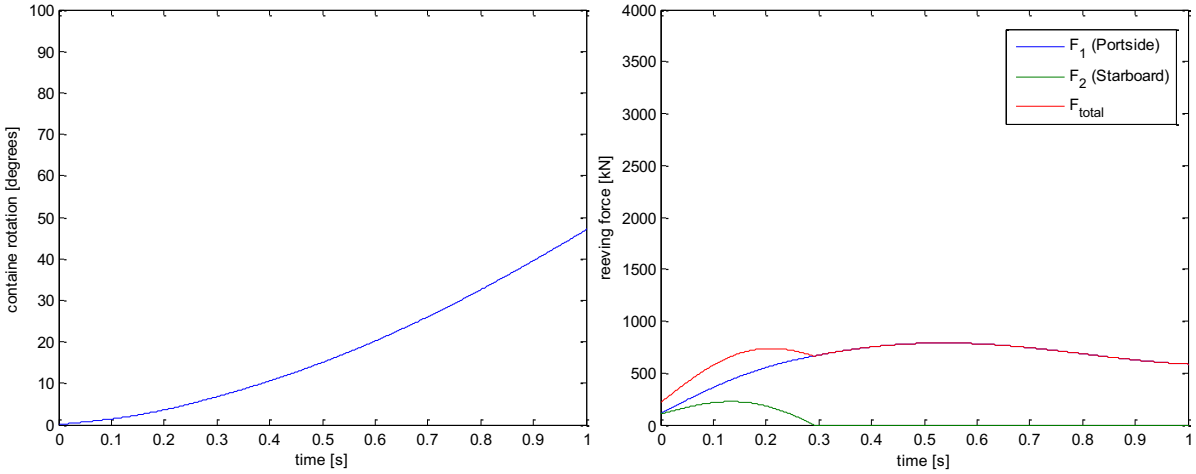

Figure 4.6: Rotation of the container and forces in starboard and portside reeving for a 2-rope snag of a 40-foot spreader, with a 23 ton load at 180 m/min

20'-spreader, 138 m/min

The biggest difference between snags with a 20'-spreader vs. a 40'-spreader is the speed at which the tension in the portside rope increases. Because of the short distance between the point of rotation and the hoisting sheaves (dimension a) there is very little vertical displacement of these sheaves.

The drop in rope tension of the starboard rope parts is also slower compared to a 40' spreader, because of the reduced dimension b.

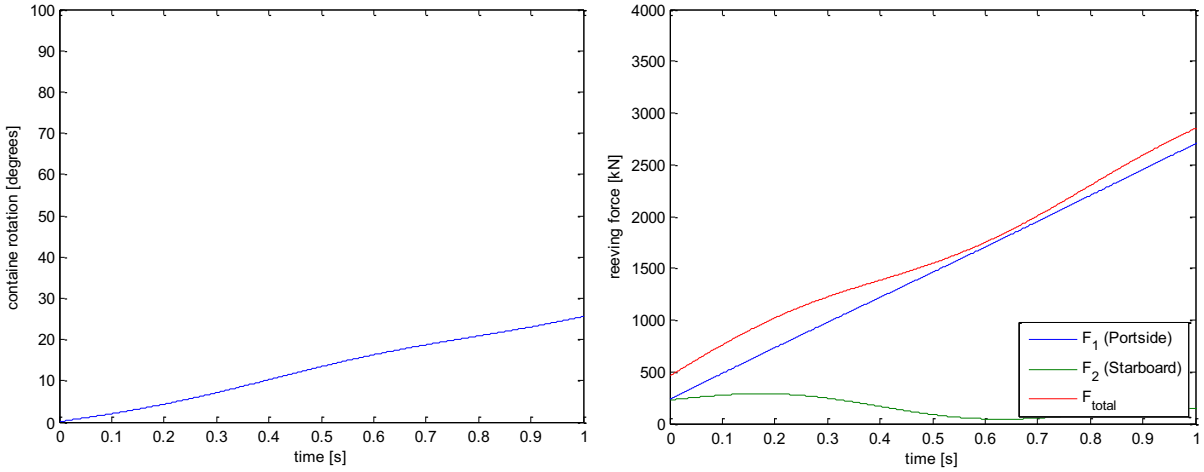

Figure 4.7: Rotation of the container and forces in starboard and portside reeving for a 2-rope snag of a 20-foot spreader, with an 47.5 ton load at 138 m/min

20'-spreader, 180 m/min

With an empty 20' spreader, the rope tension in the starboard ropes reaches zero in 0.3 seconds. The rotation occurs almost twice as fast as the fully loaded 20'-spreader, due to the increased hoisting speed and reduced inertia of the load.

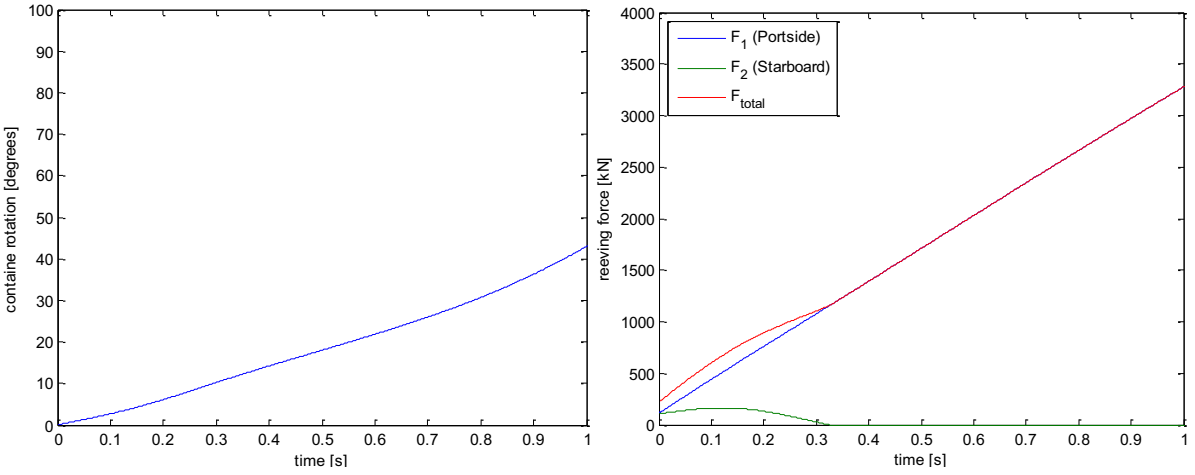

Figure 4.8: Rotation of the container and forces in starboard and portside reeving for a 2-rope snag of a 20-foot spreader, with a 23 ton load at 180 m/min

It can be concluded that a snag with a 20'-spreader is highly unfavourable to the crane, compared with a 40'-spreader. The rope tension rises much faster, due to the small distance between the point of rotation and the hoisting sheaves.

20'-spreader, 180 m/min, impact close to rope sheave

It is possible for the load to snag very close to the wire rope sheaves, especially when getting stuck behind a part of the ships construction. Due to a very short distance "a", the rotation of the container has almost no influence on the increase in rope tension. The portside rope tension increases almost linearly, while the starboard rope tension oscillates and slowly decreases towards zero tension.

The total load after one second is approximately 3500 kN, compared to 3250 kN when the edge of a 20'-spreader snags. This difference can be explained by the decrease in dimension "a".

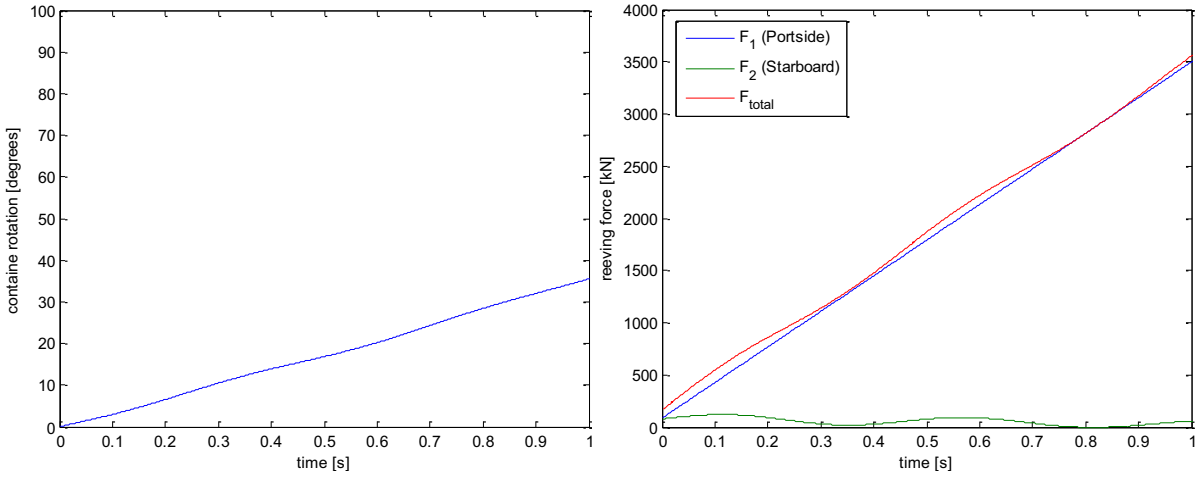

Figure 4.9: Result for a 2-rope snag with an impact close to the wire rope sheaves (a=0.05 m). 180 m/min with a 23 ton load

4.4 Conclusions

The worst case snags for an STS crane are the load cases that result in either the highest rope tension or the highest load on the crane structure. A faster increase in tension will result in a higher resulting crane load, since the time it takes to stop the winch will be approximately the same.

The analysis of the movement of the container performed in this chapter therefore showed that the load cases to cover the worst case scenarios are:

- 2-rope snag on a 20-foot spreader with impact close to the wire rope sheaves
- 4-rope snag (spreader mode is irrelevant)

The situation of 2-rope -> 4-rope snag will not be examined, since the result will be unpredictable, and will be somewhere in between the 2-rope and the 4-rope snag result. It has no use to analyze a 2-rope snag on a 40'-spreader, since this leads to slower increase in rope tension, due to spreader rotation.

The increase of the load on the crane can be approximated by the linear approximation described in (4.24).

4.5 Implementation of results into snag calculation

The results show a remarkable linear behavior of the total load during the first part of a snag. The length of this period depends on the type of snag, but ranges between approximately 0.2 seconds for a 2-rope snag on a 40'-spreader, to over 1 second for a snag close to the rope sheaves.

Since the impact close to wire rope sheaves is the load case of interest, this case will now be approximated using linear approximation of the rope tension. By using this approximation, the analysis of snag loads can be simplified.

4.5.1 Formulation

Using the following assumptions, a linear approximation is used to simplify the calculations for the analysis of snag loads:

- The total load can be expressed as the sum of the tension in the free ropes and the snagged ropes.
- The tension in the free rope parts is assumed to be constant at the static rope tension.
- The force in the snagged rope parts is determined by the reeving stiffness and the hoisting speed.

The total load can then be expressed as:

$$F_{total} = F_1 + F_2 \tag{4.23}$$

$$F_{total} = \frac{m \cdot g}{2} + \left(\frac{m \cdot g}{2} + v_{hoist} \cdot k_{reeving}\right) = m \cdot g + v_{hoist} \cdot k_{reeving} \tag{4.24}$$

4.5.2 Results

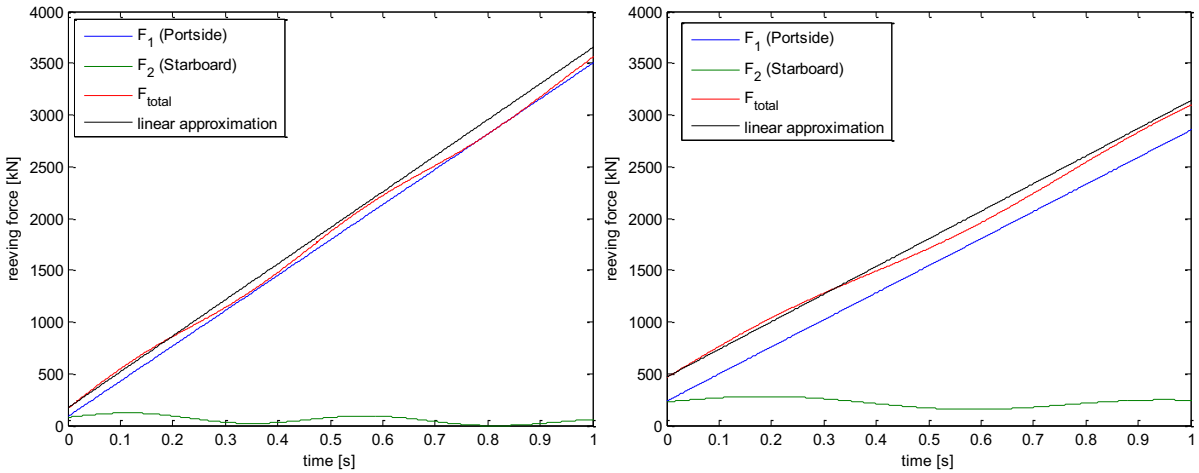

Figure 4.10: Results of the linear approximation on a snag with an empty (left) and a fully loaded 20'-spreader (right), both with an impact close to the wire rope sheaves

This approximation matches the results from the dynamic analysis closely for the first 0.2-0.3 seconds of a snag, depending on the mode of the snag. Due to vibrations of the load, the accuracy varies during later stages of the snag.

The linear approximation will be used to calculate the response time of the control system due to a snag. The accuracy of this method will be examined in paragraph 5.2.2.4.

5. The calculation model

This chapter will start with the explanation of the calculation model. Next some phenomena occurring in the crane during snag will be analyzed and implemented into the model if they have a significant influence on the snag load.

5.1 Modelling of the mechanical system

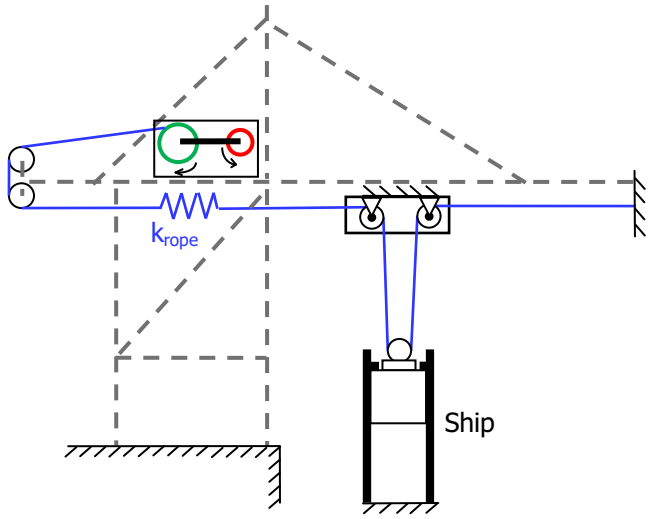

Figure 5.1: Schematic drawing of the model used for calculation (not to scale)

5.1.1.1 Operating principle

The essence of the model is a rotating inertia, in this case the hoisting winch, connected to tension springs which model the snagged hoisting ropes. The tension springs are being stretched by the rotating winch. The winch is stopped by a combination of braking torque and torque caused by the hoisting ropes.

The brakes are activated after the snag is detected. This detection can be performed by the monitoring system of the AC motors or by the tension monitoring system.

5.1.1.2 Crane structure

The influence of the crane structure is taken into account by reducing the rope elongation by 6%. This reduces the complexity of the calculations, since the crane structure itself won't have to be modelled. This will be explained in section 5.3.5.

5.1.1.3 Load cases

The different types of snag that will be examined are:

- 2-rope snag of a 20-foot spreader, impact close to rope sheave
- 4-rope snag

Both situations can be modelled as if the rope is suddenly stopped, since the influence of spreader rotation can be neglected.

5.1.1.4 Free ropes

For a 2-rope snag, the tension in the free ropes is assumed to remain constant at static rope tension. This assumption has been explained in chapter 4. With a 4-rope snag, all ropes are being stretched by the hoisting winch, so there will be no free ropes.

5.2 Modelling of the control system

5.2.1 Control of the AC motor

The combination of the speed and load of the motor determines the load cases for the snag calculation.

The AC drive determines the speed at which the motor runs, depending on the load of the motor.

The duty points of a crane are specified at a number of loads, for example:

- 82 ton, 90 m/min
- 17 ton, 180 m/min

When the crane lifts a load, the drive controls the motor through a control loop, to accelerate the motor to the maximum speed at which it can still support the load. The exact method of operation of this control loop is kept secret by the AC drive suppliers. This control loop will result in some sort of curve of the duty points of the motor. To be able to calculate the snag load, the duty points will be estimated using linear interpolation.

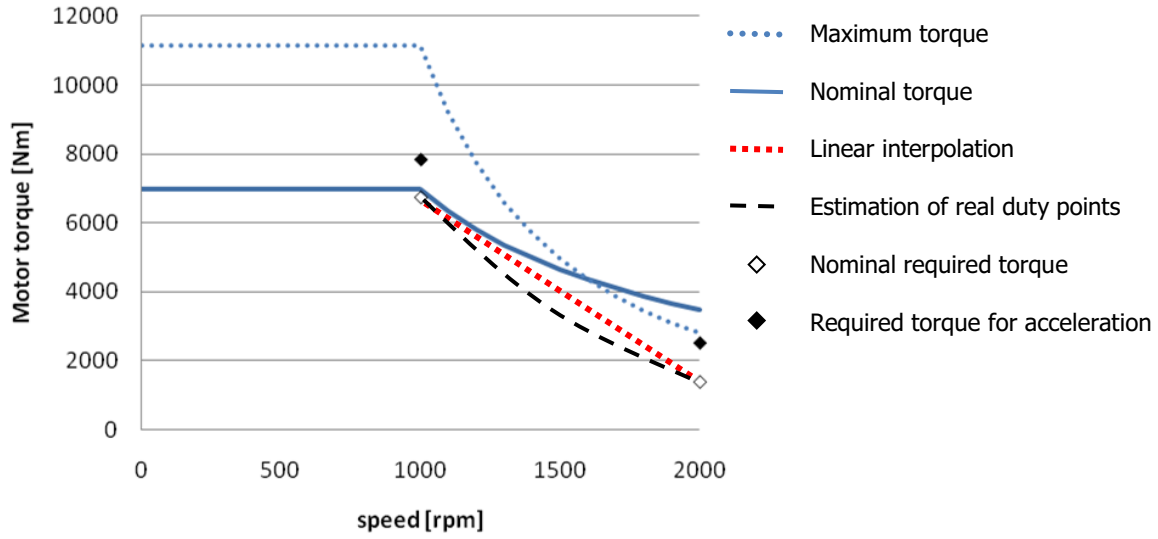

Figure 5.2: Illustration of all duty points of the AC motor, both the linear interpolation and the estimation of real duty points are illustrated

The linear interpolation will result in slightly higher hoisting speeds for a certain load, in comparison with reality. If the real duty points cannot be determined using supplier data, they could be measured during the testing of the crane.

5.2.2 The monitoring system

The control system determines the response times of the components. In section 3.2 a number of properties of the control system were discussed. In this section a method for calculating the response time of the monitoring system will be explained.

Currently a snag can be detected by the PLC in two different ways:

- Wire rope tension limit
- Overload of the electric motors

5.2.2.1 Wire rope tension limit

The time it takes to shut down the AC drive once a tension limit is reached can be expressed as:

$$total\ response\ time = \frac{tension\ limit - static\ rope\ tension}{speed\ of\ tension\ increase} + electronic\ delay\ time \tag{5.1}$$

With:

$$electronic\ delay\ time = Monitoring\ system + PLC + AC\ drive \tag{5.2}$$

$$static\ rope\ tension = \frac{total\ load\ on\ rope \cdot 9.81}{8\ rope\ parts} \tag{5.3}$$

$$speed\ of\ tension\ increase = v_{rope} \cdot k_{rope} \tag{5.4}$$

During tension monitoring, a number of limits for the rope tension are monitored:

- Total load
- Maximum single rope tension
- Underload
- Eccentric loads

The calculation of these four limits will now be explained. All limits will be rewritten to the tension limit in a single snagged rope.

Total load

The total load limit is set at 110% of the maximum allowable load of the crane. This load is typically 82 or 100 tons on the ropes, for a twinlift container crane. When this load limit is reached during a snag, the tension in the snagged ropes can be calculated using the following equation:

$$Maximum\ total\ load\ on\ ropes = maximum\ hoisted\ load \cdot 1.1 = n_s \cdot 2 \cdot T_s + n_f \cdot 2 \cdot T_f \tag{5.5}$$

n_S = number of snagged ropes

n_F = number of free ropes

T_S = Tension in snagged ropes

T_F = Tension in free ropes

The factor 2 in the equation is the mechanical advantage due to the reeving in a normal STS crane. Rewriting the equation gives:

$$T_s = tension\ limit = \frac{maximum\ hoisted\ load \cdot 1.1 - n_f \cdot 2 \cdot T_f}{2 \cdot n_s} \tag{5.6}$$

In this equation the tension in the free ropes is equal to the static rope tension.

Maximum single rope tension

This load limit is currently set at a rope tension of 265 kN.

Underload

The monitoring system checks for underload, to prevent the ropes from slacking. If the ropes would slack, they can get stuck behind objects or run of the hoisting sheaves, damaging the ropes.

The limit for slacked ropes is reached when the tension in either the portside or starboard reeving reaches below 15 kN of rope tension per side. If underload is detected, further lowering of the load is disabled and only hoisting is enabled.

Underload detection is only used when lowering the load, and is therefore not relevant for snag.

Eccentric loads

Eccentric load (or delta load) is calculated by the load monitoring system. The two eccentric loads that are monitored are:

- Portside vs. Starboard load
- Waterside vs. Landside ropes

During a snag, the relevant eccentric load is the difference between portside and starboard rope tension. The eccentric load could exceed the limit during a snag and trigger an alarm. However there are also variants of snag possible where this limit is not exceeded. To be sure to analyze the worst case scenario, this eccentric load monitoring will not be taken into account.

5.2.2.2 Overload of electric motors

During operation the electric motors try to maintain a set speed. When the motor load rises, i.e. due to load accelerations, the slip of the electric motors will increase, increasing the motor torque and current.

During a snag event the motor load increases dramatically, exceeding the maximum allowable torque. This is detected by the AC drive, which will unpower the electric motor.

The time it takes before the motor is shut down by the AC drive, due to exceeding the torque limit is:

$$total\ resp.time = \frac{Motor\ torque\ limit - static\ torque\ load}{Torque\ increase\ per\ second} + ACdrive\ resp.time \qquad (5.7)$$

With:

$$Torque\ increase\ per\ second = n_S \cdot v_{rope} \cdot k_{rope} \cdot \frac{r}{i} \qquad (5.8)$$

$$static\ torque\ load = \frac{load \cdot 9.81}{2} \cdot \frac{r_{drum}}{i} \qquad (5.9)$$

The motor torque limit is determined using torque characteristics like the one shown in Figure 3.9.

5.2.2.3 Resulting response time

The resulting response time for motor shut down will be the minimum of the response times calculated above.

5.2.2.4 Verification of monitoring system modelling

The equations described above will have to be compared to results from section 4.2, since these equations do not take the influence of container rotation and accelerations into account.

Figure 5.3 shows the calculated response times with the response times from the dynamic model from section 4.2.

For the rope tension monitoring, the maximum error in response times using this method is a 4% (6 ms) deviation of the linear approximation from the dynamic result. The response times on the motor load have a maximum error of 9%, or 7 ms.

These errors are negligible when comparing these to the other time delays in the system, like the PLC and the brakes.

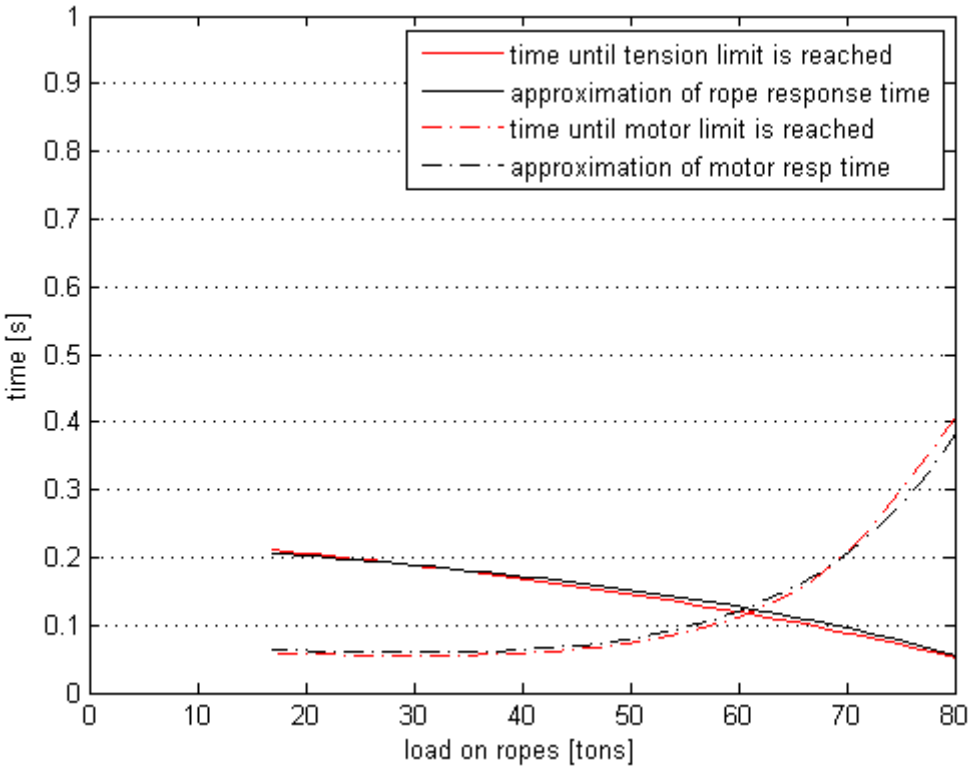

Figure 5.3: Results for the response times of the system to a 2-rope snag of a 20-foot container

5.3 Influences on snag load

In this paragraph the following phenomena will be examined, to check if they have a significant impact on the snag load. If one proves to have a significant impact, it will be implemented in the calculation model.

- Hoisting rope
  - Variation of wire rope stiffness during its lifetime
  - Rope sag
  - Tension wave propagation speed
  - Vibration of the hoisting rope during a snag
- Reeving system
  - Friction

- Rope sheave inertia

- Vertical movement of the load during snag
- Movement of the ship
- Stiffness of the crane

For the calculations performed in this paragraph, data is used from a super-post panamax STS crane installed at the MSC-Home terminal at the Delwaidedok in Antwerp, which is shown in Figure 1.4 (middle).

General properties	Outreach	56 (22 containers)	m
	Railspan	30	m
	Backreach	25	m
	Lifting height above quay level	35	m
	Hoisting speed (empty spreader)	3	m/s
	Load on ropes (empty spreader)	19	tons
	Hosting speed (twinlift)	1.5	m/s
	Nominal load on ropes (twinlift)	82	tons
Winch	Electric motors (6-pole AC)	Wölfer ODRKF 400L-6T	
	Power	2x730	kW
	Nominal speed	1000	rpm
	Maximum speed (at max hoisting speed)	2000	rpm
	Inertia	59.2	kgm^2
Gearbox	Transmission ratio	15.3	-
Hoisting rope	Type	6x36 WS + IWRC	-
	Diameter	30	mm
	Young's modulus	$1.05 \cdot 10^5$	N/mm^2
	Minimum breaking load	640	kN
	Tensile strength	1960	N/mm^2
	Cross section	414	mm^2
	Specific mass	3.17	kg/m
	Length	300	m
	Resulting rope stiffness	145	kN/m
Emergency brakes	Braking torque	2 x 160.000	Nm
Service brakes	Braking torque	2 x 10.400	Nm
Spreader + Headblock	L	12.192	m
dimensions	b	2.435	m
	AB	1.10	m
	AC	5.10	m
Snag load assumptions	Load per rope part	250	kN
	Corresponding rope elongation	1.72	m
	Time between snag and winch stop	0.8	s

Table 5.1: Data of MSC crane, used for calculations

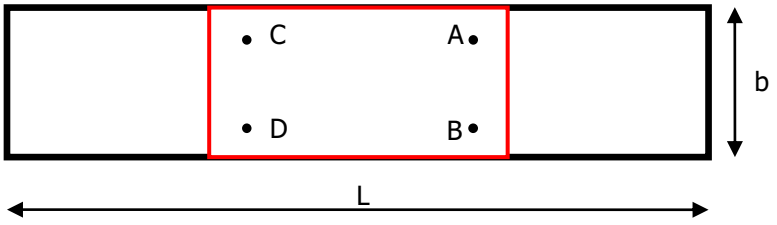

Figure 5.4: Schematic top view of the headblock and spreader

5.3.1 Hoisting rope

5.3.1.1 Variation of wire rope stiffness during its lifetime

The properties of a wire rope change during its lifetime, due to fatigue damage to the wire rope. The strands can compact, and individual wires can break.

During the early stages of the lifetime of wire rope the stiffness increases rapidly. This increase is caused by the settling of the wire rope strands. When the rope has settled, the stiffness will slowly decrease during the rest of its lifetime.

At the end of the lifetime of rope, the stiffness can decrease by 26% of its maximum stiffness. 10% decrease is found to be a good average and is recommended as a failure criterion for wire rope [18] [19].

For a snag load a higher stiffness results in higher snag loads. The stiffness decrease during the lifetime of the wire rope will therefore not be taken into account.

5.3.1.2 Rope sag

The weight of a wire rope causes the rope to sag when it spans a horizontal gap, in this case the bridge girder. When a rope sags, the total length of rope between the support points will increase. During a snag the rope tension will increase, which will decrease the rope sag. Therefore the rope sag acts as a small buffer for the hoisting rope.

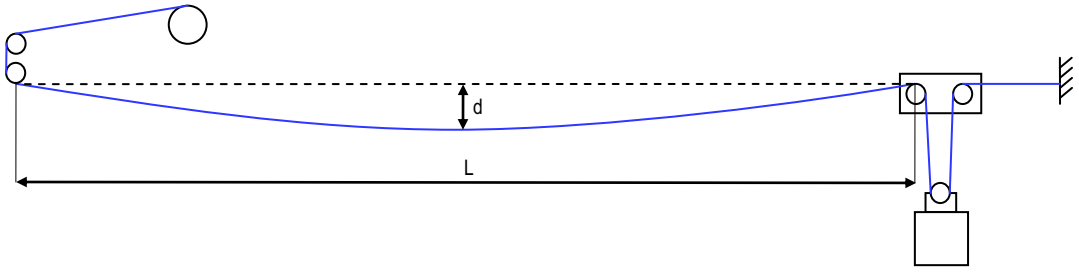

Figure 5.5: Hoisting rope sag for a reeve-through trolley system

First an unsupported rope length L of 100 m is examined. Other horizontal rope parts, like the part from the machinery house to the back of the girder will be neglected. The following equations will be used [20]:

$$d = \frac{g \cdot L^2}{8 \cdot p} \tag{5.10}$$

$$\Delta L_{sag} = \frac{8 \cdot d^2}{3 \cdot L} = \frac{8 \cdot \left(\frac{g \cdot L^2}{8 \cdot p}\right)^2}{3 \cdot L} = \frac{g^2 \cdot L^3}{24 \cdot p^2} \tag{5.11}$$

d = wire rope sag

g = weight per meter [N/m]

L = Unsupported horizontal length of the rope

p_{empty} = empty spreader rope tension

p_{snag} = rope tension during snag

The case that would create the largest rope buffer would be an empty spreader snag. For an unsupported horizontal rope length of 100 m, this would lead to the following results:

	d	ΔL_{sag}
Empty	1.72 m	0.08 m
Snagged	0.16 m	0.7 ·10-3 m
Resulting rope buffer		**0.08 m**

Table 5.2: Results for hoisting rope sag for an empty spreader and for a snag situation.

For STS-cranes with a total girder length of more than 100 meters, support systems are used to decrease sagging and slapping of the hoisting ropes. These movements of the ropes cause the load of the crane to swing and oscillate, which make it hard to control the load for the crane driver. Examples of these support systems are catenary trolleys and continuous rope support systems.

For a system with two catenary trolleys, the length for one span will decrease to approximately half of its original length, depending on the trolley's position. For a total girder length of 150 m, the unsupported length L will be 75 m, resulting in two 0.03 m rope buffers.

Continuous rope support systems usually have an unsupported rope length of 30 m. In case of a 150 m girder, this would result in five rope buffers of 0.002 m, leading to a total buffer of 0.009 m.

Because of this small wire rope sag, the effect will be neglected in snag load calculations.

5.3.1.3 Tension wave propagation speed

When a load snags, the rope tension has to be transferred from the headblock through the hoisting rope to the location where the load cells are located. The speed of this longitudinal wave is equal to the speed of sound through this medium, with has value of 5100 m/s for steel. However, the speed of sound through wire rope is lower due to its construction. 3000 m/s is found to be a conservative estimation. [21] [22]

$$t = \frac{L}{c} \tag{5.12}$$

The sag of hoisting rope influences the tension wave speed [23], as is described in the following equation:

$$c^* = c \cdot \sqrt{\frac{1}{1 + \frac{(qL)^2 EA}{12T^3}}} \tag{5.13}$$

c* = Tension wave speed

c = Speed of sound through rope

q = Weight per meter

T = Rope tension

L = unsupported rope length

When hoisting an empty spreader, the rope tension of 23 kN results in a reduction of the tension wave speed by 50%. For a horizontal rope length of 100 m and a vertical rope length of 50 meters, the travel time will be 0.08 s. Currently the STS cranes are built with a continuous rope support system, with a span of 30 m between each support. This leads to a total travel time of 0.05 seconds. This delay time will be taken into account in the calculations.

5.3.1.4 Vibration of the hoisting rope during snag

Due to vibration in both longitudinal and transverse direction of the wire rope, the tension in the hoisting rope will vary through time. The calculations assume all energy that is added to the winch is absorbed either by brakes, the motor or rope elasticity. When the ropes would vibrate, some of the potential energy from wire rope deformation is transferred into kinetic energy of the wire rope. The total wire rope deformation will therefore not increase.

5.3.2 Wire rope reeving

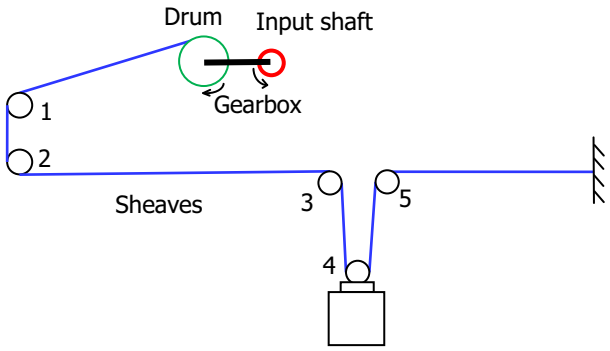

Figure 5.6: Schematic view of the reeving of a single hoisting rope

5.3.2.1 Friction

Friction in the reeving system and the hoisting winch transfers kinetic energy into heat. In calculations used at Kalmar for dimensioning motors the total efficiency is estimated at 0.89, so the total friction will be 11% of the total force required. This friction has influence on load measurements, as well as on stopping of the winch.

Reevingfactor (includes $\eta_{sheaves}$)	0.97
η_{drum}	0.97
$\eta_{gearbox}$	0.95
η_{total}	**0.89**

Table 5.3: Distribution of the friction on the hoisting rope and winch

Load measurements

The load can be measured using load shafts in the rope sheaves. Depending on the location of this load shaft, the measured load differs from the load in the rope falls by a certain factor:

$$F_{measured} = F_{load} + F_{friction} = \frac{F_{load}}{(\eta_{sheave})^{nr\ of\ sheaves}} \quad (5.14)$$

This means that the rope tension increases with every rope sheave that is passed by the rope, starting at the headblock (the location of the actual load).

For three sheaves with an efficiency of 0.99 each, the load in the ropes at the load shafts in the backreach is 3% higher. For motor calculation, the estimated friction will be on the high side to be sure the motors can cope with all possible loads. It is possible the friction is significantly lower; therefore it will be neglected in calculating the snag load. This approach is also used by Kalmar in emergency brake calculations during the crane design.

Emergency stop of the winch

During a snag, the friction in the reeving system together with friction in the winch will assist in stopping. However, the influences will be neglected for the same reasons as mentioned in the previous paragraph.

5.3.2.2 Rope sheave inertia

For a reeving system with four hoisting ropes, there are a total of 3 rope sheaves rotating at the same speed as the drums, and one sheave rotating with half this speed.

An 850 mm rope sheave has a weight of 180 kg. Assuming all mass located at a distance of 400 mm from the center, the total inertia of the sheaves on a single hoisting rope can be calculated using $I=mr^2$:

$$I = 3 \cdot 180 \cdot 0.4^2 + \left(\frac{1}{2}\right)^2 \cdot 180 \cdot 0.4^2 = 101\ kgm^2$$

This inertia will be added to the inertia of the hoisting winch, depending on the number of snagged ropes and the ratio of the gearbox.

5.3.3 Vertical movement of the load during snag

Besides the rotations studied in chapter 4, the load could also translate vertically during a snag event, sliding along the cell guides and deforming them. Because these movements are unpredictable, they movements will be neglected.

5.3.4 Movement of the ship during a snag event

Due to movement of the ship, the distance between the headblock and trolley can decrease, which decreases the rope tension during a snag. Therefore these movements will be estimated, to see if they have a significant influence.

Natural movements of a moored ship

Even though a ship is moored to the quay during loading and unloading operations, the ship can still perform roll, pitch and heave movements. Values of heave at which ports still operate vary between 0.3 and 0.8 m. Typical natural periods for heave and roll movements are 100s and 10s respectively, for 'a large vessel'. Natural periods for pitch are comparable to heave [24].

Because of these long natural periods, the movement of the ship will be neglected during the calculation of the snag event itself. However, the movement does require a fast release of the rope tension after the snag situation, to prevent the rope tension from increasing further due to ship movements, after the hoisting winch has stopped.

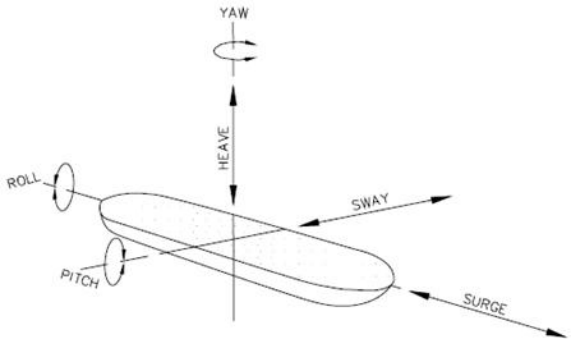

Figure 5.7: Definitions of ship movement [25]

Forced movements caused by the snag load

A snag load is a vertical force acting on the ship. This vertical force can cause a heave, roll and pitch movement.

Pitch and heave can be neglected based on the size of a ship. The vertical force would need to accelerate the ship and the water around the ship.

Roll could be possible, since this would not require water to displace, and the moment of inertia of the ship is smaller in this direction compared to pitch.

Length	397	m
Beam	56	m
Draft	15.5	m
deadweight	156 907	ton
Container capacity	14770	TEU

Table 5.4: Typical dimension of Maersk E-class container ship used for estimating forced movements caused by the snag load [26]

The deadweight mentioned in the table above is the amount of weight the ship can carry safely, including cargo, fuel, personnel etc. The total mass or displacement of the ship is unknown, so as an estimate a total mass of $200{\cdot}10^3$ ton will be used for calculations.

During a snag, the rope tension will rise from nominal load, i.e. 50 kN, to a value up to 250 kN. The following calculation will use the average of 150 kN.

When a load snags at one side of the ship, a moment is exerted on the ship, causing it to roll:

$$M = F \cdot d = 4 \cdot 2 \cdot 250kN \cdot 25m = 50 \cdot 10^6\ Nm$$

$$I = \frac{1}{2}mr^2 = \frac{1}{2} \cdot 200e3\ ton \cdot \left(\frac{56}{2}\right)^2 = 78 \cdot 10^9\ kgm^2$$

$$\ddot{\alpha} = \frac{M}{I} = \frac{50 \cdot 10^6\ Nm}{78 \cdot 10^9 kgm^2} = 6.3e \cdot 10^{-4}\ rad/s^2$$

$$rotation = \frac{1}{2}\ddot{\alpha}t^2$$

$$t = 0.8\ s$$

$$\alpha = \frac{1}{2} \cdot 6.3 \cdot 10^{-4} \cdot 0.8^2 = 0.20 \cdot 10^{-3}\ rad$$

$$0.20 \cdot 10^{-3}\ rad \cdot 25\ m = 0.003\ m$$

Due to the wire rope reeving, this vertical displacement of the ship will lead to a decrease in rope elongation of 0.006 m. This is less than one percent of the total rope elongation. Therefore this effect will be neglected.

smaller cranes and ships

The ship used in this calculation was extremely big, because the snag calculation is based on the worst case scenario. Smaller cranes would be able to handle only smaller ships. When crane dimensions are reduced from 22 to 13 containers wide (Panamax), the inertia is reduced with a factor of:

$$\left(\frac{13}{22}\right)^3 \cdot \left(\frac{13}{22}\right)^2 = 0.07$$

This results in a vertical displacement of 0.04m and a decrease in rope elongation of 0.08 m. So ship movements could decrease rope tension by less than 5% in the most favourable case. Therefore it will not be taken into account. Also, cranes which are this small usually have low hoisting speeds, and there do not require an anti-snag device anyway.

5.3.5 Stiffness of the crane

In this paragraph the stiffness of relevant components of the crane will be examined. All the deformations are regarded at the location where they influence the required rope length, which, in most cases, are the locations of the wire rope sheaves.

In the final section of this paragraph, the total stiffness of the crane structure will be calculated, together with its influence on the rope elongation.

The stiffness of the crane structure will be examined using the FEM-calculation program KRASTA. Two cranes will be examined:

- 22-wide Double box girder crane described in Table 5.1, installed in port of Antwerp (Belgium)
- 17-wide Monobox crane installed in the port of Altamira (Mexico), shown in Figure 1.4 (left)

Due to the time constraints of the research, the lattice girder will not be examined in detail. The lattice girder is known to have roughly the same properties as the other two cranes.

The following components will be examined:

- Main construction
    - Deflection
    - Compression
    - Torsion of double box girder caused by centric loading
    - Torsion of total girder caused by eccentric loading
- Trolley
- Spreader
- Headblock
- Rope sheave mountings

First the deformations will be described. The results will be examined in paragraph 5.3.5.6.

5.3.5.1 Main construction

Deflection: The deflection of the crane will be analyzed at two different trolley locations, being the minimum and maximum outreach. This will be done by checking the deformation caused by a known load.

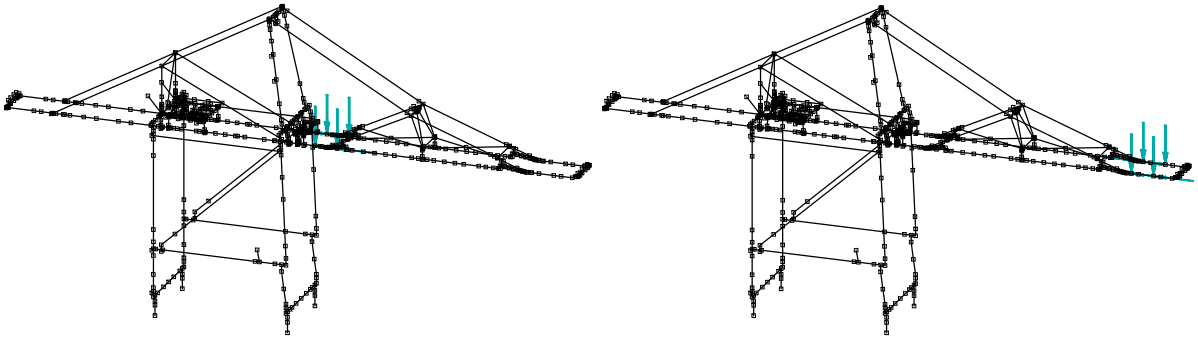

Figure 5.8: Load cases used for evaluating the stiffness of a double box girder crane: Minimum outreach (left), maximum (right)

Compression: During loading, the main girder will be compressed by the rope forces. The compression of the girder will decrease the distance between the hoisting rope sheaves at the portside and waterside of the girder, reducing the required rope length.

Torsion of a double box girder caused by centric loading: In case of a double girder crane, the trolley rails are positioned on top of the side plate of the box profile. This will cause each box to rotate during loading. The rotation, and corresponding vertical displacement of the rails will be checked.

The Monobox girder is not subjected to torsion caused by this effect.

Figure 5.9: Cross section of one of a double box girder, with the rotation caused by a centric trolley load

Torsion of girder caused by eccentric loading: During a 2-rope snag, the eccentric loading will cause a rotation of the girder, for both the Monobox and double box girder. Due to its construction, a Monobox girder has a higher torsion stiffness compared to the double box girder.

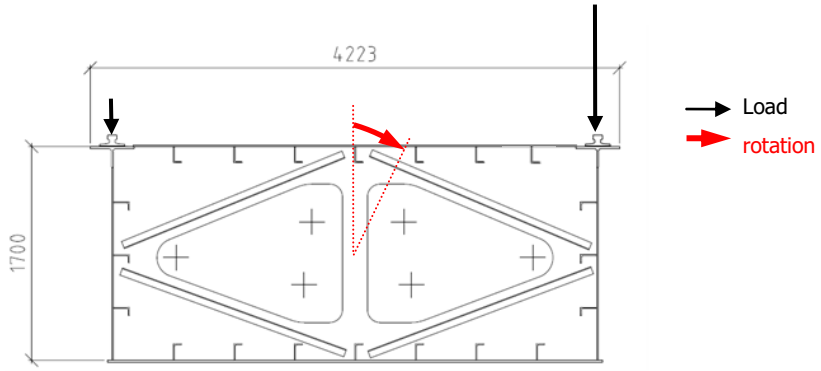

Figure 5.10: Example of an eccentric load on a Monobox girder

5.3.5.2 Trolley

The trolley stiffness is determined for both the Monobox and the double box girder crane. The relevant stiffness is determined by the displacement of the wire rope sheaves caused by a known rope tension.

5.3.5.3 Spreader

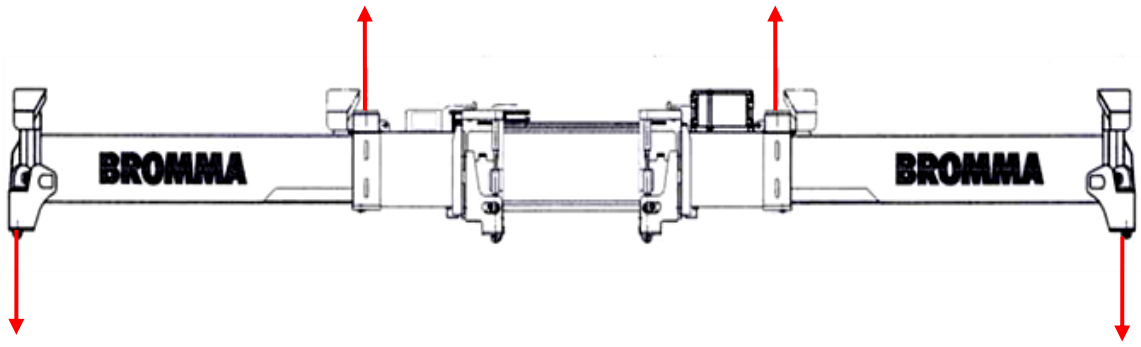

Figure 5.11: Side view of a twin lift spreader, with arrows indicating the forces acting on the spreader during snag

From testing results of a Bromma STS 45 spreader, the relevant stiffness of the spreader can be found. This stiffness is calculated using the deformation of the headblock connection relative to the container connection.

Proof loading is performed for a 51 ton single lift operation. Deflection of the spreader at the location of the headblock connection is 41 mm. This results in a stiffness of:

$$k = \frac{51 \cdot 9.81}{0.041} = 12.2 \cdot 10^3 \, {}^{kN}/_{m}$$

5.3.5.4 Headblock

The rope sheaves on the headblock are located directly above the connection between the headblock and the spreader. Therefore the only relevant deformation of the headblock is the tensile deformation. Because of the small size of the headblock in this direction, the stiffness of the headblock in this direction will be assumed infinite.

5.3.5.5 Rope sheave mountings

The rope sheave mounting will deform under load. However, compared to the deformation of the rest of the crane structure, these deformations will be negligible and will therefore not be taken into account.

5.3.5.6 Resulting stiffness

The crane can be seen as a series of springs, of which the stiffnesses are calculated in previous paragraphs. The total stiffness can be calculated by:

$$\frac{1}{k_{crane}} = \sum \frac{1}{k_{components}} \tag{5.15}$$

	min. outreach [·10^3 kN/m]		max. outreach [·10^3 kN/m]	
	Monobox	Double box	Monobox	Double box
Main girder deflection	48	42	4.2	6.4
main girder compression	180	82	180	82
Torsion caused by centric load	N.A.	2400	N.A.	1200
Torsion caused by eccentric load	111	30	56	7.1
trolley	120	210	120	210
spreader	120	120	120	120
Resulting stiffness centric load (4-rope)	**23**	**20**	**3.8**	**5.5**
Resulting stiffness eccentric load (2-rope)	**19**	**12**	**3.6**	**3.1**

Table 5.5: Stiffness results for both Monobox and double box crane at minimum and maximum outreach

5.3.5.7 Influence of stiffness on the wire rope elongation

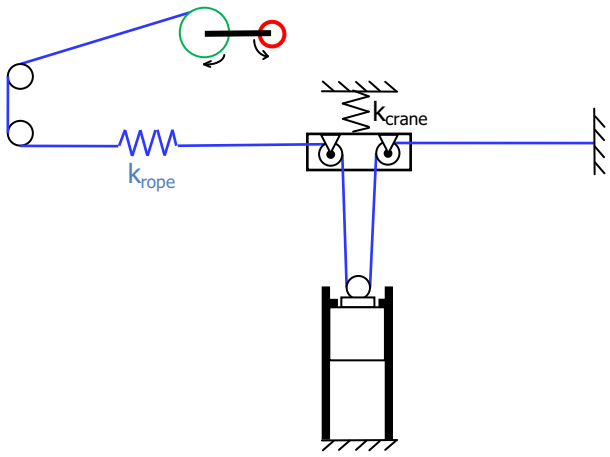

Figure 5.12: Model of a wire rope and crane structure

For a Monobox crane the stiffness at minimum outreach is 19e3 kN/m, compared to a wire rope stiffness of 156 kN/m. However, due to the wire rope reeving, the influence of the crane stiffness is not simply the ratio of these two stiffnesses.

The deformation of the crane as a function of the rope tension can be expressed as:

$$u_{crane} = \frac{F_{crane}}{k_{crane}} = \frac{2 \cdot n \cdot F_{rope}}{k_{crane}} \tag{5.16}$$

Where the factor 2 expresses the mechanical advantage of the reeving, and n equals the number of snagged ropes.

The decrease in rope elongation Δu_{rope} due to crane deformations can now be expressed as:

$$\Delta u_{rope} = 2u_{crane} = \frac{4 \cdot n \cdot F_{rope}}{k_{crane}} \tag{5.17}$$

A snag on 4 ropes at minimum outreach with a rope tension of 250 kN will result in a decrease in rope elongation of 0.17 m, resulting in a decrease in rope tension of 27 kN (11% of the original rope tension of 250 kN). This is a significant decrease in rope tension and therefore the influence will be taken into account.

5.3.5.8 Implementation of stiffness in the calculation model

The model described in section 5.1 models only the wire rope stiffness. The crane stiffness will now be combined with the wire rope stiffness, to prevent complicating the model.

Both the crane and the rope will be regarded as linear elastic springs:

$$F_{rope} = k_{rope} \cdot u_{rope} \tag{5.18}$$

$$F_{crane} = k_{crane} \cdot u_{crane} \tag{5.19}$$

The ropes have a mechanical advantage of 2, and n stands for the number of snagged ropes:

$$2 \cdot n \cdot F_{rope} = F_{crane} \tag{5.20}$$

Inserting (5.18) into (5.20), to remove F_{rope} from the equation:

$$2 \cdot n \cdot u_{rope} \cdot k_{rope} = k_{crane} \cdot u_{crane} \tag{5.21}$$

The rope stretch u_{rope} is equal to the rotation of the drum, minus the reduction of rope length caused by deformation of the crane. This reduction is equal to twice the crane deformation, due to the mechanical advantage:

$$u_{rope} = \alpha \cdot r_{drum} - 2 \cdot u_{crane} \tag{5.22}$$

Rewriting for u_{crane}:

$$u_{crane} = \frac{\alpha \cdot r_{drum} - u_{rope}}{2} \tag{5.23}$$

Eliminating u_{crane} from equation (5.21) using (5.23):

$$2 \cdot n \cdot u_{rope} \cdot k_{rope} = k_{crane} \cdot \frac{\alpha \cdot r_{drum} - u_{rope}}{2} \tag{5.24}$$

Rewriting for u_{rope} returns the equation:

$$u_{rope} = \frac{k_{crane}}{4 \cdot n \cdot k_{rope} + k_{crane}} \cdot \alpha \cdot r_{drum} \tag{5.25}$$

So to calculate the rope elongation form the rotation of the drum, the displacement of the rope has to be multiplied with a factor of:

$$\frac{k_{crane}}{4 \cdot n \cdot k_{rope} + k_{crane}} \tag{5.26}$$

Using equation (5.26), the influence of the crane stiffness can be modelled. The wire rope stiffness equals 145 kN/m for the double box and 156 kN/m for the Monobox, respectively. The crane stiffness can be found in Table 5.5.

	Min. outreach		Max. outreach	
Nr of snagged ropes	Monobox	Double box	Monobox	Double box
2	0.94	0.91	0.74	0.73
4	0.90	0.90	0.61	0.70

Table 5.6: Reduction factor of rope elongation during a snag

The elasticity of the structure causes a reduction of the rope elongation of 6% to 30%, depending on the type and location of the snag event. The difference between the 2-rope and 4-rope snag is very small for the double box girder, because of the low torsion stiffness of this construction.
Since the stiffness has a significant influence on the rope elongation, equation (5.26) will be used to calculate its influence. The stiffness used in the calculations will be the stiffness at minimum outreach of the Monobox crane, since this construction is stiffer, and this design type is currently the focus of Cargotec:

- Centric snag: $23 \cdot 10^3$ kN/m
- Eccentric snag: $19 \cdot 10^3$ kN/m

5.3.6 Conclusions

From the influences checked in this paragraph, the following will be taken into account for calculations:

- Extra time delay of 0.08 s due to tension wave travel time
- Inertia of the hoisting rope sheaves
- Stiffness of the crane structure, using the reduction factor described in (5.26)

The following influences will be neglected, because they are too small to be significant, especially in a worst case scenario.

- Wire rope sag
- Reeving system friction
- Ship movement during snag

The following influences were neglected because of other reasons:

- Variation of wire rope stiffness (will only decrease during life, which decreases snag loads)
- Vibration of the hoisting rope (will not increase calculated tension)

It is recommendable to release rope tension quickly after a snag, preventing further tension increase due to ship movements.

6. Calculation of snag loads

The calculation is performed using two different methods: a simplified calculation and a Matlab/Simulink simulation. Both are based on the same model, but the simplified calculation neglects the influences of the brakes and the regenerative braking, since it is complicated to their characteristics into a mathematic calculation.

The main benefit of Simulink is that the behaviour of the motor and brakes, with their own characteristics can be easily programmed.

6.1 Simplified calculation

6.1.1 Calculation of the snag load

The simplified calculation splits up the rope elongation in three parts:

- Static elongation
- Elongation caused by motors
- Elongation caused by kinetic energy of the hoisting winch

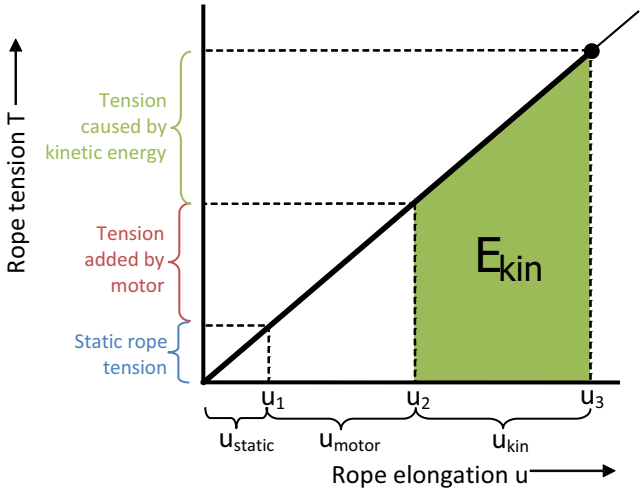

Figure 6.1: Tension vs. elongation of a linear elastic spring

Static rope elongation

The static rope elongation is present before the snag occurs:

$$u_1 = u_{static} = \frac{load}{n_{rope\ parts} \cdot k_{rope}} \tag{6.1}$$

Elongation caused by hoist motors

Once the load has snagged the motors will continue to produce torque, stretching the ropes even further. At a certain point in time the maximum allowable torque is reached and the AC drive shuts down the motor to prevent it from stalling. The torque the motors deliver at the moment of shut down can be described by:

$$Torque\ at\ motor\ shutdown = Torque\ increase\ per\ second \cdot response\ time \tag{6.2}$$

The rope elongation achieved by the motor can be expressed by:

$$u_2 = \frac{Torque\ at\ motor\ shutdown \cdot \frac{i}{r}}{n_{snagged\ \ ropes} \cdot k_{rope}} \tag{6.3}$$

$$u_{motor} = u_2 - u_1 \tag{6.4}$$

Elongation caused by kinetic energy

When the motors have been shut down, the kinetic energy stored in the motors will be absorbed by the snagged ropes in the form of rope elongation, and some energy will dissipate in the displacement of the free ropes. No brakes are implemented in this calculation.

The amount of kinetic energy that needs to be absorbed is:

$$E_{kin} = \frac{1}{2} J \omega^2 \tag{6.5}$$

This energy is equal to the potential energy in the ropes at the end of the snag event, which can be seen as the green area in the tension-elongation graph above:

$$E_{kin} = E_{pot} = n_{free\ ropes} \cdot F_1 \cdot u_{kin} + n_{snag\ ropes} \cdot F_2 \cdot u_{kin} + n_{snagged\ \ ropes} \cdot \frac{1}{2} \cdot k_{rope} \cdot u_{kin}^2 \tag{6.6}$$

$$u_{kin} = u_3 - u_2 \tag{6.7}$$

$$=> E_{kin} = n_{free\ ropes} \cdot F_1 \cdot u_{kin} + F_2 \cdot (u_3 - u_2) + \frac{1}{2} \cdot k_{rope} \cdot n_{snagged\ \ ropes} \cdot (u_3 - u_2)^2 \tag{6.8}$$

Because u_2 is already known, this equation can now be solved for u_3.

6.1.2 Example

As an example, the snag load will now be calculated for all duty points of the STS crane used in chapter 5. The electric motors operate at a nominal speed of approximately 1000 rpm when hoisting the maximum load on the ropes of 80 tons. At lower loads, the AC motors operate in field weakening range.

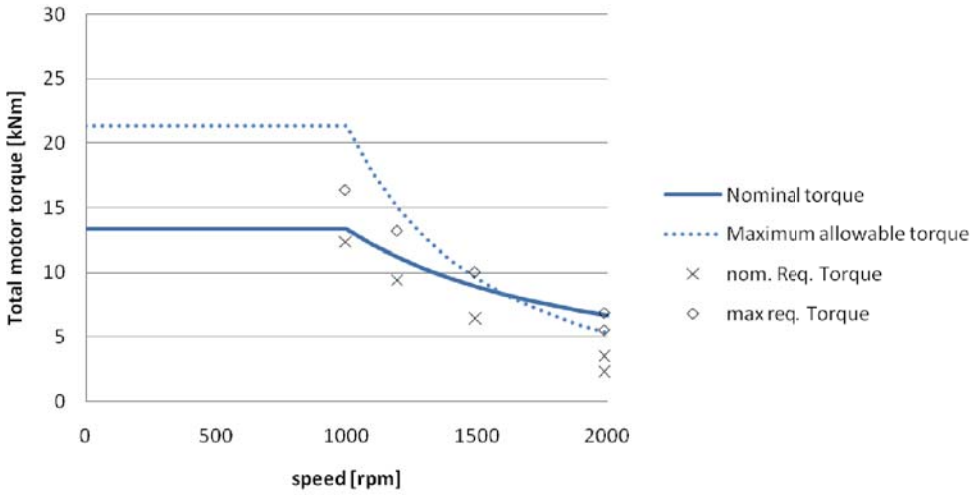

Figure 6.2: Duty points of the AC motors used in the MSC crane installed in Antwerp

Load on ropes [tons]	15	23	42	61	80
Load speed [m/s]	3.0	3.0	2.25	1.8	1.5
Total motor torque [kNm]	2.31	3.54	6.47	9.40	12.3
Motor speed [rpm]	1990	1990	1492	1194	995

Table 6.1: Duty points of the example crane

The results for this calculation can now be plotted for all duty points mentioned in Table 6.1 using either the load on the ropes (Figure 6.3) or the motor speed (Figure 6.4).

The resulting rope tension indicated in purple is built up from the three parts described in section 6.1.1:

- Static rope tension F_s (blue)
- Tension caused by motor reserve F_{mr} (red)
- Kinetic energy F_{kin} (green)

The most irregular behaviour of these three influences is seen at the tension added by the motor reserve. This is caused by the characteristics of the motor in combination with the rope tension monitoring, which result in a different motor reserve at the different duty points.

By using this type of graph, it can be seen that currently the kinetic energy has the most influence on the resulting snag load: up to 75% of the total load comes from the kinetic energy at maximum hoisting speed.

Another benefit of this type of graph is that it can quickly show at what duty point the snag load is the highest. For this particular example, the snag load is the highest at the maximum speed.

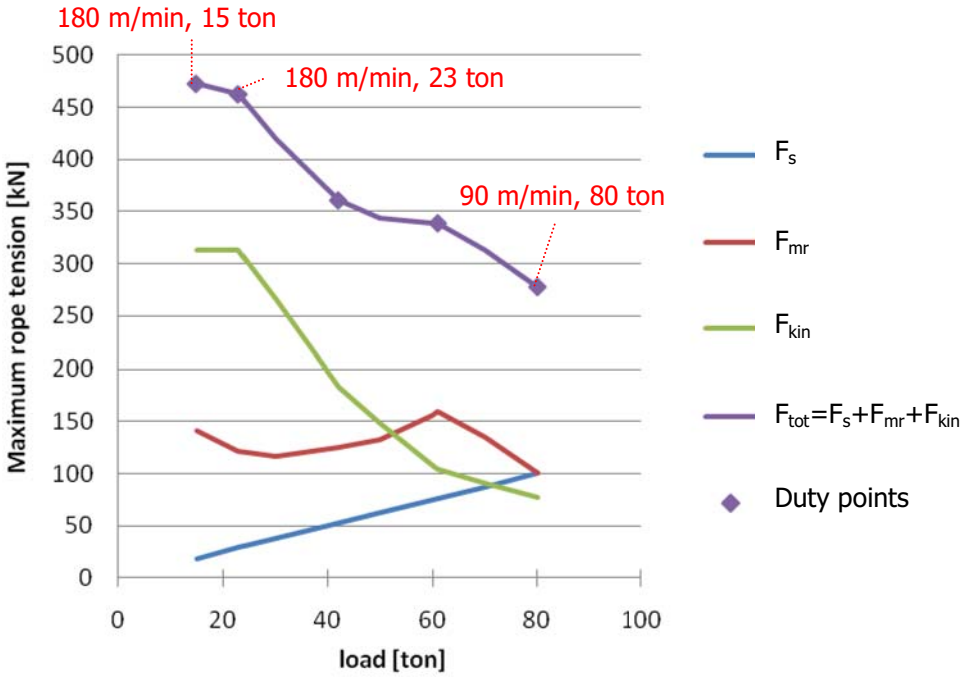

Figure 6.3: Results from simplified calculation of snag loads throughout the operating range of the electric motor

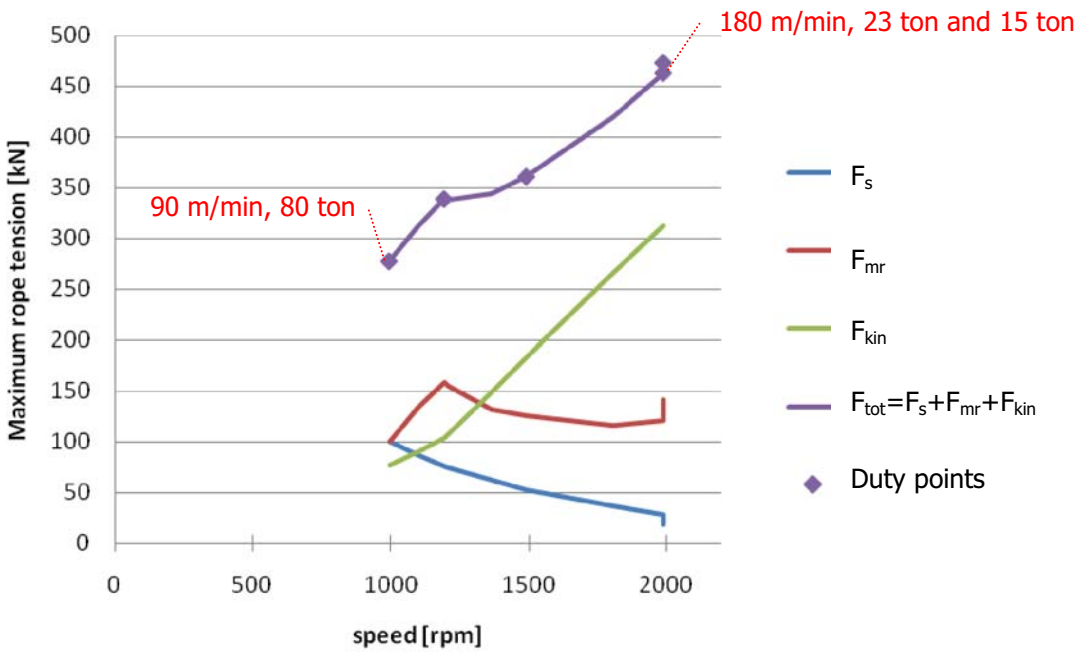

Figure 6.4: Results from simplified calculation of snag loads for all possible motor speeds

6.2 Simulink model

Matlab/Simulink is a tool for simulating dynamic systems. These systems can be a combination of different types of systems, like electronic, mechanical, thermal, etc.

6.2.1 Model description

The Simulink model simulates the hoisting winch as a rotating inertia on which several torques are applied, which vary throughout time:

- Rope (tension acting on the hoisting drum)
- Hoisting winch:
    - Electric motors
    - Operational brakes
    - Emergency brakes

By dividing the resulting torque with the inertia, the deceleration of the input shaft is calculated. By integrating the decelerations, the rotation of the input shaft can be determined. This rotation determines the elongation of the hoisting rope, through the gearbox and rope drum diameter.

The simulation starts at the moment that the load snags and the hoisting ropes start to stretch and ends when the hoisting winch has stopped. The model can be found in Appendix E, together with the code used to run the simulation.

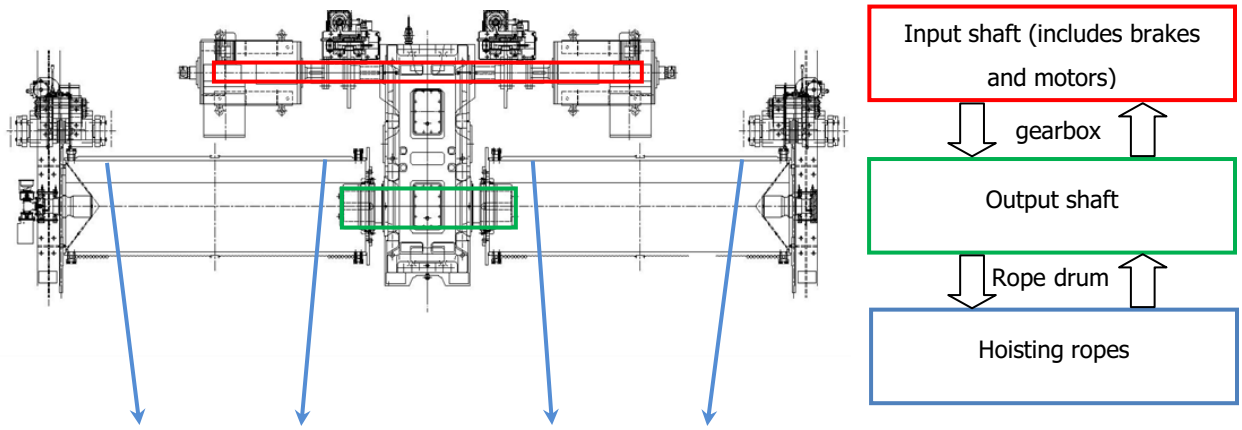

Figure 6.5: Layout of the Simulink model

6.2.2 Example

The same example is used as with the simplified calculation in 6.1.2, to show the possibilities of the simulation model.

A single simulation run will return a number of results, of which the most important ones are plotted in Figure 6.6, for a 2-rope snag on the example crane. The figure shows the following results through time:

- Rotational speed of the input shaft
- Rope elongation of the snagged ropes
- Rope tension of the snagged ropes
- Torque on the hoisting winch, exerted by the wire rope and by the driveline components

At t=0 the load snags and therefore the rope tension and motor torque start to rise. The speed of the motor remains constant, since the motor and rope are still in equilibrium. When the motor exceeds its limit, the motor is shut down, and the winch starts to slow down. When the delays of the PLC and brake controllers have passed, the brakes start to apply torque to the winch. Together with the tension of the rope on the drum, this stops the hoisting winch.

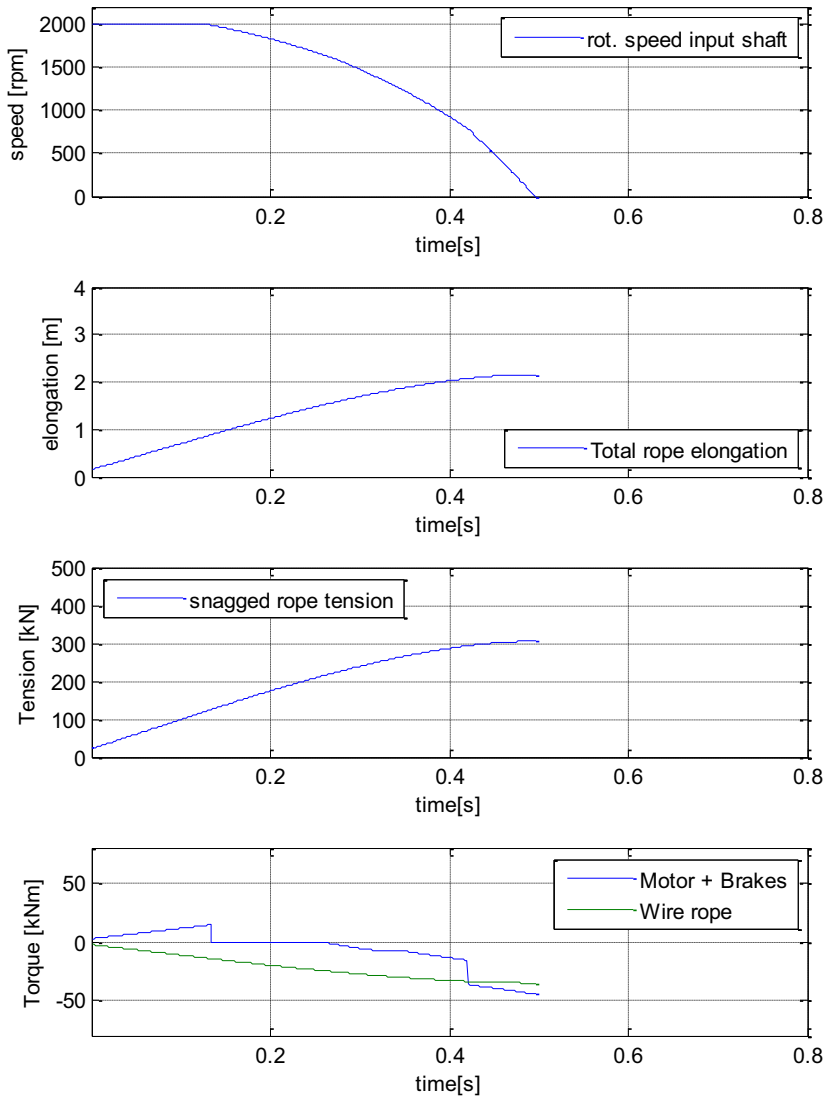

Figure 6.6: Example result of a single simulation run on a 2 rope snag

Another capability of the simulation model is that the loads on components of the winch during a snag can be calculated. This way all components can be checked on strength, to see if they aren't loaded over their maximum allowable load. In Figure 6.7, both the motor coupling on the input shaft and the output shaft of the gearbox are loaded beyond their limit.

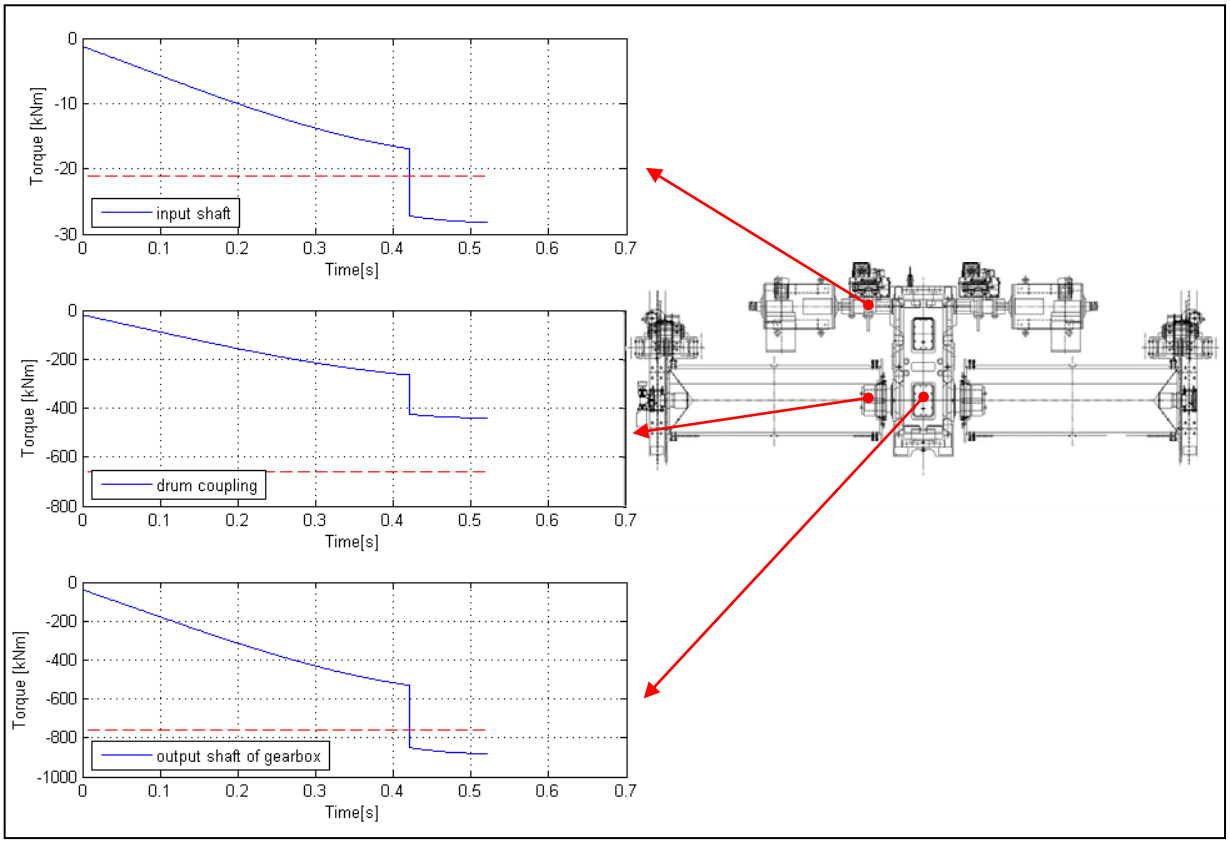

Figure 6.7: Development of the torque on several components of the winch, together with their maximum allowed load

The load and corresponding speed of the winch can be varied, to create a same type of result as in Figure 6.3. This will be used in the next section, to verify the calculation model.

Besides a more accurate result, the benefit of the simulation is that the influence of different design parameters can be analysed by performing a number of runs, varying a single design parameter. This way the simulation can be used as a design tool for snag loads on the hoisting winch (see chapter 8).

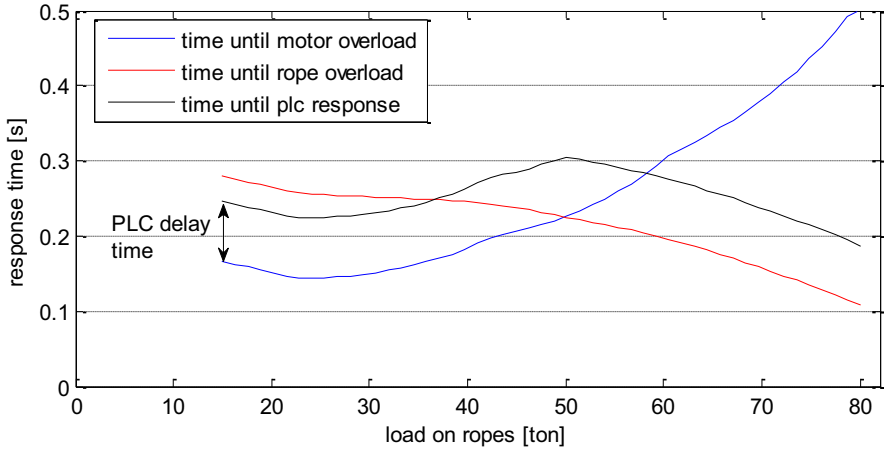

Figure 6.8: Time until PLC response, as a function of the overload times for rope and motor

6.3 Verification and validation

The simplified calculation can be used to verify the results of the simulation. Unfortunately, no measurements on snag loads are currently available for validation of the simulation results.

6.3.1 Verification

Verification is the check whether or not the model is implemented correctly, and no programming errors have been made. The verification is performed in two ways. The first is a comparison of a snag result from the simplified calculation with the simulation. The second method is to analyze the energy balance of the system.

6.3.1.1 Comparison with simplified calculation

For the example crane used previously in this chapter a simulation is run for all duty points, without the use of brakes or reversed motor torque. These results should match the results for the simplified calculation on the same crane, which were displayed in Figure 6.3.

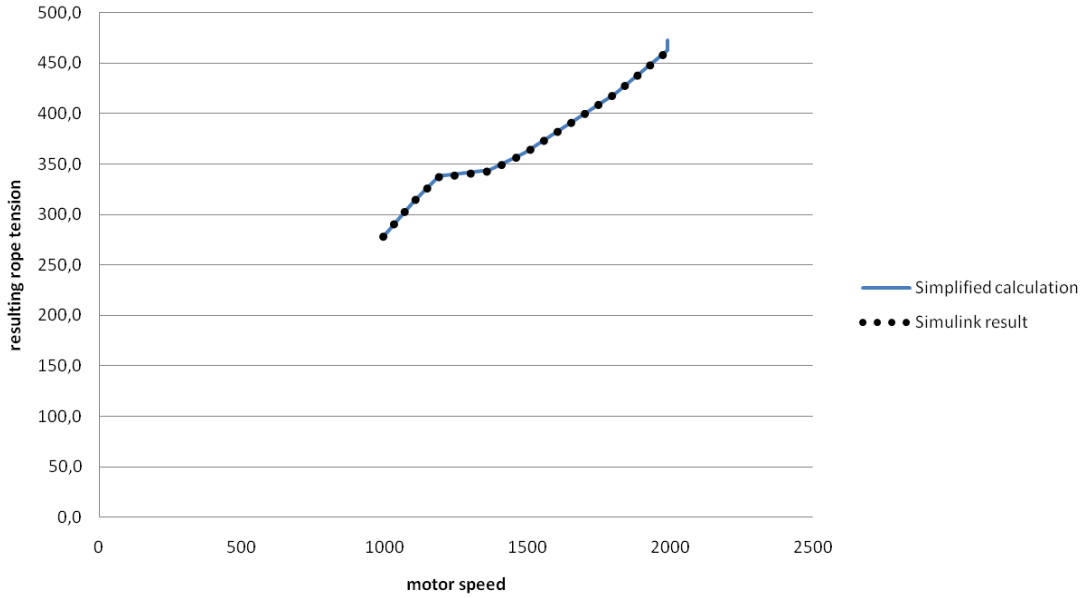

Figure 6.9: Simulation results for all duty points described in Table 6.1

Speed of input shaft [rpm]	995	1100	1194	1210	1367	1492	1807	1990	1990
Corresponding load [ton]	80	70	61	60	50	42	30	23	15
Simplified calculation [kN]	278.0	312.5	339.1	338.3	343.8	361.1	420.0	462.8	472.8
Simulation [kN]	277.6	312.3	338.6	337.6	343.1	360.3	419.0	461.6	471.6

Table 6.2: Comparison of the resulting rope tension for the simplified calculation and simulation, at all duty points

As can be seen in the table and figure above, the results match closely with a maximum difference of 0.3%. This small difference could lie in the numerical calculation of Simulink, or the improved accuracy of the data used.

6.3.1.2 Energy balance

Another method to verify the calculation is to see if no energy has disappeared in the system. This means the energy put into the system has to be equal to the energy going out of the system. The analysis is performed for the example shown in section 6.2.2, being a 2-rope snag of an empty spreader at 180 m/min.

$$E_{in} = E_{kin} + E_{motors} + E_{rope,static} \tag{6.9}$$

$$E_{in} = \frac{1}{2} \cdot J \cdot \omega_{input}^2 \tag{6.10}$$

$$+\sum_{t=0}^{t_{end}} T_{motor}\,[t] \cdot \left(\alpha_{input\ \ shaft}\,[t] - \alpha_{input\ \ shaft}\,[t-1]\right)$$

$$+4 \cdot \frac{1}{2} \cdot k_{rope}\ \cdot u_{rope\ ,static}^{2}$$

Source of energy	Energy [MJ]
Kinetic energy	1.47
Energy added by motors	0.29
Static rope elongation	0.0064
Total	**1.77**

Table 6.3: Energy present in the system before a snag

The main source of the energy is shown to be the kinetic energy present in the hoisting winch. The motors also add a significant amount of energy, even though they have little torque reserve at high speeds. For an empty spreader, the static rope elongation is negligible.

$$E_{out}\ = E_{pot\ ,snagged\ \ ropes}\ + E_{pot\ ,free\ ropes}\ + E_{pot\ ,crane}\ + E_{brakes} \tag{6.11}$$

$$\begin{aligned} E_{out}\ = {} & n_s \cdot \frac{1}{2} \cdot k_{rope}\ \cdot u_{rope}^{2} \\ & + n_f\ \cdot u_{rope}\ \cdot F_{rope\ ,static} \\ & + \frac{1}{2} \cdot k_{crane}\ \cdot u_{crane}^{2} \\ & + \sum_{t=0}^{t_{end}} T_{brake}\,[t] \cdot \left(\alpha_{input\ \ shaft}\,[t] - \alpha_{input\ \ shaft}\,[t-1]\right) \end{aligned} \tag{6.12}$$

Energy dissipated by	Energy [MJ]
Snagged rope elongation	0.95
Potential energy dissipated by free rope displacement	0.055
Crane deformation	0.0024
Energy dissipated due to braking	0.81
Total	**1.82**

Table 6.4: Distribution of energy after a snag

Most of the energy is dissipated in the form of rope elongation and the application of the brakes and reversed motor torque.

There is a small discrepancy between the energy before and after the snag of 3%. This error is acceptable; it can be explained by the numeric calculation of the energy shown in equations (6.10) and (6.12).

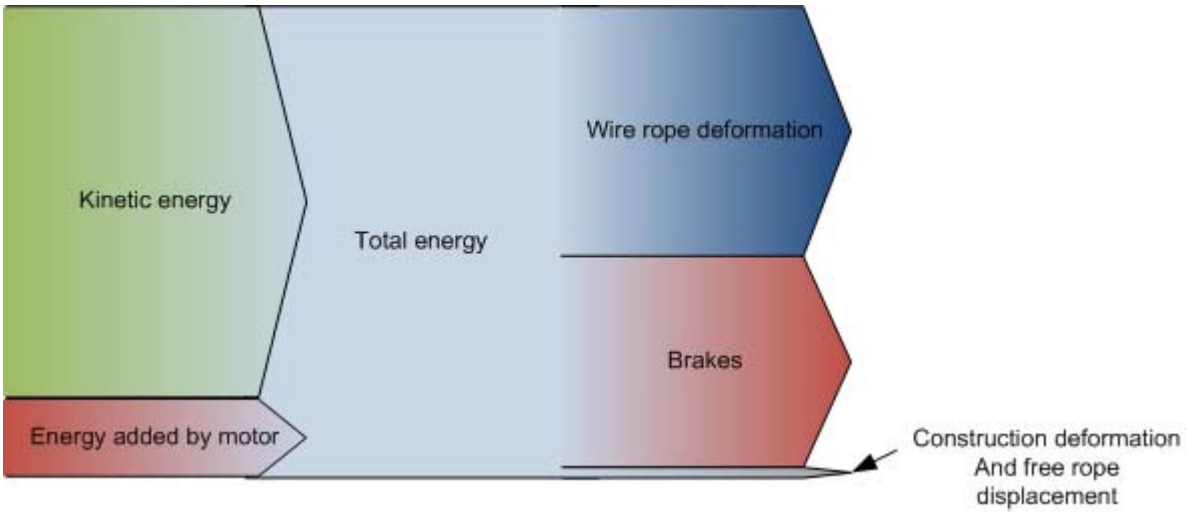

Figure 6.10: Sankey diagram illustrating the distribution of energy before and after a 2-rope snag at 180 m/min. Static rope elongation is too small to be visible

6.3.2 Validation

The validation of the model is the check whether or not the model behaves the same as the modelled crane behaves in the real world.

Unfortunately, there are currently no measurements available on snag loads, which can be used for validation. There are some measurements available on cranes, however these did not contain snag loads, or were of insufficient resolution to be of any use.

It is recommendable to perform measurements on an existing crane without an anti-snag device, to be able to validate the model. This would make the results of this study more convincing, especially to potential clients of Cargotec.

7. History and development of the STS Crane driveline

In this chapter a selection of cranes produced by Cargotec or one of its predecessors (Kalmar or Nelcon) will be evaluated using the simulation model described in the previous chapter. The cranes are selected throughout a range of different constructions, hoisting speeds and type of drives.
Using the results, an attempt will be made to see if there is a link between some of the variables and the resulting snag load.

7.1 Evaluated cranes

The table below lists the cranes that will be evaluated, together with a characteristic property of the crane, indicating the reason for its choice. Appendix F contains all the relevant data of these cranes.

	Name	Year of construction	Reason for selection of crane	Anti-snag
1	HNN	1989	High inertia DC driveline	No
2	Dubai	1995	Boom collapse caused by fatigue, initiated by snag	No
3	Ect-Home (North Side)	1997	Small crane, relatively long ropes	No
4	Noordnatie	1998	Siemens DC driveline	No
5	RST	1998	Machinery on trolley, Johnny walker rope reeving	No
6	Le Havre	2000	120 m/min Lattice girder crane	No
7	Eurogate	2003	Machinery on trolley	Yes
8	HNN MSC	2007	180 m/min double box girder, Heavy AC driveline	Yes
9	Finnsteve	2008	150 m/min double box girder	Yes
10	Evyap	2010	Recent Monobox crane	No
11	SPRC	2011	Large Monobox crane, high inertia AC driveline	yes

Table 7.1: Cranes selected for evaluation

The response times of the control system are considered to be the same for all cranes, because it is hard to retrieve this data. This assumption is unlikely, since the computational power of electronic systems was significantly lower two decades ago than it is nowadays; however the assumption had to be made due to time constraints of the thesis.
All results are calculated as if there is no anti-snag system installed on the cranes. A number of these cranes do have an anti-snag system installed, as can be seen in Table 7.1.

Remark on RST

The RST crane has a Johnny-Walker rope reeving system. This reeving system consists of 8 rope falls, just as the normal reeving system. The difference is the configuration of this falls, as is shown in Figure 7.1. This configuration reduces the sway of the load, allowing for easier positioning. Unlike the regular wire rope reeving, all hoisting ropes are connected to the rope drums. The wire rope speed is therefore equal to the hoisting speed, when neglecting the effects of the angle of the hoisting rope to the vertical.

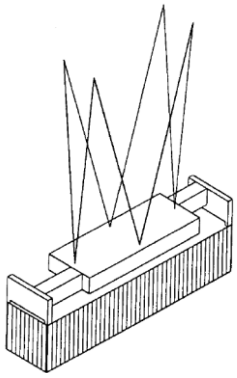

Figure 7.1: Johnny Walker wire rope reeving [7]

7.2 Results

For all cranes described in the previous paragraph, the results have been calculated.

As a comparison: During normal operation, the rope tension in a STS crane is equal to approximately 100 kN per rope, when hoisting a 80 ton load. During design, an extreme rope tension between 200 and 250 kN is used.

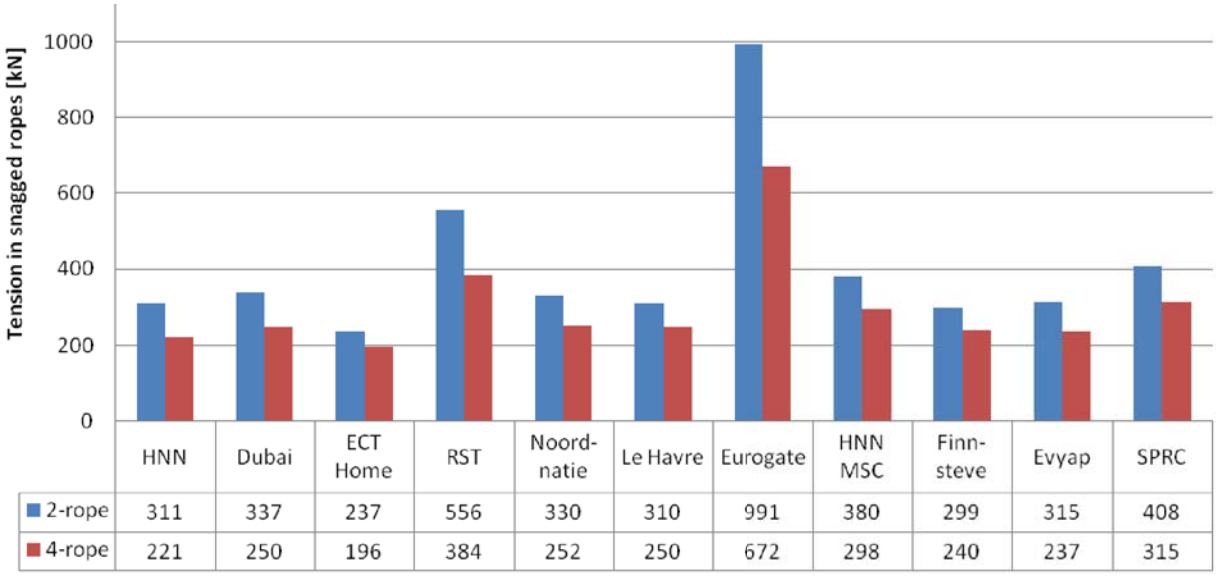

	HNN	Dubai	ECT Home	RST	Noord-natie	Le Havre	Eurogate	HNN MSC	Finn-steve	Evyap	SPRC
2-rope	311	337	237	556	330	310	991	380	299	315	408
4-rope	221	250	196	384	252	250	672	298	240	237	315

Figure 7.2: Results from the Simulink simulation for a 2 rope snag

7.2.1 General observations

Most of the cranes exceed the rope tension which was considered the extreme rope tension during the design of the crane. Some of the cranes have an anti-snag system installed to prevent the crane from reaching this rope tension during a snag. However, some cranes without an anti-snag system also exceed a rope tension of 250 kN in the simulation results, while no damage due to snag has occurred. This could be explained by a number of reasons:

- The extreme rope tension of 250 kN was not normative for the design
- The components are stronger than they were calculated at, due to safety factors
- Some plastic deformation occurs, but not enough to result in visual damage

7.2.2 Reeve-through vs. Machinery on trolley

When evaluating the results shown in Figure 7.2, the resulting rope tension from the machinery trolleys stands out. This is caused by the very short hoisting ropes of these systems, which lead to a high stiffness of these ropes.

For all reeve-through trolley cranes, the resulting rope tension varies between approximately 200 kN and 400 kN.

7.2.3 2-rope snag vs. 4-rope snag

As expected, the resulting rope tension for a 4-rope snag is lower than the rope tension for a 2-rope snag. To check if there is a correlation between these two types of snag, the ratio between the resulting rope tensions is calculated.

The average ratio between these types of snag is 0.75, with a standard deviation of 0.05.

This ratio can be explained by performing a simplified calculation of the snag, where only the hoisting ropes absorb the kinetic energy of the motor:

$$\frac{1}{2}k \cdot u^2 \cdot n_s = E_{kin} \tag{7.1}$$

$$u = \sqrt{\frac{2 \cdot E_{kin}}{n_s \cdot k_{rope}}} \tag{7.2}$$

For a 4-rope snag and a 2-rope snag, the kinetic energy and the rope stiffness are equal. The only difference is the number of snagged ropes: n_s.

$$\frac{u_{4-rope}}{u_{2-rope}} = \frac{\sqrt{\frac{2 \cdot E_{kin}}{4 \cdot k_{rope}}}}{\sqrt{\frac{2 \cdot E_{kin}}{2 \cdot k_{rope}}}} = \sqrt{\frac{1}{2}} \approx 0.71 \tag{7.3}$$

The variation of the value of this ratio can be explained by the free rope tension, which absorbs some of the energy. Another explanation is the variations in winch design, like the installation of larger emergency brakes.

7.2.4 Different hoisting speeds

Most new cranes have an empty spreader hoisting speed of 120, 150 or 180 m/min. It is interesting to compare the results for these speeds.

By evaluating the results of Evyap, Finnsteve and HNN MSC, the influence of different load speeds can be checked, since the cranes have been constructed throughout the last 4 years, and therefore have a similar state of technology of the drives.

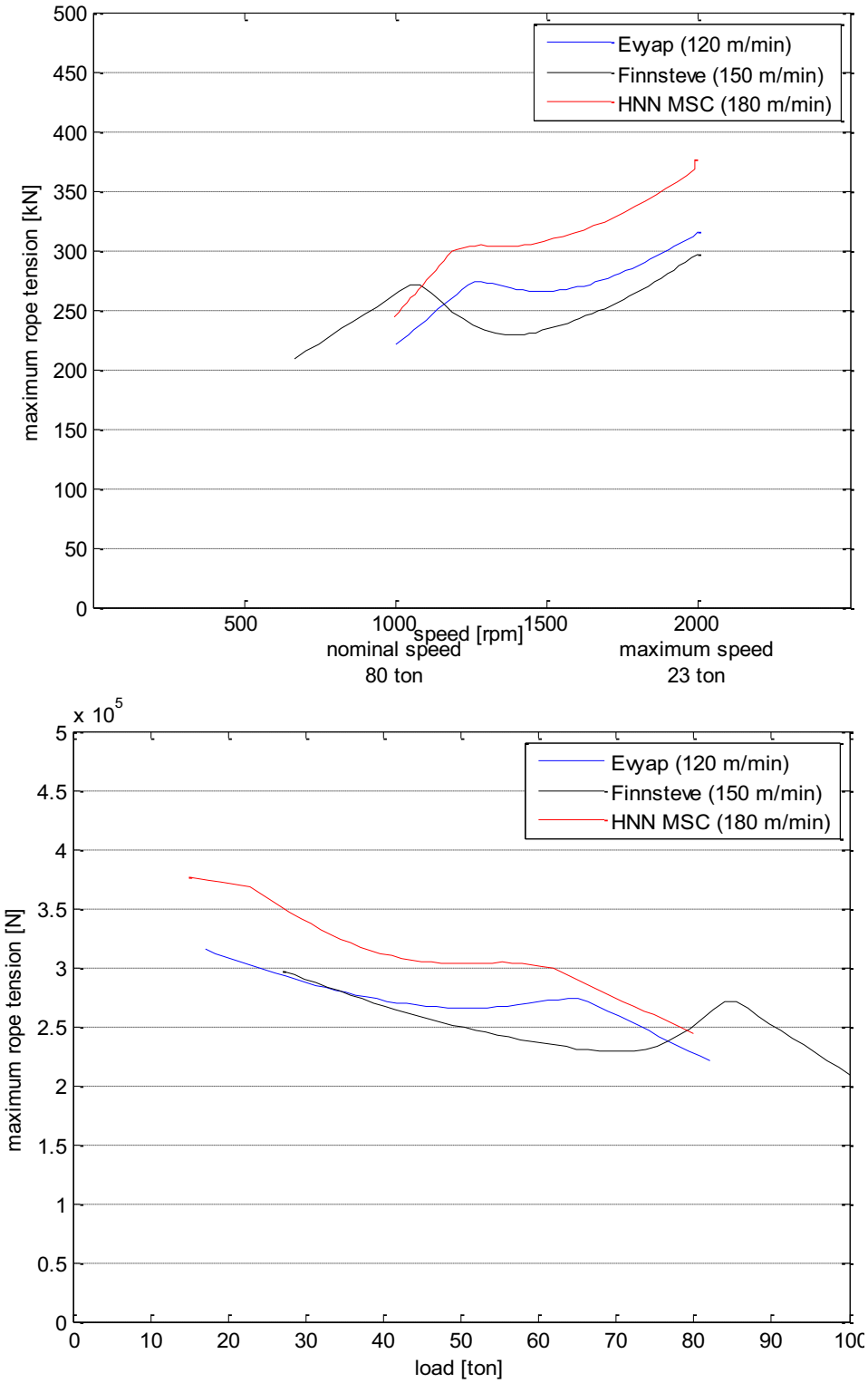

Figure 7.3: Results for three existing STS cranes with a different maximum hoisting speed for a 2-rope snag

All electric motors are operated up to a speed of 2000 rpm. However, the power and therefore the size of the motors increase with increasing hoisting speeds. This speed is acquired by the selection of the gearbox ratio and rope drum diameter.

The results show that the snag load does not correspond directly to the hoisting speed, because of other influencing factors:

- **Rope stiffness:** Finnsteve and HNN have a wire rope reeving as shown in Figure 3.3, while the Evyap wire ropes from Evyap are much shorter, since this crane uses a reeving as shown in Figure 3.2. Therefore the ropes from Evyap have a higher stiffness, causing a higher snag load.
- **Maximum load:** Finnsteve is able to lift a 100 ton load vs. a maximum of 80 tons of Evyap and HNN. This higher maximum load causes the load limit to be higher as well. Therefore it takes a longer time for the monitoring system to reach the tension limit at high speeds.
- **Emergency brakes:** Evyap has no emergency brakes installed, resulting in a smaller braking torque when the emergency stop is initiated.

It is remarkable to see that the resulting snag load for Finnsteve is smaller than that of Evyap, while Finnsteve has an anti-snag system installed to reduce the snag loads and Evyap has not. The local maximum of the snag load at speeds around 1100 rpm is determined by the monitoring system.

7.2.5 Relations between parameters and resulting snag load

To try and find a relation between the snag load and some design parameters, the snag load is plotted versus these parameters. Unfortunately no direct correlation between a single parameter and the snag load is found. A general trend can be expected from the figures, but there is a lot of variation in the results.

It can be concluded from these results that the snag load is dependent on a variety of design parameters, not just a single one. Also the design parameters are related. For example with a high empty spreader hoist speed, the installed hoisting power will also be higher. This usually leads to a higher inertia of the hoisting winch.

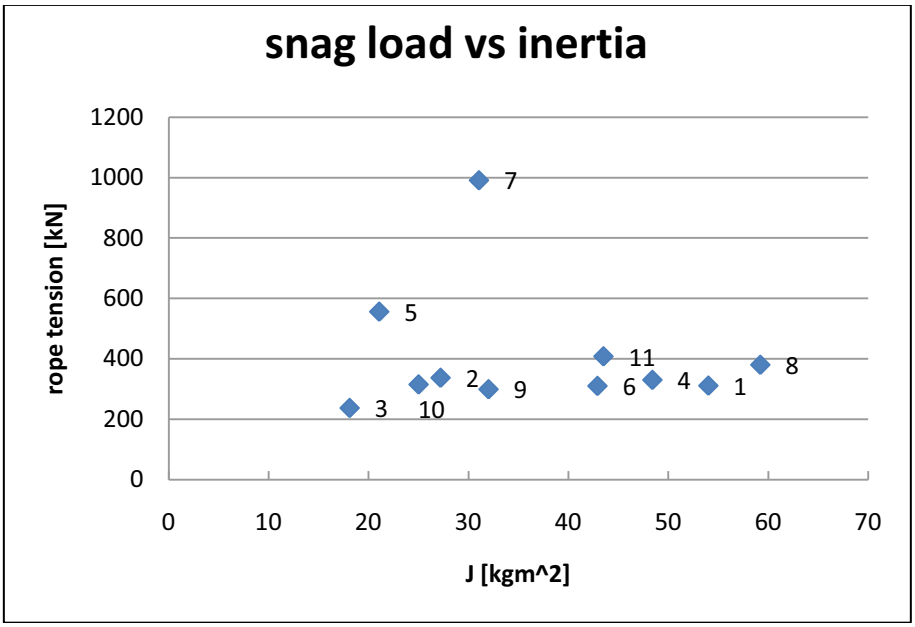

Figure 7.4: Relation between the inertia of the hoisting winch and the resulting snag load of a 2-rope snag. Only reeve through trolleys are used in analysis

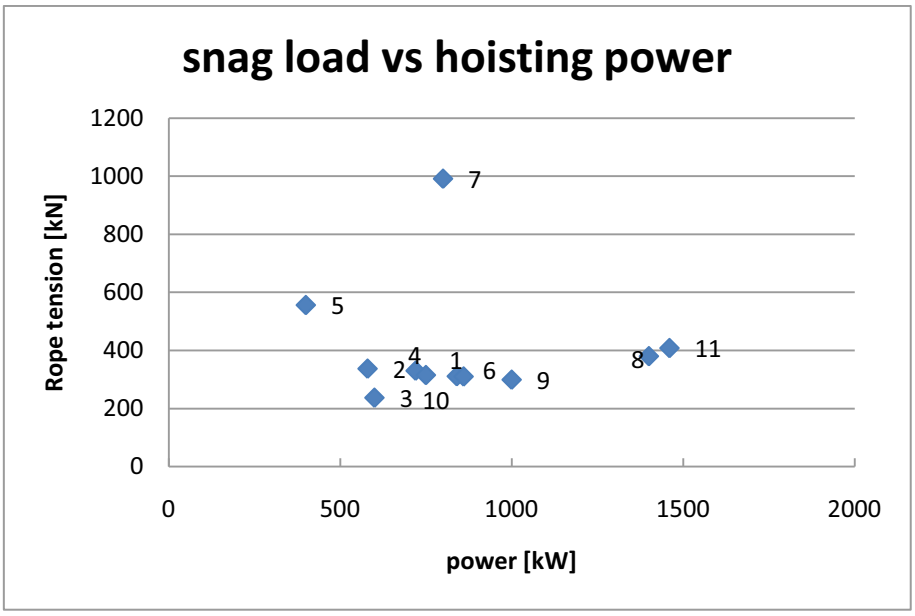

Figure 7.5: Relation between the hoisting power of the winch and the resulting snag load of a 2-rope snag. Only reeve through trolleys are used in analysis

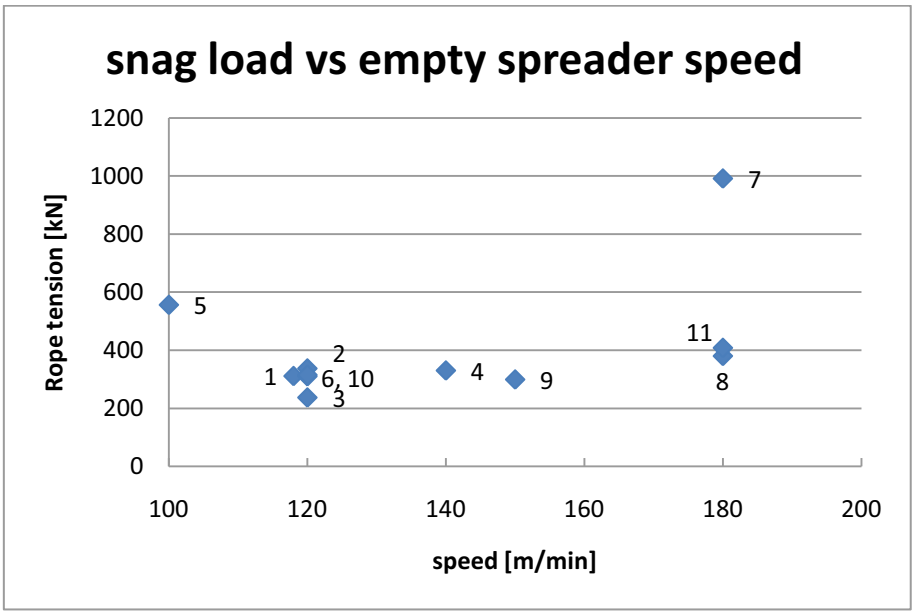

Figure 7.6: Relation between the empty spreader hoisting speed and the resulting snag load of a 2-rope snag. Only reeve through trolleys are used in analysis

7.2.6 Possibility of operating with a snag protection device

In an attempt to simplify the choice for a snag protection device, the results calculated in this chapter are plotted as a function of rope length and empty spreader hoisting speed.

Figure 7.7 gives an indication on the possibility of operating without an anti-snag device. The colours indicate if it is possible to operate without an anti-snag device. There is a large yellow area, where the choice is not clear. In this area the other variables, like the inertia of the winch, play a role.

The individual resultss from this chapter have a colour, based on their snag load:

- < 300 kN = green
- 300-400 kN = yellow
- > 400 kN = red

These values are based on the improvements and the load limits calculated in chapter 8 and 9 of this thesis.

The figure indicates for example that machinery trolleys, which typically have rope lengths around 40 m, are not possible to have hoisting speeds over 100 m/min, without requiring a snag device.

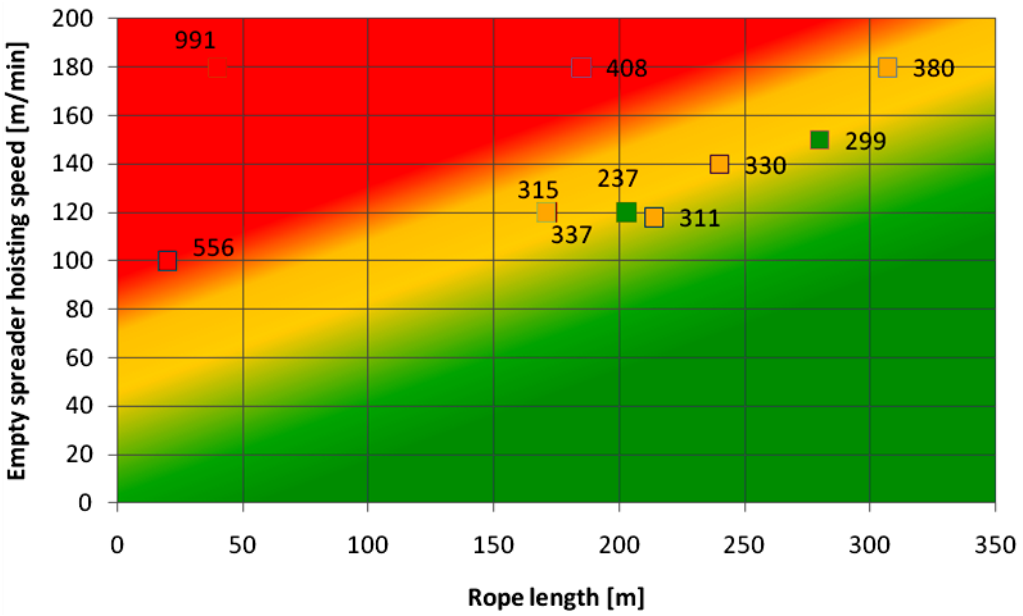

Figure 7.7: Chart to indicate if it is possible to operate without an anti-snag device. Red = snag device required, Green = no snag device required

7.3 Conclusions

In this chapter the snag loads of 11 cranes were evaluated using the simulation model. Due to a high number of influencing factors, no direct correlation between the snag load and a single parameter can be found. When analyzing the dependence of the snag load on a single parameter, a lot of variance if found in the results, which is caused by the other parameters.

8. Design improvements to reduce snag loads

Adjustments of the hoisting winch will now be examined using the Simulink model, to check the possibilities for reducing snag loads within the current hoisting winch configuration.
Each possible improvement will be investigated separately, comparing its influence to the standard configuration. All values and results mentioned in this chapter are obtained from the example crane used in previous chapters, unless mentioned otherwise.
The following design parameters will be evaluated:

- Monitoring method
- Selection of electric motors
- Winch inertia
- Braking response time
- Braking power
- Wire rope stiffness

8.1 Monitoring method

As was described in paragraph 3.2, the load is currently being monitored by means of rope tension. An emergency stop can also be initiated when the AC drive is overloaded.
Improvements of the monitoring method allow the control system to detect a snag earlier, reducing the snag loads. The challenge for the monitoring method lies in the fact that the system should not create false alarms, while still being able to detect all the snags in time.
Possible improvements on the monitoring method are:

- Reduce time delay of monitoring electronics
- Different monitoring methods
    - Rope tension monitoring
        - Variable tension limit
        - Derivative of rope tension to time
    - Accelerations of headblock
    - Rotations of headblock
    - Position of headblock compared to desired position
    - Derivative of the motor current to time

Headblock position, rotation or acceleration measurements are very hard to perform, due to the bumping and movements of the spreader during normal operations.
The motor current signal has a lot of noise. The derivative of this signal is therefore very irregular, and would result in a lot of false snag alarms.

8.1.1 Time delay of monitoring electronics

When a snag is detected by the monitoring system, it will send a signal to the PLC. The PLC will then go through its cycle, after which it will decide to initiate an emergency stop.

PLC response time

By improving the response time of the PLC, the response time of the total monitoring system can be reduced, therefore reducing the snag load, as can be seen in Figure 8.1. The current PLC has a response time of 0.08 s.

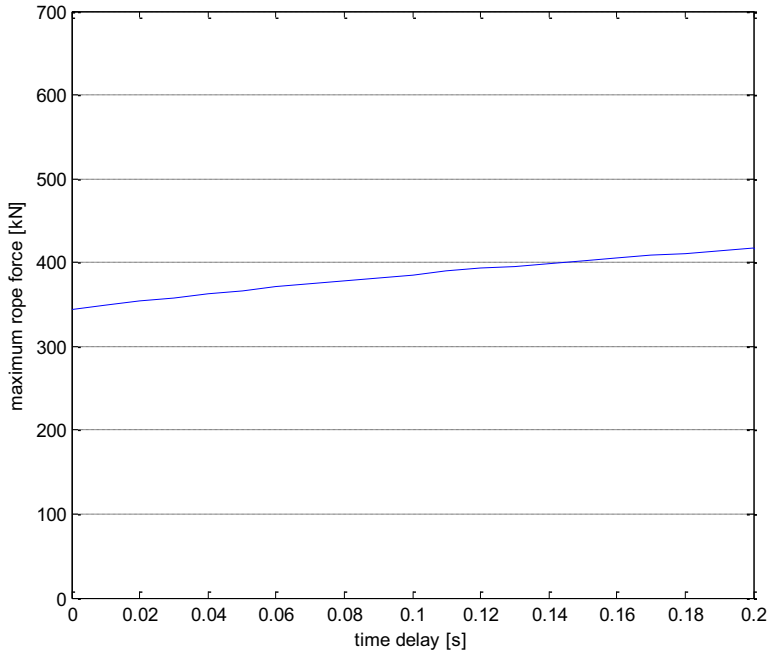

Figure 8.1: Influence on the resulting snag load of a 2-rope snag by varying the plc response time

The monitoring system that is currently in use has the possibility to send signals to the appropriate controllers, bypassing the PLC. By bypassing the PLC, the delay time of snag detection by the ropes can be reduced by 0.08 s.

Location of the load cells

To reduce the effect of the delay caused by the tension wave described in section 5.3.1.3, it would be beneficial to measure the rope tension close to the spreader to minimize the travel time of the tension wave. Several locations would be possible:

- Twistlocks of the spreader
- Headblock rope sheaves
- Trolley: hoisting rope sheave
- Rope sheaves at the backreach

Currently the rope tension is monitored using load shafts in the rope sheaves at the backreach. This position is the furthest away from the origin of the tension wave, being the headblock/spreader. This leads to a delay time due to the tension wave propagation speed of 0.05 seconds, as was calculated in section 5.3.1.3.

Load monitoring in the twistlocks does not detect snags with an empty spreader and is therefore not recommended.

Load monitoring in the trolley or the headblock rope sheaves is possible, however this would require transformation of the weak load cell signals, which introduces a new delay to the system. Besides this

delay, additional noise could be added due to interference of power cables running through the crane. Because of these disadvantages, its recommendable to maintain the rope tension monitoring position and accept the delay of 0.05 s. This delay time will be taken into account in the calculations.

8.1.2 Normal variations in rope tension

In 2007, Kalmar performed measurements for a period of 3 days on a crane similar to the HNN MSC crane, to determine the maximum load factor of that crane. The load factor is the difference between the average load and the maximum load, during a single lift. The load factor had an average of 1.22 and a maximum value of 1.53.

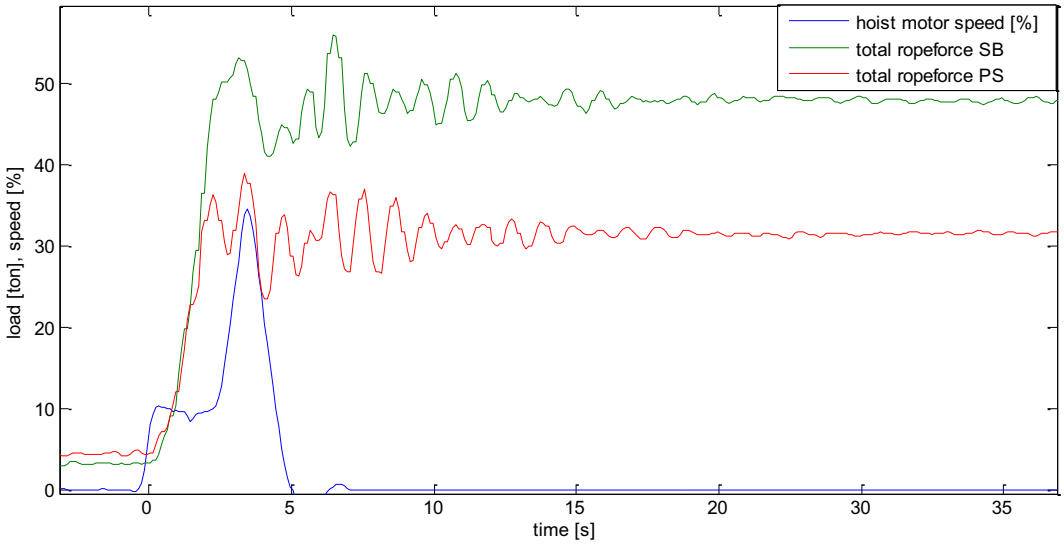

Figure 8.2: Normal tension variation during the start of a hoist operation on an eccentric load

Figure 8.2 contains a very small section of these measurements, showing the natural variation of the rope forces during the pickup of a load. Starting at t=0, a creep speed of 10% of the maximum speed is initiated, to lift up the container. After 2 seconds, the load is approximately estimated, full hoisting speed is enabled. The total rope force of the port side and starboard differ because of an eccentric load.

8.1.3 Variable tension limit

Operating principle

Currently the rope tension limit does not depend on the load that is being hoisted. This is disadvantageous to the snag load, since the maximum snag loads occur at high speeds, while only hoisting a small load. The load limit however is determined at a value defined by the maximum allowable hoisted load. As a result, it will take a relatively long time for the total rope load to exceed the load limit.

A method to shorten the time it takes to reach a tension limit is to implement a variable tension limit. This tension limit is set at a certain margin over the current rope tension:

$$variable\ tension\ limit = overload\ factor \cdot static\ rope\ tension \tag{8.1}$$

This could even be implemented as setting a different tension limit for all four hoisting ropes, to account for eccentric loading of the container.

The static rope tension is determined during the start of a hoist operation, when the crane is operating at creep speed. This creep speed is already being used currently to determine the mass of the container being lifted, which is required to calculate the maximum allowed speed. This method of lifting is also beneficial for the crane loads, since it reduces the impact of the loading on the crane, which is expressed in the dynamic factor used in calculating design loads on the crane. (i.e. see FEM1.001, booklet 9.3)

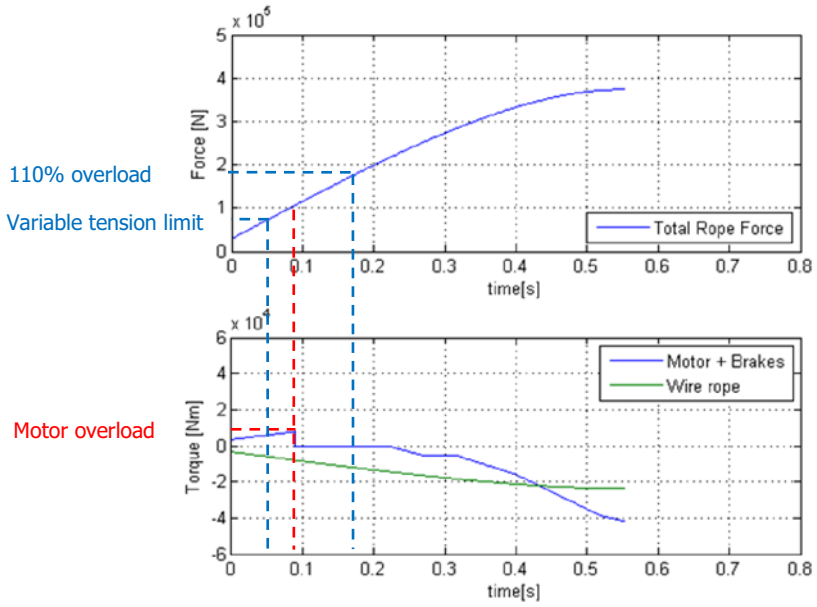

Figure 8.3: Implementation of a variable load limit of two times the static rope tension

Value of the overload factor

To prevent the monitoring system from creating false alarms, the overload factor has to be higher than the normal variation in rope tension that occurs during hoisting. This factor was determined at 1.53 in paragraph 8.1.2. However, from literature a value of 1.25 is recommended [6]. The exact value of this overload factor will have to be determined in practice, since it might be possible that the variations are even larger, but did not occur during the measurements.

For now, a value of 1.53 is used as the overload factor.

8.1.4 Tension variation through time

8.1.4.1 Operating principle

The tension variation through time can be calculated by dividing the difference of the last two samples by the sample time:

$$\frac{\Delta T}{\Delta t} = \frac{T[n] - T[n-1]}{sample\ time} \tag{8.2}$$

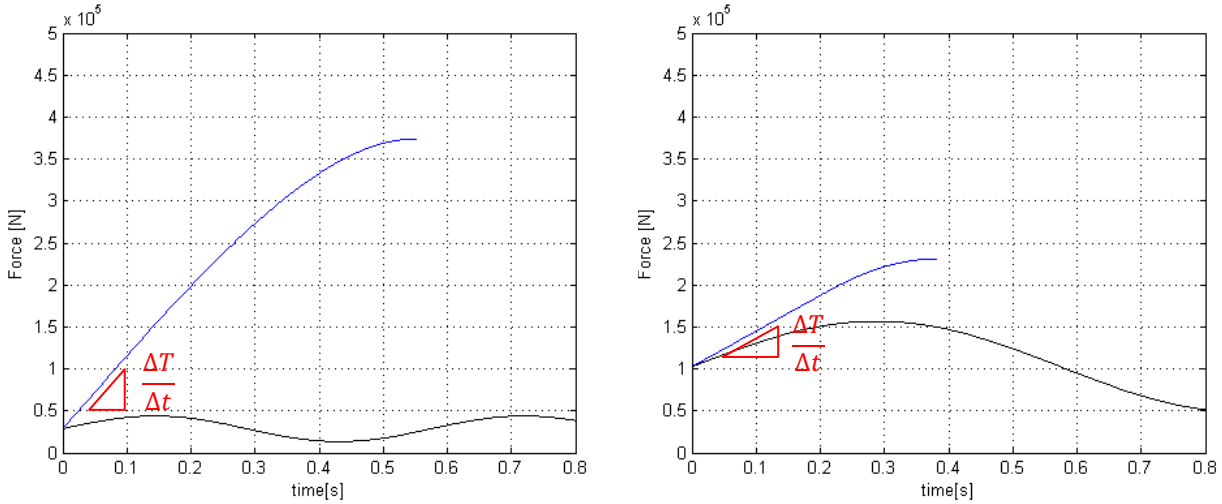

Figure 8.4: Rope tension vs. time of a 180 m/min (left) and a 90 m/min (right) snag. The black line indicates the natural vibration of the hoisting rope

During a snag, the increase in rope tension is equal to:

$$\frac{\Delta T}{\Delta t} = v_{rope} \cdot k_{rope} \tag{8.3}$$

This results in an increase in rope tension of approximately 450 kN/s for a 90 m/min snag and 900 kN/s for a 180 m/min snag.

8.1.4.2 Natural vibration of the load

This increase will have to be larger than the increase which occurs due to natural vibrations of the load. The speed of increase due to natural vibrations can be determined using the eigenfrequency of the load.

The eigenfrequency can be calculated using:

$$\omega_n \left[{}^{rad}/_{s} \right] = \sqrt{\frac{k}{m}} \tag{8.4}$$

$$k = 4 \cdot \frac{4EA}{L} = 1600 \frac{kN}{m} \tag{8.5}$$

Using above equation, a 62 ton load results in an eigenfrequency of 0.99 Hz. The measurements described in section 8.1.3 can be used for verifying this result: the frequency of the vibration of a 62 ton load can be determined at approximately 1 Hz.

The measurements also showed a maximum load variation of 1.53 x static load.

From these results, the maximum increase of rope tension during normal hoist operation can be determined at:

$$T_{rope} = T_{static} \cdot (1 + 0.53 \cdot \sin(2\pi \cdot \omega_n \cdot t)) \tag{8.6}$$

$$\frac{\Delta T}{\Delta t} = 2\pi \cdot \omega_n \cdot T_{static} \cdot 0.53 \cdot \cos(2\pi \cdot \omega_n \cdot t) \tag{8.7}$$

$$\max\left(\frac{\Delta T}{\Delta t}\right) = 2\pi \cdot \omega_n \cdot T_{static} \cdot 0.53 \tag{8.8}$$

load	Tension increase at snag	Tension increase due to vibrations	ratio
82 ton at 90 m/min	450	294	1.5
17 ton at 180 m/min	900	134	6.7

Table 8.1: Comparison of tension increase due to snag and due to natural vibrations

At low speeds, the difference between natural variation of the rope tension and tension increase due to snag is small, as is shown in Table 8.1. Added to that is the effect of eccentric loading of the container, which could lead to a higher static rope tension and therefore a larger variation in tension due to the vibrations.

The tension variation monitoring should therefore only be implemented at high speeds.

8.1.4.3 Sampling frequency and noise

It will be important for the monitoring system to have a high sampling frequency, to assure a short response time. However, when the sampling frequency is increased, the noise will increase as well. The measurements mentioned earlier in this paragraph were performed with a 100 Hz frequency, thus implying a 0.01 s cycle time.

The noise on the load cell signal needs to be low, especially at high sampling frequencies, to prevent false alarms of the monitoring system. If the noise of the load cell is too high, filters will have to be applied, which will increase the response time of the system.

From experiences by Cargotec, a similar system proved to be very hard to implement, due to a high number of false alarms by the system. Still the method will be taken into account, to see if the improvement might be big enough to justify the work required to tune the system.

To model this type of monitoring in the simulation, the same method as described in paragraph 8.1.3 will be used. As an estimate, the overload factor will be set at 1.01, and an extra time delay of 3 cycle times (0.03 seconds) will be added to the time delay of the monitoring system.

8.1.5 Results

When implementing the improvements in rope tension monitoring in the simulation, the following results are obtained:

Values in [kN]	Static load limit	Variable limit	Tension variation monitoring
With PLC	381	369	375
Bypassing PLC	381	**335**	342

Table 8.2: Rope tension for a 2-rope snag on the SPRC crane for different monitoring improvements

The bypass of the plc only has use when some sort of load dependent rope tension monitoring is used. When only the static limit is monitored, the winch is too slow to respond in time, as the winch is only stopped by the tension of the ropes.

The variable limit and the tension variation monitoring have a similar improvement. The values of the parameters used by such a tension monitoring method are still unknown, and have to be determined in practice.

Because the tension variation monitoring system isn't significantly better than the variable limit method, the variable limit method, together with bypass of the PLC, will be the recommended improvement to the rope tension monitoring.

8.2 Selection of electric motors

8.2.1 3-phase asynchronous motor with variable speed drive

In this paragraph the current 6-pole AC motor is compared with two other AC motors:

- 6-pole motor with high overload factor
- 4-pole motor with high overload factor

8.2.1.1 Overloading 6-pole motor

Because of technological advances, it is possible to overload AC-motors to a higher level compared to the motors used in STS cranes of the past decades. This way, smaller motors can be used in the hoist drive, while still being able to produce the same amount of torque and power required for hoisting. This results in a lower motor inertia on the input shaft.

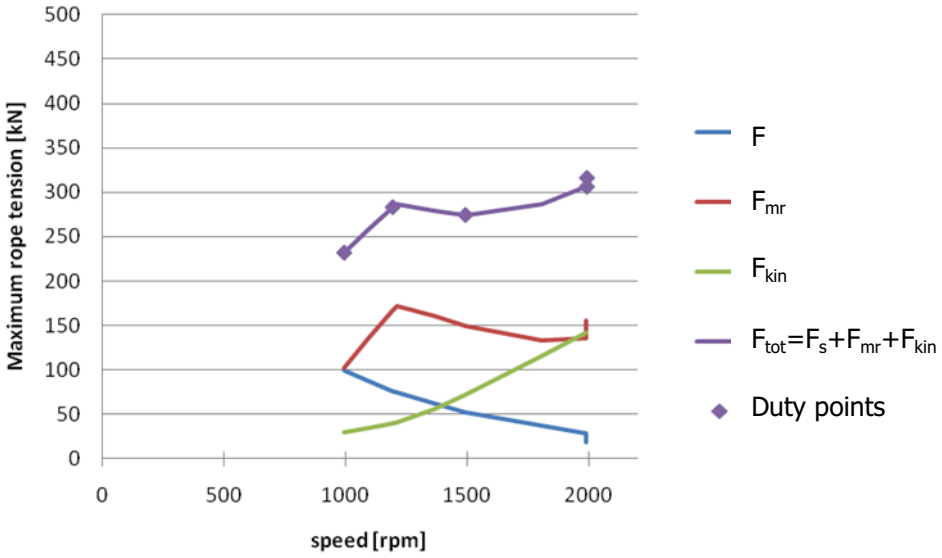

Figure 8.5: Resulting snag load for the simplified calculation of a 2 rope snag using overloaded 6-pole motors

8.2.1.2 4-pole AC motor

For selection of the 6-pole motors used currently in the STS cranes, the duty point at the highest speed is governing for the motor selection, due to the scaling of the maximum allowable torque. By selecting a 4-pole a smaller motor can be used, while maintaining the same duty points. The size of the 4-pole motor is usually determined by the duty point at nominal speed, as shown in Figure 8.10.

A disadvantage of the 4-pole motor is that it has a large torque reserve at the highest speeds. Therefore the motor will be able to increase torque for a longer period of time before the maximum allowable torque will reached.

These influences can be clearly seen when comparing Figure 8.6 with Figure 6.4. Figure 8.6 shows a higher tension added by the motors. A benefit of this larger torque reserve is that the torque can be used for braking when the snag has been detected. Better snag detection will be required at high speeds, which will prevent the motor from stretching the rope too far due to its large torque reserve.

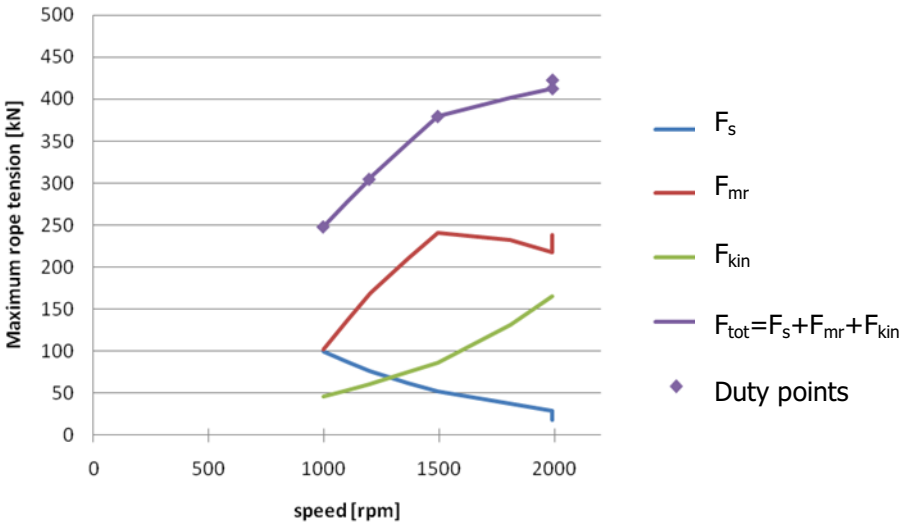

Figure 8.6: Resulting snag load for the simplified calculation of a 2 rope snag using 4-pole motors

8.2.2 AC Synchronous motor

The difference between the asynchronous and synchronous AC motor is the way the magnetic field in the rotor is generated. The rotor of the synchronous motor has a permanent magnet, or its own power supply to generate a magnetic field. Therefore it does not require slip to generate torque, and runs synchronous with the speed of the stator field.

These types of motors can produce high torques at very low speeds. Because of the low speeds, a low amount of kinetic energy is present in the system, which will be beneficial for a snag situation.

In some cases the low speed allows for direct drive: a direct coupling between the motor and rope drum without a gearbox. By using variable frequency drives, the motor speed can be adjusted to the demands from the driver.

An example of a synchronous motor as a hoist drive can be found in a walking dragline powered by Siemens motors, which is shown in Figure 8.7. This motor delivers a power of 9600 kW at speeds below 35 rpm, with the stator containing 36 poles. Because of the elimination of the gearbox together with the extra shaft and bearing, efficiency of the total driveline was improved from 74% for the old DC motor system to 89% to this AC synchronous system [27]. Even though this motor has much more power than required for an STS crane, it does prove that the concept is viable.

Figure 8.7 (left and center): AC synchronous motor installed in a walking dragline
Figure 8.8 (right): Section of the hoisting winch of the king post crane

Another example of this motor type is the main hoist of a king post crane developed by National Oilwell Varco. It consists of a low speed AC synchronous motor installed inside the rope drum. It is connected to the rope drum through a planetary gearbox. [28]

Summarizing, the following advantages and disadvantages can be listed, compared to the current winch configuration:

Advantages:

- Reduced snag load due to lower speeds
- Fewer rotating components (no gearbox and high speed shaft, motor couplings etc)
- More accurate control

Disadvantages:

- Price (4 or 5x normal AC motor price)
- Larger dimensions
- Higher weight

Due to the high price, the large dimensions and the high mass of this motor, it will not be taken into consideration. It will be too hard to implement in the current configuration of STS cranes. It is not in the scope of this research to completely redesign the hoisting system.

8.2.3 DC Motor

DC motors were the standard drive for hoist winches up to 10 years ago. The last ten years however, they were overtaken by the AC motor, which is more robust and has a better power factor. However, it is still interesting to see what the influence of a DC motor is on the snag load.

The DC motor characteristics resemble those of the AC motor, with one important difference. In the field weakening range the maximum allowable torque scales by constant power: T*n=constant. Therefore the DC motor will have a larger torque reserve at high speeds compared to the AC motor.

The inertia of the current DC motors, like those from Siemens and ABB, is found to be higher than the currently used AC motors from Wölffer.

The DC motors will not be investigated any further, because of this disadvantage in combination with other reasons to pick AC motors over DC, mentioned at the start of this section.

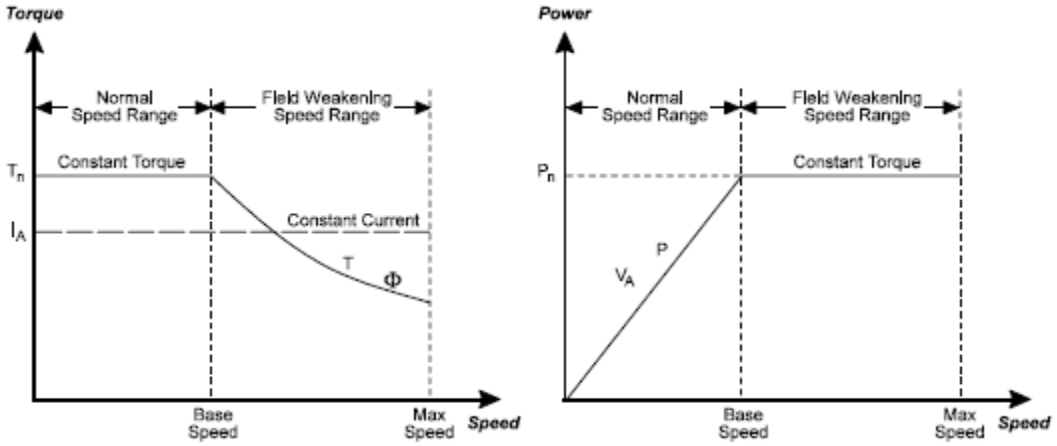

Figure 8.9: Speed-torque and speed-power diagram of a DC-motor [13]

8.2.4 Example

The influence on snag load of the three valid options for motor selection will now be calculated using the simulation model.

8.2.4.1 Input

Table 8.3 shows the current motor of the example crane, compared with the 4-pole and 6-pole replacements.

In Figure 8.10 the duty points of the crane are plotted with the characteristics of the three possible motors in the winch. It shows that sometimes the nominal required torque exceeds the nominal produced torque of the motor. This is possible because the hoist motors are only operating around 30 or 40% of the time, allowing the motors enough time to cool down after each overload.

	Current motor	4-pole replacement	Overloaded 6-pole	
name	ODRKF400L-6T	ODRKF 315L-4bb	ODRKF 315X-6	
Nameplate power	unknown	500	425	kW
Duty cycle	S3-60%	S3-60%	S3-60%	-
Nominal power	700	590	500	kW
Stall torque	3.12	3.31	3.4	-
Motor inertia	20.4	5.65	7.91	Kgm^2
number of poles	6	4	6	-
Nominal speed	1000	1500	1000	rpm
Maximum speed	2000	3000	2000	rpm
Overload factor	1.6	2.2	2.6	-
Nominal torque	6.7	3.8	4.8	kNm

Table 8.3: The current motor versus an overloaded 6-pole motor and a 4-pole motor (all values are per motor, 2 motors are installed in the winch)

The characteristics of the three motors are shown below. The maximum required torque is determined by the required acceleration and the motor inertia. The 4-pole and the overloaded 6-pole motor will therefore have a lower required torque than displayed in the figure below. The actual points are not shown to improve the readability.

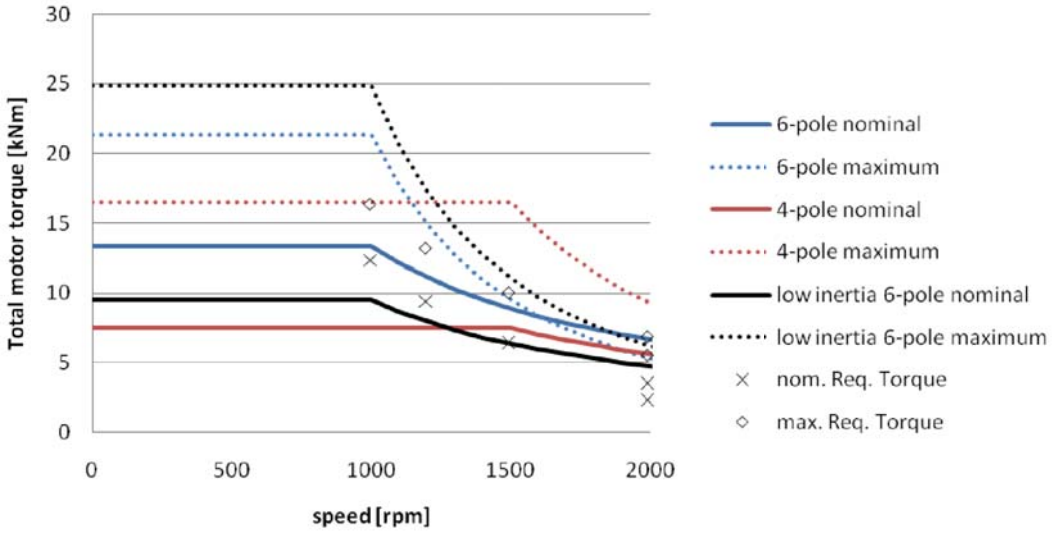

Figure 8.10: Three different types of motors plotted with the duty points of the crane. The solid lines represent the nominal torque of the motors; the dotted lines represent the maximum allowable torque

8.2.4.2 Results

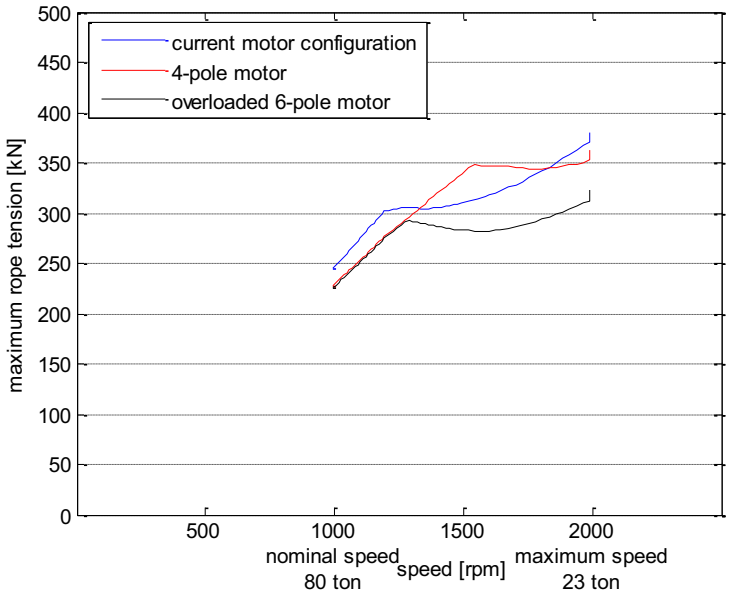

Figure 8.11: HNN MSC results for a 2-rope snag, static load limit

When only implementing the improvement of the AC motors, the results as displayed above are obtained. It shows a slight reduction in snag load when implementing an overloaded 6-pole motor. A 4-pole motor actually leads to a large increase of the snag load, due to the high overloading capability of the motor at high speeds. This effect can be negated using a variable tension limit, as is illustrated in Figure 8.3. The results of the 4-pole motor and the overloaded 6-pole are now very close.

Therefore these motors will both be taken into account when analysing the case in chapter 10.

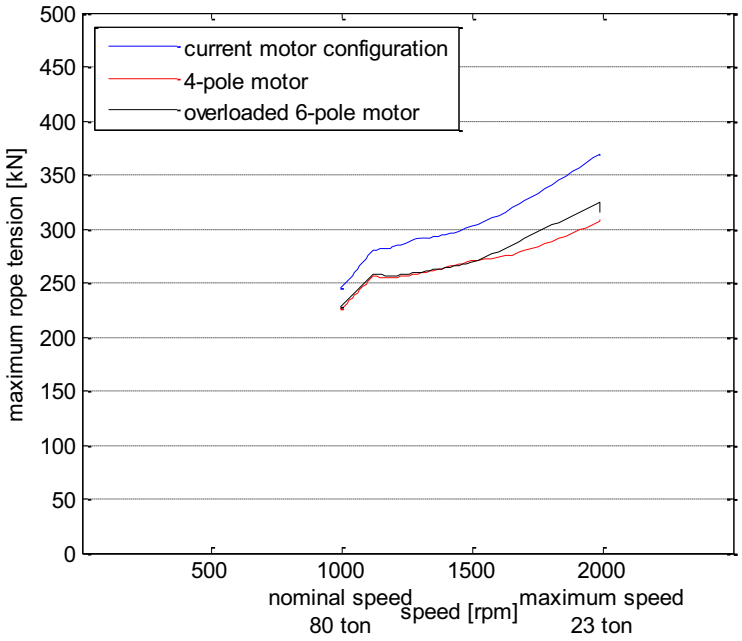

Figure 8.12: HNN MSC results for a 2-rope snag, dynamic load limit

8.3 Winch inertia

8.3.1 Current inertia distribution

The total inertia of the winch consists of the inertia of the input shaft and output shaft. The inertia of input shaft is the sum of the inertia of the motors, brakes, couplings and gearbox, which are all specified by their respective manufacturers.

The inertia of the low speed components comprises of the rope drums, couplings and hoisting sheaves. The rope drum inertia can be calculated using:

$$I = \int_m r^2 dm \tag{8.9}$$

This returns a mass moment of inertia of 946 kgm^2 for the rope drum with a diameter of 900 mm.

The inertia of the low speed components is reduced through the gearbox:

$$I_{high\ speed} = \frac{I_{low\ speed}}{\left(i_{gearbox}\right)^2} \tag{8.10}$$

The following table shows the inertia of the hoisting winch for three characteristic hoisting speeds.

		Evyap 120 m/min	Finnsteve 150 m/min	HNN MSC 180 m/min	
High speed components	Electric motors	13.9	15.8	40.8	kgm^2
	Operating brake discs	7.7	11.7	11.7	kgm^2
	Couplings	2.3	1.6	1.4	kgm^2
	Gears	1.1	2.9	5.4	kgm^2
Low speed components (reduced to input shaft)	Rope drums and couplings	3.5	6.4	8.2	kgm^2
	Rope sheaves	0.7	1.1	1.7	kgm^2
Total		**29.2**	**39.6**	**67.5**	**kgm^2**

Table 8.4: Inertia of the input shaft for three common maximum hoisting speeds

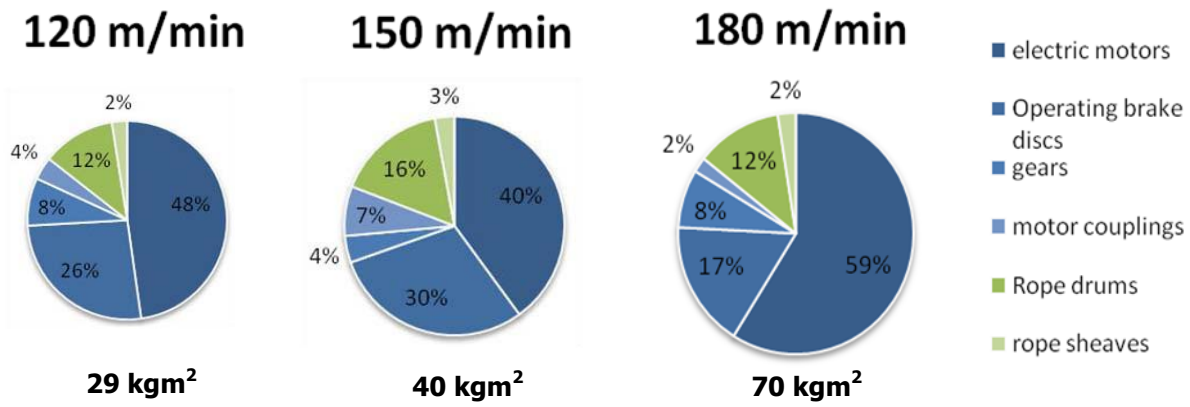

Figure 8.13: Inertia distribution of the complete hoisting winch, high speed components in blue, low speed in green. Values can be found in Table 8.4

The table shows that faster hoisting speed generally result in higher hoisting winch inertia. More power is required, resulting in larger motors and heavier couplings. Because the motors of these three cranes all run at the same speed, higher hoisting speed is acquired by using a lower gearbox ratio. Due to the lower gearbox ratio, the reduced inertia of the output shaft increases. However due to a higher total inertia its fraction will remain at about 15-20% of the total inertia.

8.3.2 Possible inertia reductions

Reducing the inertia will decrease the amount of kinetic energy that needs to be dissipated.

The biggest opportunity for improvement lies in the selection of different motors and braking discs, as is shown in Figure 8.13.

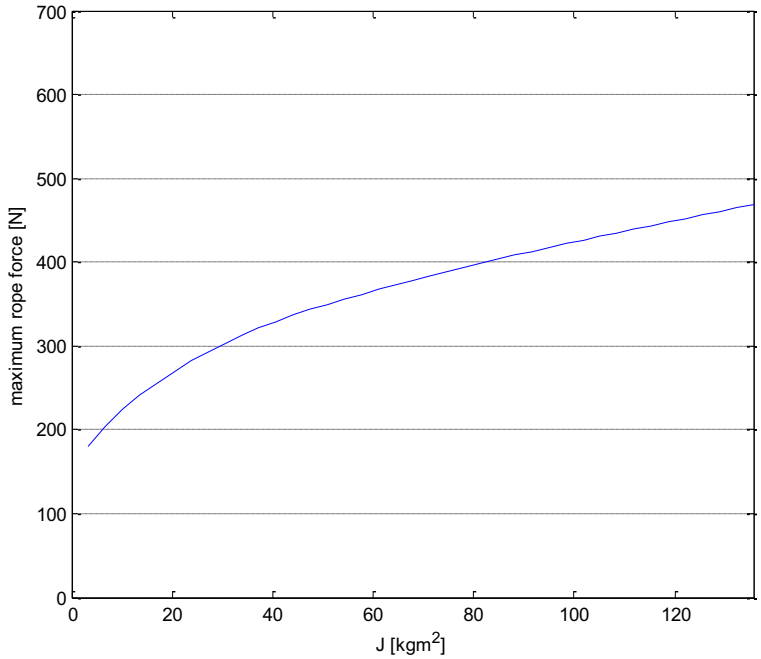

Figure 8.14: Influence of varying the inertia of the driveline on the resulting rope tension for a 2-rope snag

Motors

The selection of smaller motors was already described in section 8.2.1.1. The rotors of these motors have a lower inertia.

Brake discs

The inertia of the brake discs is determined by its mass and diameter.

Current industrial brake discs are manufactured from steel, although manufacturers are trying to find different materials to improve the properties of the disc.

The Litec brake disc manufactured by Bubenzer is constructed out of alloyed aluminium, reducing the inertia of the disc by 60%. Unfortunately these brake discs are reported to have problems regarding separation of the top layer of the disc. This causes the friction coefficient to drop, due to sliding of this top layer.

In other industries, like the car industry, ceramic composite materials are used on high-performance cars. The benefits of these materials are enhanced durability and a weight reduction of 50%. However, no application of these types of materials can be found in industrial brakes.

To decrease the radius while maintaining the same braking torque, the clamping force of the brakes has to be increased. Sibre improved their TEXU brake design, allowing the brake disc diameter to decrease from 710 to 500 mm, while providing a braking torque between 6500 and 14000 Nm per brake. This will decrease the inertia of a single motor coupling + disc brake from 6.67 kgm^2 to 3.12 kgm^2, which is a 53% decrease.

8.4 Brake response time

The current brakes respond too slowly to have a significant impact on the snag load. Historically, the brakes were never specifically designed to cope with snag loads. The operational brakes were designed to hold the load when motors are unpowered, while the emergency brakes were designed to catch the load in case of an emergency.

However, brake manufacturers are currently developing brakes with shorter response and ramp up times. I.e. in the SOS-system described in section B.2.1, these new brakes are used. The emergency brakes used in that system have a closing time of 20 ms, and a ramp up time of approximately 80 ms. [29]

The response time of the electric motors is a lot faster than the brakes, so there is little room for improvement on the electric motors.

Brake type	Parameter	Current system	Improved brakes	
Operational brakes	Controller response time	0.15	0.01	s
	Closing time	0.35	0.14	s
	Braking torque	2 x 10 000		Nm
Emergency brakes	Controller response time	0.02	0.01	s
	closing	0.2	0.09	s
	Braking torque	2 x 150 000		Nm

Table 8.5: Properties of the brakes currently used in Kalmar STS cranes

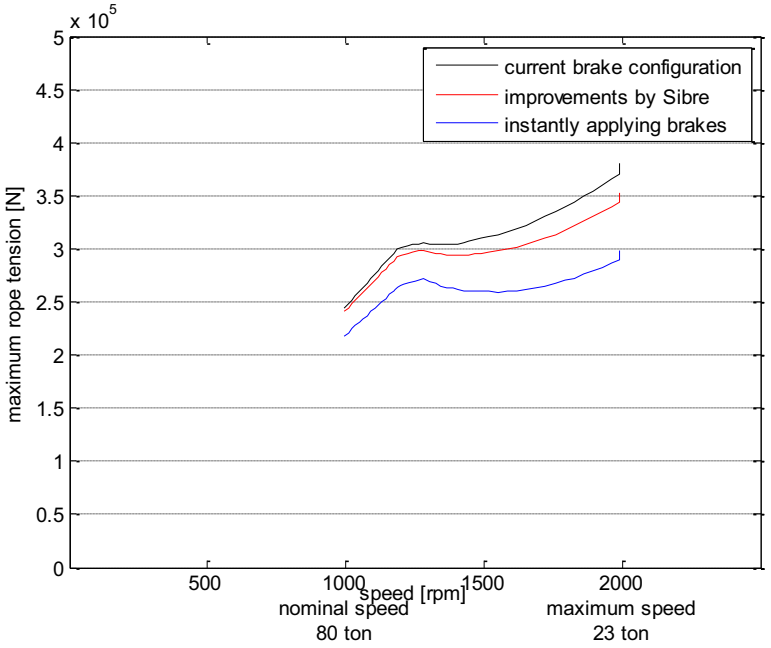

Figure 8.15: Decrease in resulting snag load when improving brake response times

8.5 Braking torque

Installing more braking torque will result in bigger deceleration of the input shaft during the emergency stop. The maximum braking torque is limited by the strength of the driveline components, which have to transfer the torque from the brakes to the load (the input shaft electric motors). This problem is described in more detail in section 9.3.2.

The braking torque of the electric motors is limited by the maximum torque the motors can deliver at their shaft speed and will therefore not be examined in this chapter.

Using the simulation, it is found that increasing the braking torque has little influence on the resulting snag load. This is caused by the slow snag detection and application of the brakes. These delays in the system ensure that the brakes are applied at the last fraction of the snag, when the winch has already been slowed down significantly by the increasing rope tension.

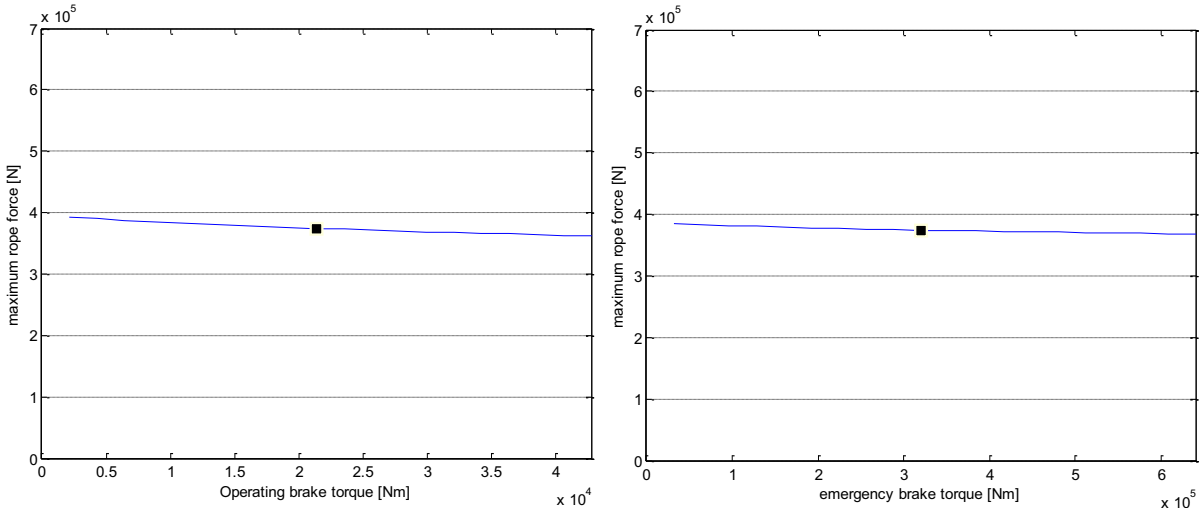

Figure 8.16: Influence of varying torque of emergency brakes (left) and operating brakes (right). Black dot indicates current braking torque

Because of the limitation in braking torque by the strength of the components and the little influence of increased braking torque, increasing braking torque has low priority. When the braking disc diameter needs to be increased to increase braking torque, it can even have an adverse effect on the resulting snag load, due to the increase in inertia of the winch.

8.6 Wire rope stiffness

By decreasing the stiffness of the wire rope, the tension rise in the rope during a snag can be decreased. The wire rope stiffness is described by the following equation:

$$k = \frac{EA}{L} \tag{8.11}$$

The Young's-module is dependent on the type of wire rope construction and the material type. The wire rope construction and material type greatly influence other properties of the wire rope, like the fatigue strength and wear resistance. This is therefore not a value that is easily changed.

The length of the wire rope is determined by the design of the crane. Extra rope length could be installed to decrease the stiffness, but this would be an expensive solution.

The cross-sectional area can be changed by selecting a smaller diameter wire rope. Currently two types of standard wire rope are the most common ropes in use:

Rope type	Diameter	Area	Minimum breaking strength
8x25 WS + IWRC	28 mm	311 mm^2	547 kN
6x36 WS + IWRC	30 mm	414 mm^2	640 kN

Table 8.6: Two common wire rope constructions used in STS cranes

As long as the strength of the 28 mm rope is sufficient, it is highly recommended over the 30 mm wire rope. For the HNN MSC crane, a change to the 28 mm rope would result in a 25% decrease of stiffness, decreasing the snag load by 20%.

Due to the reduced diameter, the minimum breaking strength reduces as well, influencing the safety factor of the wire rope on snag. For the 30 mm wire rope, the safety factor on snag load is 1.74. For the 28 mm wire rope the safety factor will be 1.86. The introduction of the 28 mm wire rope will therefore have a larger safety factor for the wire rope during a snag load.

If it is possible to use a 28 mm wire rope depends on other factors, like the maximum load the crane is required to lift. But due to the large improvements of the selection of a smaller rope, it should definitely be taken into account during the design phase of a crane.

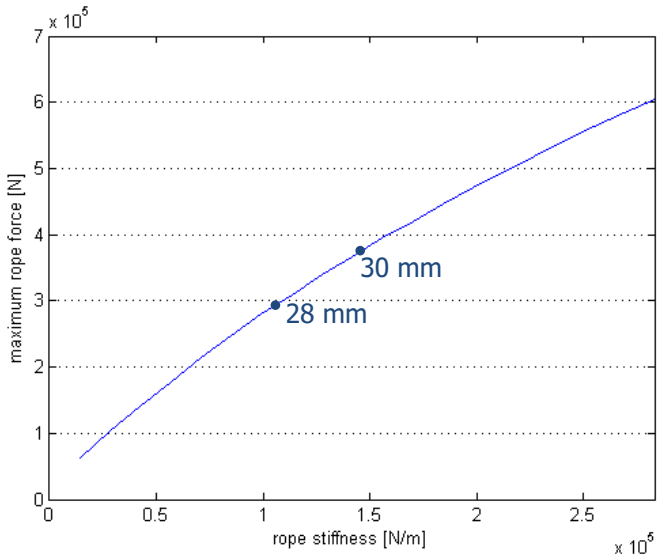

Figure 8.17: Influence of the wire rope stiffness on the maximum rope tension

8.7 Conclusions

In this chapter a number of improvements to the current hoisting winch configuration have been investigated using the Simulink model. The improvements are mainly aimed at decreasing response time, decreasing the inertia, decreasing wire rope stiffness.

The response time of the control system should be minimized, to ensure a quick stop of the winch. Therefore it is recommended to bypass the PLC when applying an emergency stop initiated by rope overload. The snag will be detected more quickly by varying the limit of the tension monitoring system.

The inertia of the winch should be reduced as much as possible, to reduce the kinetic energy stored in the winch. The inertia should be reduced by selecting small operating brakes and heavily overloaded motors. So far there are no known successful improvements in the area of brake disc material for industrial brakes.

The selection of a 4-pole motor can also be beneficial for the snag load, since it reduces the inertia of the motor, and allows for a higher braking torque. However, an improved monitoring method is required to be able to utilize this braking torque. If the normal monitoring method is used, the motor's characteristics actually lead to a higher snag load.

The stiffness of the ropes has a lot of influence on the resulting stiffness. When possible, it is highly recommended to use a 28 mm wire rope in favour of a 30 mm rope.

Selecting stronger brakes has little to no influence on the resulting snag load. This is therefore not of interest, until the monitoring system is fast enough for the brakes to make a difference.

9. Maximum allowable snag load

Now that it is possible to calculate the snag load, the maximum allowed snag load must be determined, in order to see if it is possible to operate without a snag protection device.
It would be possible to make an extremely strong crane with very strong components, but this would result in a crane that is too heavy and too expensive to sell.
The maximum allowable snag load will be determined by setting a limit to the rope tension developed during snag. The maximum allowable rope tension will be determined as the maximum tension that is not governing for the design of the crane.
The analysis will be split in four parts, which will be analysed separately:

- Wire rope
- Crane structure and related mechanisms (i.e. pylonhead or forestay)
- Mechanical components of the reeving and winch
- Hoisting tools

For both the wire rope and the mechanisms connected to the rope the 2-rope snag is governing, since it results in higher rope tensions. For the crane structure, the 4-rope snag has to be examined as well, since a 4-rope snag leads to a higher total load on the crane.

9.1 Wire rope

The maximum tension allowed for a rope is determined by the safety factor of the rope on the minimum allowable breaking load, which is the guaranteed minimum load a wire rope can support before breaking. I.e. for a 28 mm wire rope with an 8x25 Warrington seale (WS) + internal wire rope core (IWRC), this load is reached at a tension of 547 kN.
Design standards, like the NEN 3508, define a minimum safety factor depending on the load spectrum and usage class of the crane. Depending on these factors, the required safety factor varies between 5 and 6.
The safety factor is sometimes defined in customer inquiries, which define a factor of 5 as well.
However, during normal operation the safety factor of the wire rope can already decrease to 3 due to extreme load conditions, like a twinlift of one empty and one maximum loaded 20' container.
In the design process, there is no concrete minimum safety factor on the wire rope, and it's proven to be a case of experience and customer demands.
The maximum load on the wire rope is therefore not examined separately, since no exact limit can be defined.

9.2 Crane structure and related mechanisms

The snag load will be compared to the load used for fatigue calculations, since this is usually normative for most parts of the crane. Other parts of the crane where the stiffness is normative will already be strong enough to sustain the snag load, i.e. the machinery floor and the trolley. The comparison is performed using the following idea:

$$snagload \cdot extreme\ load\ safety\ factor \leq fatigue\ load \cdot safety\ factor \tag{9.1}$$

$$maximum\ extreme\ load = \frac{fatigue\ safety\ factor}{extreme\ loadcase\ safety\ factor} \cdot fatigue\ load \tag{9.2}$$

Fatigue load is determined in Case I with a safety factor of 1.5 to the yield stress using:

$$y_c \cdot (S_G + S_L \cdot \varphi) \tag{9.3}$$

S_G = Dead load

S_L = Working load = 820 kN

S_H = two most unfavourable horizontal loads = 0 kN

The amplifying coefficient y_c for an STS-crane has a value of around 1.17, depending on the group classification of the crane.

The Dynamic factor φ depends on the hoisting class and the hoisting speed during the lifting of an unrestrained load from the ground. The speed during this part of the operation is called the creep speed, which is usually 10% of maximum hoisting speed. This results in a dynamic factor of 1.2.

Snag load is evaluated as an extreme load, and is thus described by Case III with a safety factor of 1.1 to the yield stress:

$$(S_G + S_L \cdot \varphi) \tag{9.4}$$

S_G = Dead load

S_L = Resulting snag load (to be determined)

Now the maximum allowable snag load can be determined by comparing case I to case III.

Case III<Case I:

$$1.1 \cdot (S_G + S_{snag}) < 1.5 \cdot y_c \cdot (S_G + S_L \cdot \varphi) \tag{9.5}$$

$$S_{snag} < \frac{1.5}{1.1} \cdot y_c \cdot (S_G + S_L \cdot \varphi) - S_G \tag{9.6}$$

9.2.1 4-rope snag

Equation (9.6) will now be used to determine the allowable snag load for a 4-rope snag.

The loads on the crane during a 4 rope snag can be compared to the vertical load on a crane during the normal load situation.

For example: for loads on the boom the dead load is equal to the trolley weight, which has a value of 300 kN. This results in a maximum allowable snag load of 1748 kN, which corresponds to a rope tension of 219 kN. For the forestay the dead load also includes the weight of the boom girder, which weighs between 100 and 150 tons, resulting in a higher allowable snag load.

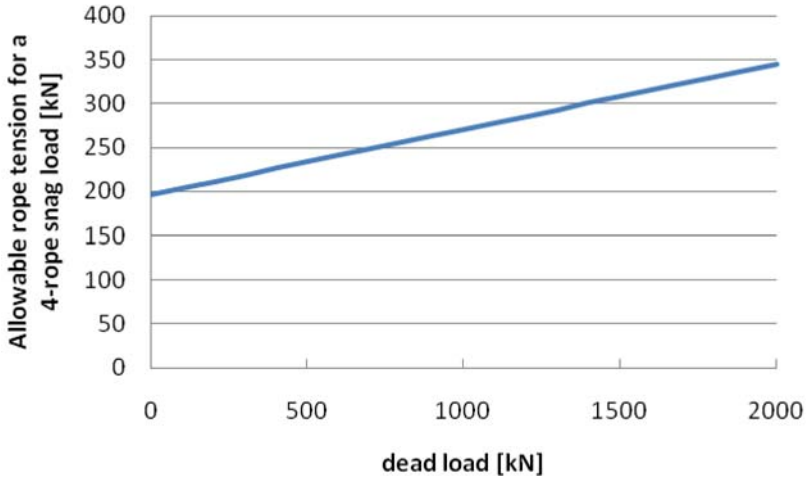

Figure 9.1: The maximum allowable rope tension during a 4-rope snag expressed as a function of the dead load on a component

As can be seen above, the allowable snag load is linearly dependent on the rope tension.
The limiting construction element will therefore be the element that is affected by the least amount of dead load, which would be the bridge girder and the trolley. These are only affected by the weight of the trolley. This leads to a maximum allowable rope tension of 219 kN for a 4-rope snag.

9.2.2 2-rope snag

The same method for comparing the snag load with the fatigue as was used for the 4-rope snag can be applied to a 2-rope snag load. The difference between the 4-rope and 2-rope snag lies in the values used when applying equation (9.6). Also, a difference has to be made between the double box girder and the Monobox, due to their difference in torque stiffness.

9.2.2.1 Double box girder

When considering an eccentric snag on a double box girder, it is assumed that the girders have little influence on each other. This assumption can be proven valid when looking at the difference in stiffness for a 2 and a 4-rope snag. During a 2-rope snag only half of the construction is loaded, while the stiffness of the crane during a 2-rope snag is also almost halved compared to a 4-rope snag (as shown in Table 5.5). Therefore the double-box girder can be regarded as two separate girders, not influencing each other.

Figure 9.2: Schematic front view of a 4-rope and a 2-rope snag on a double-box girder

To calculate the maximum allowable snag load for a 2-rope snag, the maximum fatigue load on one side of the girder will be used as the working load. This will be a 10% eccentrically loaded twinlift operation, resulting in a load of 479 kN on a single beam.

The dead load for the analysis will be halved for some of the analysed components, depending on the location. Like with the 4-rope snag situation, the allowable snag load is lowest at a location closest to the load, being the bridge girder. The dead load will then be half the trolley weight: 150 kN. Inserting these values into equation (9.6), results in a maximum allowable snag load of 1006 kN, corresponding to a rope tension of 251 kN.

9.2.2.2 Monobox girder

The vertical stiffness of a Monobox STS crane for an eccentric snag is comparable to the stiffness for centric snag, due to the high torsion stiffness of the girder. Therefore the total dead load can be taken into account, instead of half the dead load for the double box girder.
A 2-rope snag will therefore result in an allowable snag load on the bridge girder of 273 kN.

9.3 Mechanical components of the reeving and winch

These components are required to have sufficient strength to cope with the high rope tension caused by snag, or the high torque developed during an emergency stop caused by snag. The following components need to be checked (see Figure 3.6 for their location):

- Tension loaded components
    - Rope sheaves and sheave bearings
    - Rope drums
    - Drum bearings
    - Drum shaft
    - Drum coupling
- Torque loaded components
    - Gearbox
    - Motor coupling
    - Drum coupling

The rope drum and drum coupling are both loaded by tension and torque. The drum coupling is bought from a manufacturer. This manufacturer defines the torque and radial load separately, and will therefore be examined separately.
The rope drum is loaded by the torque from brakes and motors, however the torque is not governing for the design and will therefore not be taken into account determining the snag load limit.
For analysis, four cranes will be checked:

- HNN MSC
- Finnsteve
- Evyap
- SPRC

9.3.1 Tension loaded components

The tension loaded components are directly related to the maximum allowable rope tension. The maximum static strength of these components will be listed. First all components will be described, after which the maximum allowable loads of these components will be listed.

These rotating components are loaded by a high rope tension during a snag. For most components, the fatigue load is normative, which leads to very high permissible extreme loads.

9.3.1.1 Drum bearings

The bearings of the hoisting rope drums in an STS crane are typically spherical roller bearings. They are only loaded by rope tension, not by the developed torque.

9.3.1.2 Rope drums

The rope drum is loaded by the torque from brakes and motors, however the torque is not governing for the design and will therefore not be taken into account determining the snag load limit.

9.3.1.3 Drum coupling

The drum coupling is loaded by a combination of torque and rope tension. According to manufacturer's calculations, both are evaluated separately. When the torque load does not exceed nominal torque, the maximum allowable tension for the drum increases, but this is not the case for snag. Therefore the tension and torque loads will be evaluated separately, each with their own limits.

The load on the drum coupling is equal to the load of a single rope, even though there are two ropes connected to a single drum. This is caused by the construction of the drum: the drum is supported by the drum bearing on the opposite site of the drum coupling. This is illustrated in Figure 3.6.

9.3.1.4 Rope sheave bearings

The loading on the rope sheave bearings depends on the rope tension and the angle of wrap of the sheave. All the running sheaves located in the crane have a safety factor between 2 and 3 on the extreme static rope tension.

The rope sheaves at the tip of the boom have a lower safety factor, since these sheaves do not rotate during normal operation, and are therefore not designed on fatigue life, but only on static strength. The safety factor on the extreme rope tension of these bearings ranges between 1.25 and 1.5.

9.3.1.5 Resulting loads

For some cranes, the values for certain components could not be found, but enough values have been found to draw conclusions on the maximum allowable rope tension.

All values in [kN]	HNN MSC	Finnsteve	Evyap	SPRC
Drum bearings	821	433	987	987
Rope drum	394	311	460	287
Drum coupling	unknown	unknown	250	265
Sheave bearings	650	648	482	632
Boom end sheave bearing	349	313	414	unknown
Drum shaft	378	680	569	564
Minimum allowable rope tension	**378**	**311**	**250**	**265**

Table 9.1: Minimum allowable rope tension for the tension loaded components of the four example cranes

The maximum rope tension of the drum coupling for Evyap and SPRC was defined by the manufacturer as a maximum loading. No details were included if this was just a maximum load or the extreme load. It is likely that this load is a maximum load and therefore the allowable extreme load will be higher. This should be investigated in more detail, by contacting the suppliers.

For Finnsteve and HNN MSC, the data of this coupling was not available. The minimum value found when regarding all components and cranes together is 250 kN.

9.3.2 Torque loaded components

The torque on these components consists of two parts:

- Torque due to rope tension on the rope drum
- Torque developed by brakes and electric motors

These components will not be considered in determining the maximum allowable rope tension, since a large part of the torque is determined by the brakes. The maximum torque on these components during snag does have to be taken into account during snag analysis. The torque on all components is not equal, due to their location in the drive train.

9.3.2.1 Drum coupling

The torque on the drum coupling is equal to the braking torque of a single emergency brake, together with the torque generated by the two ropes on the drum. The critical drum coupling will be the one connected to the snagged ropes, since these will have the highest rope tension.

$$T_{drum\ \ coupling} = T_{emergency\ \ brake} + 2 \cdot T_{rope,snag} \tag{9.7}$$

In case of mechanism group M8 from FEM1.001, the manufacturers subscribed a safety factor of 2 on the maximum motor torque. However there is no safety factor defined specifically for extreme situations.

9.3.2.2 Gearbox

The torque on the gearbox is equal to the total braking torque of the emergency brakes, together with the torque developed by all four ropes acting on the drums:

$$T_{gearbox\ \ output\ \ shaft} = 2 \cdot T_{emergency\ \ brake} + T_{rope,total} \tag{9.8}$$

From data from the manufacturer of the gearbox the following values can be found.

9.3.2.3 Motor coupling

The torque on the motor coupling is equal to the torque on the gearbox output shaft, reduced by the gearbox ratio, together with the torque of one operating brake. The torque from the gearbox output shaft is divided equally over the number of motors.

$$T_{motor\ \ coupling} = \frac{2 \cdot T_{emergency\ \ brake} + T_{rope}}{n_{motors} \cdot i} + T_{operating\ \ brake} \tag{9.9}$$

The motor couplings are currently designed to have a certain safety factor on the nominal motor torque, usually at a value of 2.5. Stronger and bigger motors therefore result in larger motor couplings.

9.3.2.4 Resulting loads

All three torsion loaded components have their own limit, and also their own loads, which have to be evaluated separately, since these are not completely related.

All values in [kNm]	Finnsteve	HNN MSC	Evyap	SPRC
Drum coupling	620	620	620	660
Gearbox (output)	unknown	760	unknown	760
Motor coupling	21.2	19.8	21.2	22.1

Table 9.2: Data for maximum allowable torque loads on winch components

9.4 Hoisting tools

The hoisting tools are the components supported by the hoisting rope, which are used to pick up the load. The hoisting tools that will be investigated are:

- Headblock
- Headblock-spreader connection
- Spreader
- Twistlocks

Besides the loading of increased rope tension, the hoisting tools will sustain impact loads during a snag, which cause damage to the hoisting tools. The impact loads will not be investigated during this assignment, since it is unpredictable, and no detailed information of these tools is available.

9.4.1 Headblock

The headblock of the cranes is currently designed and constructed by Cargotec, using design standard FEM1.001. The qualification used is U8-Q2-A8-E7-82ton resulting in a dynamic coefficient of 1.25 and a group factor of 1.20.

From design calculations, it is found that the normative load case is normal service without wind (Case I), a load of 82 ton, with an eccentricity of 10% in both directions. This leads to a rope tension of 164 kN without the dynamic factors, including rope reeving efficiency. There is no dead load acting on the headblock, so S_G is zero.

Filling in equation (9.6) will result in the maximum extreme rope tension for the headblock:

$$S_{snag} < \frac{1.5}{1.1} \cdot y_c \cdot (S_G + S_L \cdot \varphi) - S_G = 335\ \text{kN} \tag{9.10}$$

9.4.2 Headblock-spreader connection

For the SPRC crane, the connection between the headblock and spreader is executed using a twistlock at each corner of the headblock. The twistlocks, with a shaft diameter of 70 mm, have been analyzed using FEM by Cargotec, and are found to have the yield limit at 70 tons of tensile load per twistlock.

9.4.3 Spreader

The spreaders are not built by Cargotec, but are bought from a manufacturer, i.e. Bromma.

The spreaders are test loaded up to a load of 150% of maximum load. This test load equals:

$$150\% \cdot (2 \cdot 32.5 + 12.3) = 116\ tons \tag{9.11}$$

$$116\ tons \cdot \frac{9.81}{8\ rope\ parts} = 145\ kN\ rope\ tension \tag{9.12}$$

The test load would resemble a load of 145 kN per rope. However, this is the test load, while the maximum allowable load of the spreader will be higher. Unfortunately, the maximum load of the spreader is unknown. If 145 kN of rope tension would be the maximum load, a lot of spreaders would have been destroyed during a snag, since anti-snag systems have a rope tension limit set in the range of 200-250 kN.

Besides structural damage because of overloading, the impact itself during a snag can cause minor damage to the spreader. These kinds of impacts will not be calculated using the model.

Because there is no sufficient information available about the spreader at this time, the spreader will not be taken into account when analyzing the snag loads. Before implementing the solutions mentioned in this thesis, the spreader strength should be checked with the supplier.

9.4.4 Twistlocks

The twistlocks are the parts of the spreader which hold the container during hoisting, with one twistlock per corner of a container. According to Bromma, the twistlocks are test loaded and certified for a tensile load up to 37 tons.

The only type of snag during which the twistlocks are loaded is indicated in Figure 9.3. This load is a combination of shear and tensile load. The exact value of the load on the twistlock depends on the deformations of the ship cell and container and friction of the cell guides, and is therefore hard to determine.

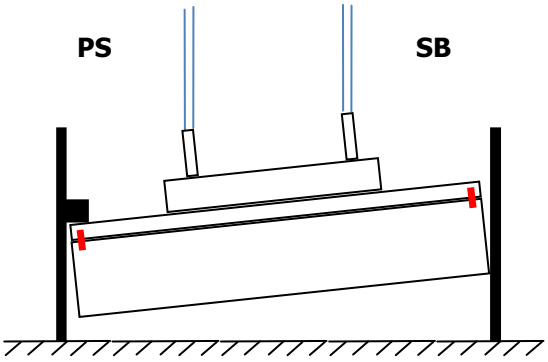

Figure 9.3: Snag during which the starboard twistlocks are loaded. Twistlocks are indicated by the red markers

9.5 Conclusion

In this chapter the maximum snag load was determined which would not be normative for the design of the crane.

The limit for 2-rope snag is limited at 250 kN by the wire rope drum.

The limit for 4-rope snag is limited at 219 kN by the construction with only the dead weight of the trolley acting on it.

During snag analysis the torque loaded components have to be taken into account as well. The allowable torque for these components is listed in Table 9.2.

This chapter showed that the allowable snag load on the crane depends on the components chosen for the crane. It is therefore recommended to take the snag load into account during the design process, when selecting these components.

10. Case: 180 m/min without an anti-snag device

In chapter 8 a number of improvements were investigated to reduce the snag loads on a crane. In this chapter, a case study is presented to examine the improvements, and to illustrate some findings from the research.

The case study comprises of a super-post Panamax Monobox crane currently under construction for a port in Colombia: SPRC. The main characteristics of the crane are shown in the table below, while the other necessary characteristics are listed in Appendix F.

parameter	Value	
Outreach	61 22	m containers
Rail span	30.48	m
Backreach	12	m
Lifting height	48	m
Duty points	Nominal load: 82 ton, 90 m/min Empty spreader: 17 ton, 180 m/min	

Table 10.1: Main dimensions of the SPRC crane

10.1 Implemented improvements

10.1.1 Control system

Two improvements that were discussed previously will be implemented for this case study:

- Bypass plc for rope tension monitoring
- Implement a variable load limit of 1.53 x static rope tension

10.1.2 Mechanical system

Three mechanical improvements will be implemented:

- Smaller brake discs
- Reduced closing time of the brakes
- Selection of smaller motor with high overload factor

The crane already has 28 mm diameter hoisting ropes, so there is no room for improvement on this part.

10.1.2.1 Brake selection

By selecting different brakes, the response time can be reduced. The total inertia increases slightly, because the original brakes used the expensive Litec brake disc option.

		Current configuration	Sibre fast solution, USB brake	
Operating Brakes	name	SB 28-800x30-301/10bb	USB3-III 710, 301/6	-
	Torque	17.5	17.2	kNm
	inertia	3.70	Included in coupling	kgm^2
coupling	name	MSC AKNXSE 0.88	ASC-15+disc	-
	inertia	3.36	7.337	kgm^2
	max torque	22.1	22	kNm
Emergency brakes	name	Bubenzer SF24	Sibre fast SHI-251	-
	clamping force	240	max. 300	kN
	max torque	153.6	192000	kNm
	notes	Litec brake discs for operating brakes		-
Total inertia on input shaft		**14.1**	**14.7**	**kgm^2**

Table 10.2: data of the implemented brakes

It has no use to apply the TEXU brakes described in 8.3.2 in this case, because the couplings required to transmit the torque from the motors are too large to fit inside the TEXU brakes. The TEXU brakes would then be the same size as the USB brake, which is cheaper, while delivering the same braking torque.

10.1.2.2 Reduced brake closing time

The response times of the brakes selected in the previous paragraph are mentioned in Table 8.5.

10.1.2.3 Smaller, overloaded motors

By selecting smaller, higher overloaded motors, the inertia of the winch is reduced. Both the 4-pole and the 6-pole replacement are taken into account, because the difference between the results of these two motors was very small in chapter 8. By calculating the resulting rope tension for both these motors, either the 4-pole or 6-pole motor will be selected.

	Current motor	4-pole replacement	Overloaded 6-pole	
name	ODRKF 355-X6	ODRKF 315L-4bbb	ODRKF 315-X6	
Nameplate power	730	550	425	kW
Duty cycle	S1-100%	S3-60%	S3-60%	-
Nominal power	730	649	550	kW
Stall torque	3.75	3.22	3.4	-
Inertia	13.6	5.92	7.91	Kgm^2
number of poles	6	4	6	-
Nominal speed	1000	1500	1000	rpm
Maximum speed	2000	3000	2000	rpm
Overload factor	1.6	2.6	2.6	-
Nominal torque	6.97	4.13	5.25	kNm

Table 10.3: Data for selected AC motors

As is shown below, the nominal required torque at low speed exceeds the nominal torque of the selected motors. The nominal required torque is the torque required to maintain constant speed at the appropriate load. This is not a problem, because the motors have time to cool down after each run and do not always have to perform at that duty point.

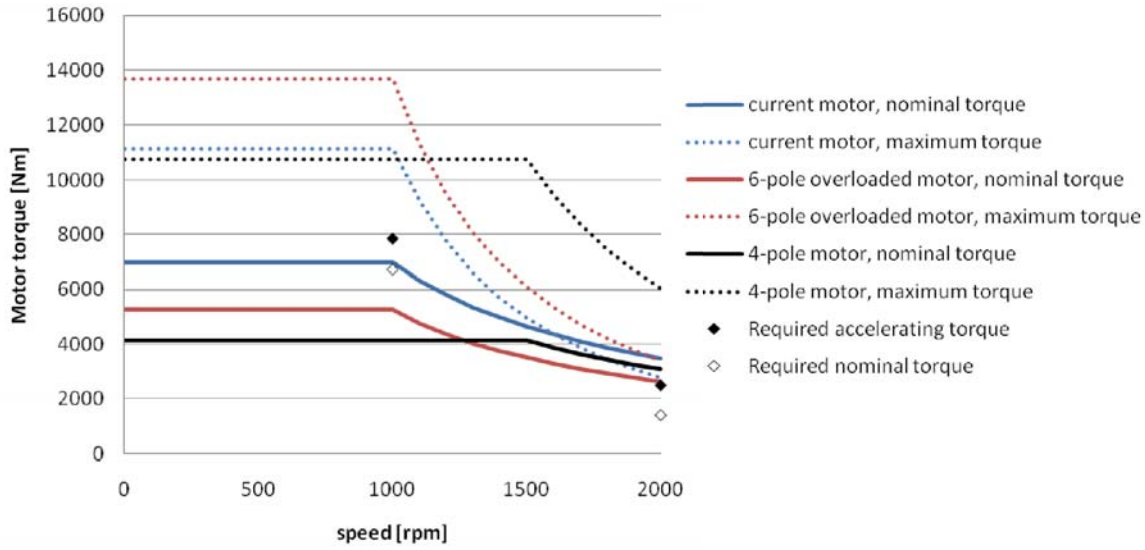

Figure 10.1: Characteristics of the motors mentioned in Table 10.3. The duty points are indicated in the figure by the diamond shapes

As is shown below, the 4-pole motor leads to a slightly lower snagload for both the 2-rope and the 4-rope snag. Therefore the 4-pole motor will be selected.

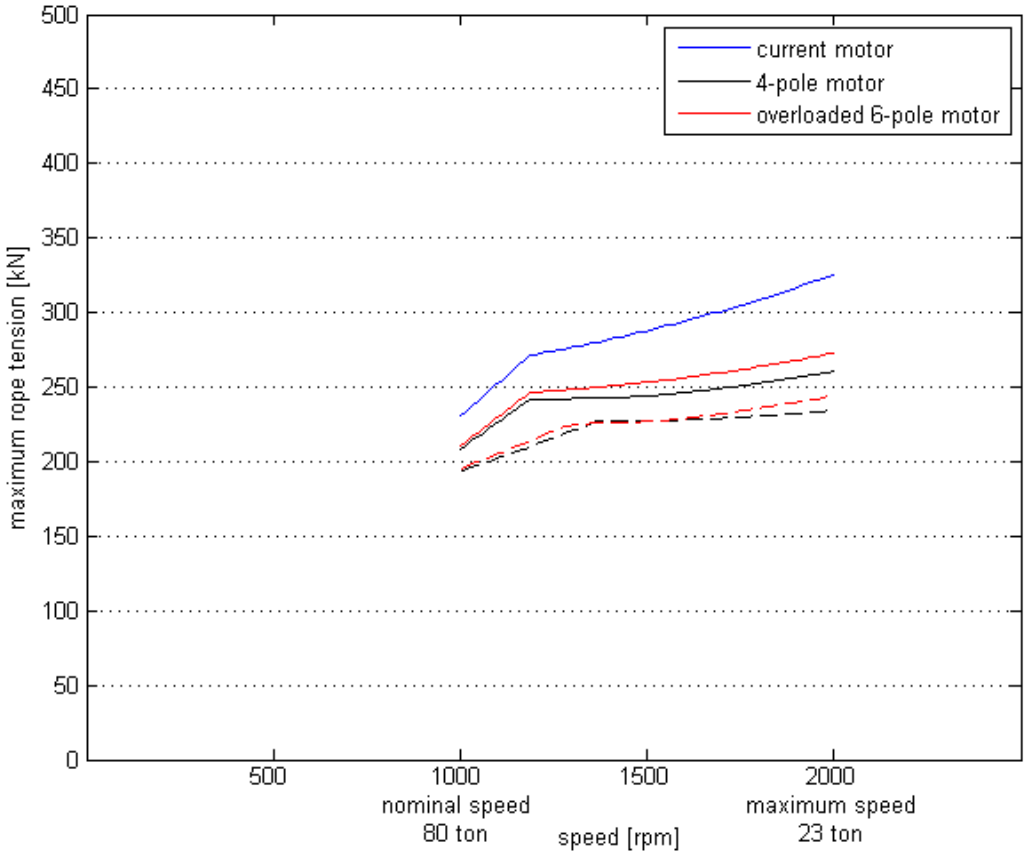

Figure 10.2: Result for both the 4-pole and the overloaded 6-pole motor. Dashed lines indicate the result for a 4-rope snag, solid lines are results from 2-rope snag

10.2 Results

When all the improvements are implemented, the impact of these adjustments can be analyzed using the simulation model. This analysis requires some iteration steps until the solution is found:

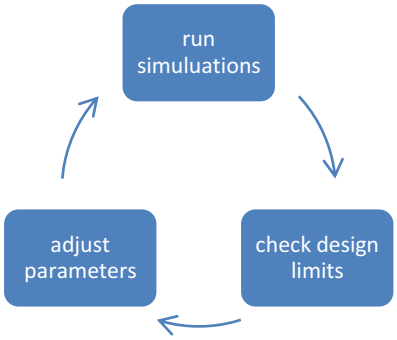

Figure 10.3: illustration of the iterative process during the analysis of snag loads

First the iterations during this case will be described, using short summaries of the results. When the final design is known, the results will be explained in detail.

			Iteration number			
	Normative load case	Limit	1	2	3	unit
construction, 2-rope snag	2-rope	279	256	264	236	kN
tension loaded components	2-rope	265				
construction, 4-rope snag	4-rope	219	**230**	**232**	217	kN
motor coupling	4-rope	22	**41**	**23.7**	21.8	kNm
drum coupling	2-rope	660	385	391	362	kNm
gearbox	4-rope	760	740	744	669	kNm

Table 10.4: Results of first iteration of the case

Iteration 1

As is shown above, the construction is slightly overloaded during the 2-rope snag. The real concern is the motor coupling, which is severely overloaded. This cannot be compensated by stronger couplings. When investigating the torque in detail, it is found that the operational brakes are activated very late, and therefore dissipate only a small amount of the total energy, while they do add a large shock on the driveline.

Iteration 2

To reduce the torque load on the motor coupling, the operating brake will not be applied when performing a snag stop. This will slightly increase the rope tension, but the torque load on the motor couplings will decrease dramatically.

Iteration 3

To reduce the snag loads to an acceptable level, the hoisting speeds inside the ship cell will be decreased. After iteration, an empty spreader speed of 160 m/min is found to be possible. The other speeds are determined using linear interpolation.

10.2.2 Tension loaded components

To illustrate the results from the design improvements, the figure below shows the resulting rope tension. The governing limit proved to be the 4-rope snag load.

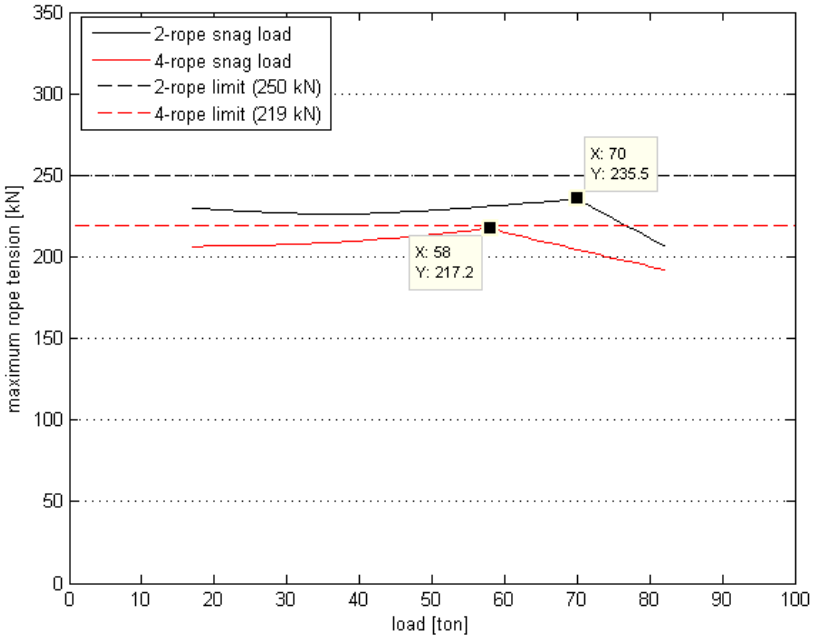

Figure 10.4: Resulting rope tension for a 2-rope and a 4-rope snag, for all duty points

10.2.3 Torque loaded components

Below are the loads through time on the torque loaded components, for both the 2 and the 4-rope snag. The most critical part is proven to be the motor coupling during a 4-rope snag.

Figure 10.5 shows the torque on the motor coupling during the critical 4-rope snag, which is a snag of a 58 ton load at 99 m/min.

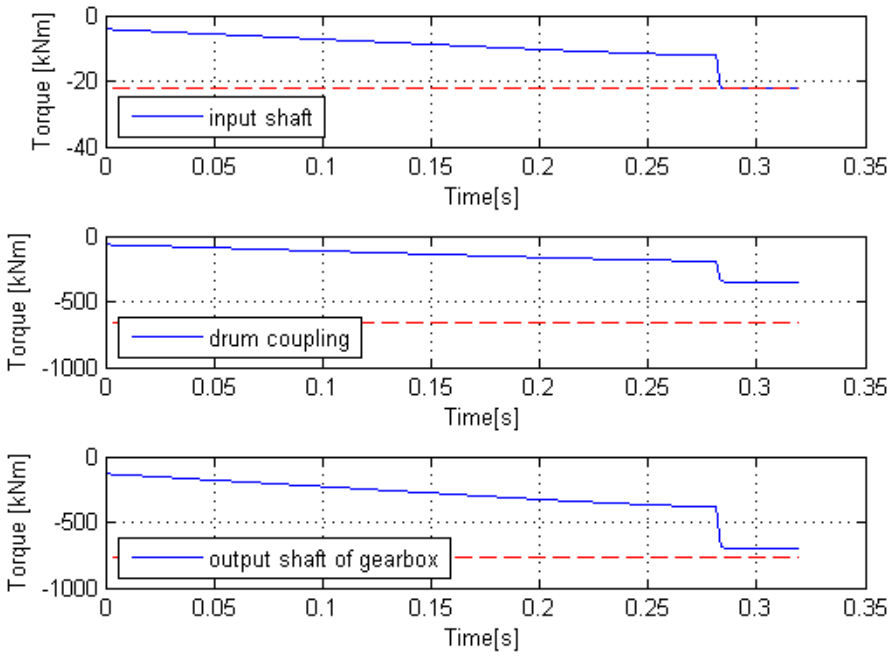

Figure 10.5: Development of the torque on components of the hoisting winch during 4-rope snag, without applying operating brakes

10.2.4 Productivity loss due to hoisting speed decrease

The productivity losses of a reduced hoisting speed inside the ship cell can be calculated.

Assuming a total height of 11 container inside ship cell equals 27.5 meters. The following equations are based on the assumption of constant acceleration up to the point where maximum speed is reached. In reality a ramp function is used to decrease shock loads on the crane.

$$t_{acceleration} = \frac{v_{hoist}}{a_{hoist}} \tag{10.1}$$

$$s_{acceleration} = \frac{1}{2} a_{hoist} \cdot t_{acceleration}^{\ 2} \tag{10.2}$$

$$s_{total} = s_{acceleration} + s_{constant\ \ speed} = 27.5m \tag{10.3}$$

$$t_{total} = \mathrm{t}_{\mathrm{acceleration}} + \frac{s_{constant\ \ speed}}{v_{hoist}} \tag{10.4}$$

Using these equations, the hoisting speed of 180 m/min results in a hoisting time in the ship cell of 11.3 seconds, and the hoisting speed of 160 m/min results in 12.2 seconds. This is an increase of 0.9 seconds.

Assuming a total cycle time of 90 seconds (corresponding to 40 moves per hour), which is relatively fast, this is an increase in cycle time of 1%.

The impact on the productivity on the total terminal is harder to determine, since the dynamics between the crane and the land operation influence each other.

10.3 Conclusion

It was not possible to hoist at 180 m/min without the use of some sort of snag protection system, using the following improvements:

- Control system
    - Bypass plc for rope tension monitoring
    - Implement a variable load limit of 1.53 x static rope tension
- Mechanical system
    - Smaller brake discs to reduce inertia
    - Reduced closing time of the brakes
    - Selection of smaller motor with high overload factor

However, when limiting the hoisting speed in the ship cell, the snag load can be reduced to an acceptable level. The hoisting speed is limited inside the ship cell at 160 m/min.
The decrease in hoisting speed led to a small increase in cycle time of 1%.

11. Conclusions

The conclusions drawn from this research will be described in this chapter, divided over three parts. First the conclusions on the analysis of the snag loads will be listed. Next the results from the study on possible improvements will be described. Finally, a number of recommendations are introduced for further research and improvements.

11.1 Analysis of snag loads

The main goal of this thesis was to redesign the hoist system in such a way, that an STS crane can withstand a snag load without the use of extra equipment. To achieve this goal, an analysis was made of the influences on the snag load, to construct a model for calculation of the snag loads.

Types of snag load

The resulting rope tension will be highest when a 2-rope snag occurs, with the collision close to the wire rope sheaves. This type of snag will not allow any vertical movement of the wire rope sheaves on the headblock and therefore results on the largest wire rope elongation.

The total load on the crane will be highest during a 4-rope snag, because in that case all four hoisting ropes are stretched.

Crane deformation

The deformation of the construction reduces the wire rope elongation. For both a Monobox and a double box girder design, the deformations were examined. The reduction in rope elongation due to the construction deformation ranges from 6% at minimum outreach, to 39% at maximum outreach. For further calculations, the 6% reduction was taken into account, since the worst case scenario has to be calculated.

Analysis of existing crane designs

The snag loads calculated in chapter 6 exceeded the limits from chapter 9 in some cases. This would mean that either the calculation is incorrect, or the components are stronger than assumed in chapter 9.

First of all, the calculation is based on a worst case scenario. This scenario involves a purely 2-rope or 4-rope snag, at minimum outreach on a large vessel. The chances on such a snag are small, and it is therefore possible that his type does not occur during the lifetime of the crane.

Secondly, the allowable snag load for the structural components is based on safety factors in relation to the yield stress. Due to these safety factors, some margin for error is maintained. This way it is possible to exceed the allowable snag load without damaging any components, or at least without endangering the cranes integrity.

The allowable snag load for the components is based on data from the suppliers. These will always maintain a certain safety factor for their components. The actual strength of the components is therefore higher than the values used in chapter 9.

11.2 Design improvements to the hoisting system

Parameters influencing snag load

It is found that machinery on trolley systems are not possible to operate safely at current standard hoisting speeds without a snag protection device. The short hoisting ropes result in a high stiffness, and are therefore not possible to absorb enough energy without exceeding the allowable rope tension.

For reeve-through trolleys a snag protection device can be avoided, but this depends on a number of design parameters:

- Response time of the control system
- Wire rope stiffness
- Drive line inertia
- Hoisting speed
- Motor selection

Especially the response of the control system is of great importance, as well as the wire rope stiffness. It is highly recommended to use a 28 mm wire rope instead of the 30 mm rope that is normally used, if the required safety factors allow it. The reduction of the wire rope diameter greatly influences the resulting snag load.

Application of design improvements through a case study

In the case study performed in chapter 10, the following improvements were applied to decrease the snag load as far as possible:

- Control system
    - Bypass plc for rope tension monitoring
    - Implement a variable tension limit of 1.5 x static rope tension
- Mechanical system
    - Smaller brake discs to reduce inertia
    - Reduced closing time of the brakes
    - Selection of smaller main hoist motor with high overload factor

This still resulted in snag loads which exceeded the limits of the crane.

To decrease the limit on the crane, it is recommendable to not apply the operational brakes. These are found to be too slow to make a difference in stopping the winch in time, while they do add a large shock load to the components of the winch.

It is found that reducing the hoisting speed inside the ship cell to 160 m/min is required to reduce the snag load to an acceptable level. This results in an increase in cycle time of only 1 second (1% of a total cycle).

When the winch has stopped, it is recommendable to release brakes slowly, so that the overload tension is released from the ropes. This way the crane is protected from tension rises due to natural movements of the ship.

11.3 Recommendations

Validation of results

The model constructed during this research should be validated using measurements, to make sure the model is correct. These measurements could be performed on an existing STS crane without an anti-snag device. These measurements should be performed over a relatively long period (i.e. a month), to have a reasonable chance of measuring one or more snags.

The measurements can be performed in the same way as measurements were done on the HNN MSC crane: Whenever the rope tension exceeds a certain limit, all data from the past and future 5 or 10 minutes are stored. This prevents excessive requirements of data storage.

Validation of input data used for calculation

The results are highly dependent on the parameters of the components, i.e. the response time of the control system. It is therefore recommended to measure these response times, to be sure the data used is correct.

The limits which were used to determine the maximum hoisting speed were taken from suppliers catalogues, and were usually described as the maximum load, while the fatigue load was also defined. However, the maximum load is often regarded as a load that occurs regularly, but at a low frequency. The heaviest snag loads will only occur a few times in a life time of a crane, so there is still a safety factor present in the values presented by the suppliers. To know the extreme strength of the components, the suppliers should be consulted.

Impact on the design process

For structural analysis, it is recommended to introduce two extreme load cases to the calculations, one for a 2-rope snag and one for a 4-rope snag, each with their corresponding rope tension. This way it can be proven to customers that snag loads are taken into account.

The limit found in chapter 9 gives an indication on what is the maximum allowable snag load. However all cranes use slightly different components, and therefore these components should be checked separately whether they can sustain the snag load.

Chapter 9 used the FEM1.001 standard to find the snag load limit for the construction of the crane. This is an old design standard, which is soon going to be replaced with the EN13001 standard. It is recommended that the calculation from chapter 9 is performed with EN13001 as well.

Due to the improvements on the design, snags at maximum hoisting speed no longer automatically result in the highest snag load. It is therefore important to check all possible load-speed combinations.

Impact on productivity of a terminal

Due to the reduced hoisting speed, the cycle time of the STS crane increases. The impact of this increase on the productivity on a terminal can be calculated using simulation software. The impact of the increase in cycle time is likely to be small, since the cranes experience all sorts of delays, like waiting for the landside operations. This can prove to the customers that the selection of slower

hoisting cranes is justified, since the savings on this cheaper crane can then be spend elsewhere, to improve terminal performance.

12. References

[1] N. Zrni and K. Hoffmann, "Development of Design of Ship-to-Shore Container Cranes:1959-2004," *History of Machines and Mechanisms*, pp. 229-242, 2004.

[2] N. Zrnic, D. Oguamanam, and S. Bosnjak, "Dynamics and modeling of mega quayside container cranes," *FME Transactions*, no. 34, pp. 193-198, 2006.

[3] A.P. Moller - Maersk Group. (2011, Feb.) Maersk orders largest, most efficient ships ever. [Online]. http://www.maersk.com/AboutMaersk/News/Pages/20110221-114659.aspx

[4] A. Bhimani, Liftech Consultants Inc., "Quay crane accidents Lessons and Prevention," in *TOC Americas 2008*, Long Beach, CA.

[5] J. Erb, W. Jones, and R. Philips, "Coping with snags," *Cargo systems*, Jan. 1993.

[6] R. Philips and W. Jones, "Don't get caught out by snag," *Worldcargo News*, Jul. 1995.

[7] J. Verschoof, *Cranes - Design, Practice, Maintenance*. 2002.

[8] H. Oja, "Incremental innovation method for technical concept development with multi-disciplinary products," PhD Thesis, Tampere University of Technology, 2010.

[9] P. J. v. Dijk, "Safety systems against snag loads in cranes," TU Delft Literature research, 2007.

[10] B. A. Miller, "Wire ropes," in *Encyclopedia of Materials: Science and Technology*, 2004, pp. 1-10.

[11] L. Wiek, "Staalkabels: Geometrie en Levensduur," PhD Thesis, TU Delft, 1986.

[12] R. Verreet, *Casar Wire rope technical documentation*. 1997.

[13] M. Barnes, *Practical variable speed drives and Power electronics*. 2003.

[14] B. Drury, *The control techniques drives and controls handbook*. 2001.

[15] I. Siemens Industries, *Basics of AC drives*. 2011.

[16] EMG Automation GmbH, "ELDRO Electro hydraulic thrusters brochure," 2006.

[17] "Hirschmann for Doosan," *WorldCargo News*, Aug. 2007.

[18] J. I. Suh and S. P. Chang, "Experimental study on the fatigue behaviour of wire ropes," *International journal of fatigue*, vol. 22, pp. 339-347, 2000.

[19] A.G. Paton e.a., "Advances in the fatigue assessment of wire ropes," *Ocean Engineering*, vol. 28, pp. 491-518, 2001.

[20] J.B. Fortuin e.a., "Polytechnisch Zakboek," p. D1/16, 2006.

[21] H. H. Vanderveldt and J. J. Gilheany, "Propagation of longitudinal pulse in wire ropes under axial loads," 1970.

[22] J.M.N. Willis et. al., "Measurement and suppression of tension waves in arresting gear rope systems," 1950.

[23] G. Lodewijks, "Belt conveyor dynamics," *Lecture presented at TU Delft*, 2009.

[24] G.-J. Goedhart, "Criteria for (un)loading container ships," Masters assingment, TU Delft, 2002.

[25] U.S. Army Engineer Institute for Water Resources. (2010) NED manual series online. [Online]. http://www.corpsnedmanuals.us/DeepDraftNavigation/DDNPart1/DDNContMain.asp?PageID=30

[26] Maersk. (2011) Emma Maersk - Container vessel of Maersk shipping line. [Online]. http://www.emma-maersk.com/specification/

[27] Z. Zhiming and S. Cotterill, "China's first AC powered walking dragline in coal mining," in *MinExpo*, 2008.

[28] H. Kverneland, "Permanent magnet motors lead way to better power efficiency, safety on cranes, winches," *Drilling Contractor*, pp. 98-101, Jul. 2008.

[29] Malmedie Antriebstechniek GmbH , "Malmedie Snag Overload System Brochure," 2009.

[30] "Hydraulic-free snag system "now proven"," *WorldCargo News*, p. 46, Oct. 2010.

[31] J. Aotola, "Non Hydraulic Snag," *WorldCargo News*, Dec. 2010.

[32] D. Zhang, "Crane trim, list, skew and snag protection system," Patent US 7,624,883 B2, Dec. 2009.

[33] "Spreading some new ideas," *Worldcargo News*, pp. 36-38, Sep. 2009.

[34] ABB drives, *Technical guide book*. 2010.

[35] "Sweframe advert," *WorldCargo News*, p. 6, Jan. 2011.

Appendix A Scientific Research Paper

This page intentionally left blank

Analysis of Snag Loads in a Ship-To-Shore Crane

B.J. de Vette[a], W. van den Bos[b], C.A. Angevaren[c], J.C. Rijsenbrij[b]

[a] Student from the department of Transport Engineering and Logistics, Technical University Delft
[b] Department of Transport Engineering and Logistics, Technical University Delft
[c] Cargotec Netherlands B.V.

June 2011

Abstract— **One of the design issues in a container crane is to deal with the effects of a snag load in the hoist system. Snag loads are the shock loads which are exerted on the crane during hoisting when the load of the crane snags behind an object or jams inside a ship cell, due to skewing of the container. This paper focuses on the analysis of these types of load. A model of the hoisting system is constructed, to be able to calculate the snag load. Using this model, a number of improvements to the driveline are introduced and applied in a case study, to see the effects of these improvements. The improvements allow cranes to operate with empty spreader hoisting speeds up to 160 m/min without installing a snag protection device.**

I. Introduction

Ever since the beginning of containerisation, container ship sizes are increasing. Because of the demands on short cycle times for the cranes, port operators required faster hoisting speeds to keep up with the increased hoisting height. These increased hoisting speeds (up to 180 m/min for an empty spreader), introduced a new problem to STS cranes: snag loads.

Snag loads are the shock loads which are exerted on the crane when the load of the crane snags behind an object or jams inside a ship cell, due to skewing of the container (Fig 1). These shock loads can greatly exceed the normal operating loads of the crane, causing damage to the crane. This damage ranges from minor damage like bent rope sheaves mounting, to an entire boom collapsing.

Fig 1: Example of a snag due to skewing of the container (source: Cargotec)

Through time, a number of different devices were invented and installed on STS cranes to absorb or reduce the snag load. These mechanisms proved to be expensive, and required maintenance. It is therefore favourable to reduce the snag loads to a level where the crane is strong enough to withstand it without a snag protection device.

II. The Hoisting Mechanism

A. Wire rope reeving

There are a number of different possible configurations possible for the hoisting winch. This paper focuses on reeve-through trolleys, because this design is currently the main focus of Cargotec. With this design the hoisting winch is installed at the stationary machinery house of the crane, while the four hoisting ropes run through the trolley, which rides over the bridge girder.

At the tip of the boom spindles or cylinders are installed, which can extend and retract, to control movements of the container.

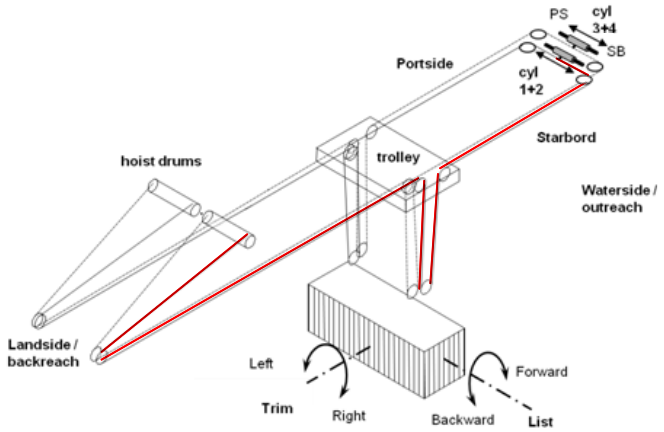

Fig 2: Example of wire rope reeving of a reeve-through trolley configuration (source: Cargotec)

The counterpart of this design would be a machinery on trolley system, where the hoisting winch is installed on the trolley. This configuration requires very short hoisting ropes.

B. Wire rope

The wire rope can be regarded as a linear elastic spring, for loads up to 55-60% of its minimum breaking load. During the lifetime of the rope, the stiffness decreases.

C. Hoisting winch

A typical hoisting winch consists of two rope drums, each carrying two hoisting ropes, and connected with each other through the gearbox. On the high speed shaft of the gearbox, one or two AC motors are installed, powered by a variable frequency drive, to control the hoisting speed. The electric motors can also be used as generators, reversing torque and converting mechanical into electric energy.

Brakes are installed on the rope drums and on the shafts of the motors.

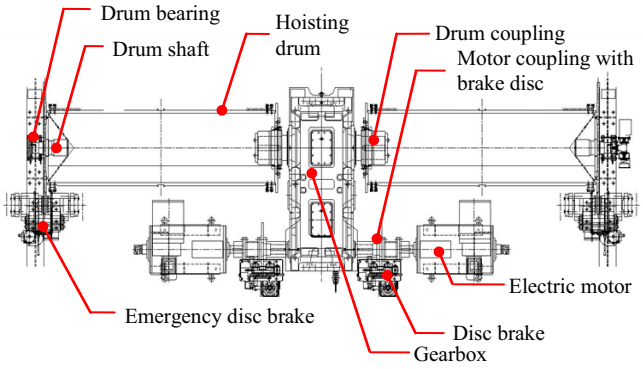

Fig 3: Layout of a typical hoisting winch with two hoisting motors

III. Description of a Snag Event

A. Types of snag

There are several possibilities in which a load can snag. The two main types which result in the highest loads on the crane are a 2-rope and a 4-rope snag.

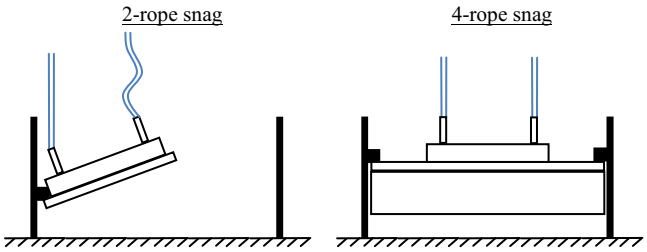

Fig 4: The load movement during a 2-rope snag on a 20' spreader, and a 4-rope snag on a 40' spreader

1) 2-rope snag: A 2-rope or eccentric snag is a snag at which only two of the four hoisting ropes are elongated by the winch. The ropes which are not stretched will eventually slack, due to the movement of the headblock and spreader. The free ropes can be assumed to maintain static rope tension, to simplify the calculation. The assumption can be verified by analysing the dynamics of the suspended load.

2) 4-rope snag: A 4-rope or centric snag is a snag at which all four hoisting ropes are elongated by the winch. Because all four ropes are stretched, the result tension in a single rope will be lower compared to the 2-rope snag, but the total vertical load on the crane will be higher.

B. Events during a snag stop

1. Load snags: rope tension starts to rise linearly, motor torque increases to maintain constant speed.
2. A load limit is exceeded:
   a. Rope tension limit: rope tension monitoring PLC sends a signal to the main PLC.
   b. Motor torque limit: The motor torque is monitored by the AC drive. When the torque limit is exceeded, the motor is switched off, and a signal is sent to the main PLC.
3. Emergency stop is activated by PLC. All brakes are applied and motor torque is reversed.
4. Together with the torque generated by the hoisting rope force acting on the drum, the winch is stopped.
5. Tension in the hoisting ropes is relieved by slowly releasing the brakes.

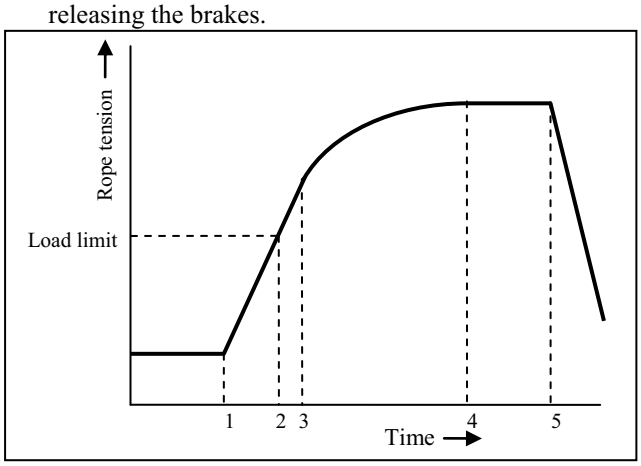

Fig 5: sketch illustrating the events during a snag using the development of rope tension through time

IV. Literature Study

There is little literature available on the subject of snag loads.

Casper & Philips consultants together with General Electric produced two articles in 1993 and 1995 regarding snag loads. The articles present the results from a calculation model on snag loads. The main conclusion from the research is that snag loads could be decreased by introducing a load limit which depends on the hoisted load. [1][2]

Design standards, like the FEM1.001 and EN13001, do not mention snag load separately, and treat the snag load as any other extreme load.

V. Model of the Hoisting Winch

The hoisting winch is modelled as a rotating inertia, which is connected to a number of linear springs, equal to the number of snagged ropes. The ropes which are not snagged will remain at static rope tension.

The following design parameters are found to have significant influence on the resulting snag load:

- Response time
- Winch inertia
- Hoisting power
- Hoisting speed
- Braking power
- Wire rope stiffness

The response times are calculated using the fact that rope tension increases linearly up to the point of detection. The increase in rope tension is determined by the hoisting speed and the wire rope stiffness.

The crane stiffness is taken into account by reducing the rope elongation with 6%. This factor was determined using FEM analysis on the crane, and corresponds to crane

deflection at minimum outreach, where the crane stiffness is highest.

VI. Calculation of the Snag Loads

A. Matlab/Simulink simulation model

Using Matlab/Simulink, the developed model can be solved using continuous simulation.

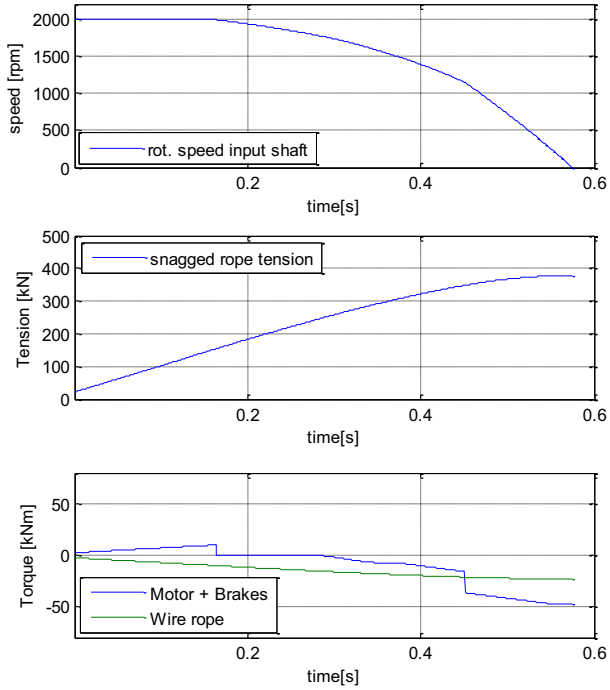

Fig 6: Result of a single simulation run of a 2-rope snag of an empty spreader at 180 m/min. From top to bottom: Rotational speed of the input shaft, rope tension and torques acting on the input shaft.

From a single simulation the results comprise of the variation of variables through time, i.e. the rope tension, speed and torque.

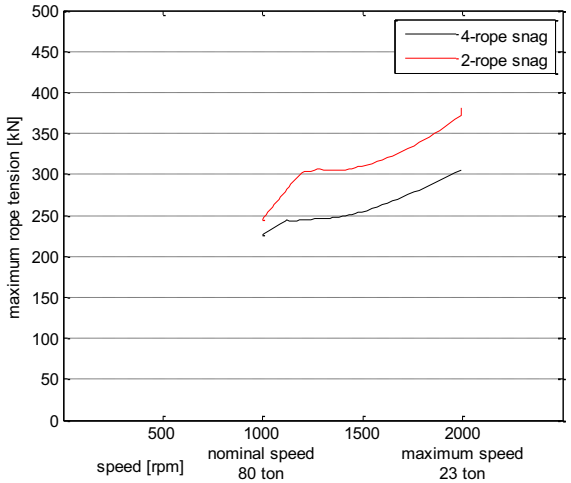

Fig 7: resulting rope tension of all possible duty points, for a 2-rope and a 4-rope snag

By executing multiple simulation runs while varying the input of the system, the dependence of the system on particular design parameters can be calculated, and the resulting rope tension for all possible duty points can be evaluated.

B. Validation

The model can't currently be validated, because no real world data is available regarding snag loads. Measurements on an existing crane should therefore be performed before implementing the improvements recommended in this research, to be sure the results of the model are correct.

C. Verification

The Simulink model is verified using a manual calculation on a simplified situation where no brakes are applied. The results from the manual calculation differ less than 1% from the simulation results.

Also an energy balance on the result of the simulation run can be performed. This shows that the total energy before and after the snag is equal, which strengthens the verification.

VII. Snag Loads on Existing STS Cranes

As part of the research, a number of cranes built between 1989 and now are analysed. Some of these cranes have an anti-snag device installed, but the influence of these devices was neglected during calculation. Using the results from this data, it is found that the snag load is not dependent on one single variable like the hoisting speed, but depends on a number of parameters (see paragraph V).

When combining the rope length and empty spreader hoisting speed, a correlation between these and the snag load is found. Using this results, and the improvements discussed later in this paper, an indication can be given of what speeds are possible without a snag protection device.

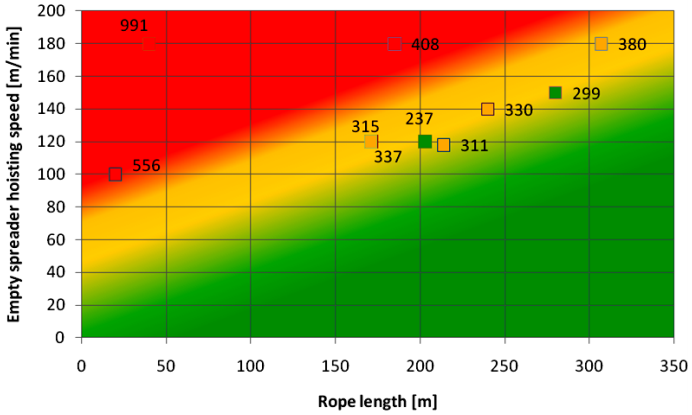

Fig 8: Indication on the possibility of operating without a snag protection device. Red = device required, green = no device required.

The figure indicates for example that machinery trolley cranes, which typically have a rope length less than 40 meters, cannot operate without a snag protection device at empty spreader hoisting speeds over 90 m/min.

VIII. Design Improvements

The design parameters mentioned in paragraph V will now be examined, to see if the snag load can be reduced.

The hoisting speed and minimum load are defined by the customer's requirements. These parameters result in a

minimum required hoisting power and braking torque. Within these requirements, there is some space to modify other parameters, which will be examined in this paragraph.

A. *Monitoring system*

The monitoring system should be improved to decrease the response time of the winch to a snag. This allows for faster stopping of the winch when a snag has occurred.

1) Bypassing PLC: When a rope tension limit is reached, the monitoring system sends a signal to the PLC, which will then start an emergency stop. By letting the monitoring system send the snag signal directly to the controllers of brakes and drives, the response time of these components to a snag is reduced by the time delay of the PLC, being 80 ms.

2) Variable tension limit: By setting a tension limit which is dependent of the actual load on the ropes, snag can be detected faster. The limit will be set at a value of the actual rope tension multiplied by a certain factor. This factor has to be set at a value as small as possible, while not creating too many false alarms due to natural variation in rope tension during hoisting operations. From prior measurements performed by Cargotec, the natural vibration of the rope tension during hoisting is found to have a maximum amplitude of 1.53 times the average tension. Therefore the overload factor will be set at 1.53.

B. *Winch inertia*

Reducing the winch inertia reduces the amount of energy stored in the winch. The winch inertia comprises of a slow speed and a high speed part. The inertia of the slow speed part is reduced through the gearbox to the high speed shaft for the calculations. Fig 9 shows the inertia distribution of the example crane. The ratio between the components is typical for STS cranes, and does not vary a lot depending on hoisting speed. However the total value of the inertia does depend on hoisting speed, since this determines the size of the motors and couplings.

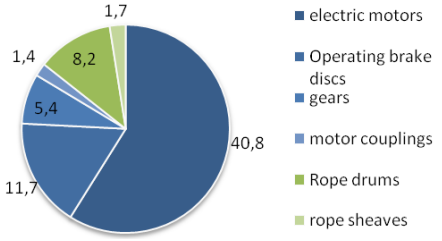

Fig 9: Inertia distribution of the example crane. Values are in kgm^2.

Fig 10 shows the influence of varying the winch inertia. It clearly shows that the winch inertia has great influence on the high speed snag, while the influence on a low speed snag is significantly smaller.

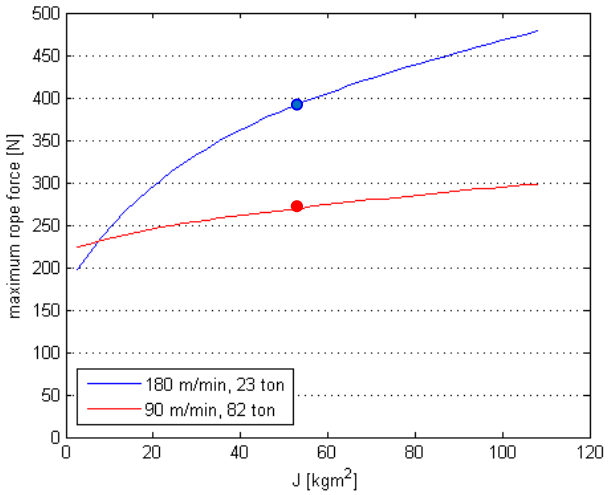

Fig 10: Influence of varying the winch inertia on the snag load of a 2-rope snag

C. *Selection of AC motors*

The required hoisting power is determined by the required speed and load. Using this required power, the AC motor is selected.

The AC motors should be as small as possible, reducing the inertia of the winch. By selecting AC motors which are just powerful enough for the task at hand, torque reserve is kept to a minimum, reducing loads on other parts of the winch. The overload also plays a role in the snag load.

1) 6-pole motor: The current motor is a 6-pole AC motor, powered by a variable speed drive. The motor can be overloaded depending on the size of drive.

2) 4-pole AC motor: By selecting a 4-pole motor, the motor size can be reduced compared with the original motor, since this motor has different characteristics. Also, by applying a high overload factor, the required motor size decreases.

3) Overloaded 6-pole AC motor: The current technology allows the AC motors to be overloaded up to a higher level compared with the 10 years ago. By selecting higher overloaded motor, a motor with smaller inertia will be able to produce the required power.

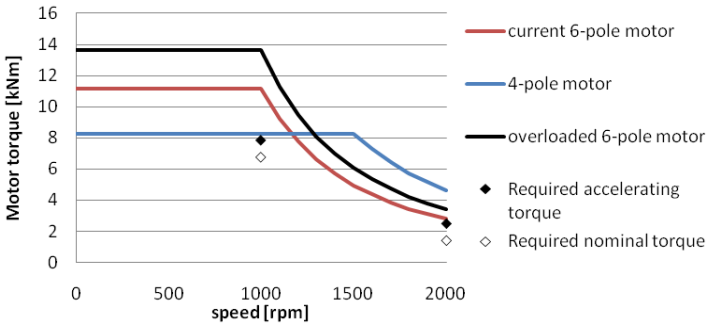

Fig 11: maximum allowable torque of three possible motors for the SPRC crane, together with two required duty points

Fig 11 shows the characteristics of the three possible motors. The 4-pole motor is determined by the nominal load at 1000 rpm, while the 6-pole motors are determined by the

high speed duty point which corresponds to empty spreader load.

In reality, the required acceleration torque for the 4-pole motor and the overloaded 6-pole will be slightly lower than the duty points for the original motor. This is caused by the reduced inertia of the motor.

D. Brake selection

Apart from the minimum required braking torque for safe stopping of the winch, the brake should be selected with two goals in mind: reducing brake response time and reducing brake inertia.

The braking torque is found to have little influence on the snag load, since the brakes respond relatively slow. It is therefore important to improve response time rather than torque.

The response times of the brakes depend on the closing time of the hydraulic thrusters. Brake manufacturers are currently working on faster closing operational and emergency brakes. These brakes should be selected to reduce the snag load.

The inertia of the brake can be reduced by selecting small brake discs.

E. Wire rope stiffness

Reducing the wire rope stiffness reduces the speed at which the rope tension rises during a snag. This allows the brakes to dissipate more energy. The hoisting ropes typically have a diameter of 28 or 30 mm. If safety factors on the nominal load allow it, it is highly recommended to use 28 mm rope, because it greatly reduces the stiffness.

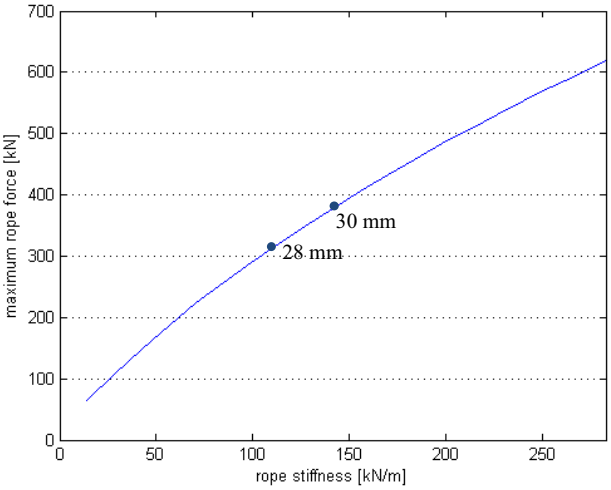

Fig 12: Influence of the wire rope stiffness on a 2-rope snag load

IX. MAXIMUM ALLOWABLE SNAG LOAD

The maximum allowable snag load will be regarded as the maximum rope tension at which the snag load is not normative for the design of the crane.

A. Construction

For the construction, this load can be calculated using the calculations from design standards, in this case FEM1.001. For most part of the construction of the crane, the fatigue load is governing. The snag load is treated as an extreme load case.

The fatigue load has a safety factor of 1.5 with respect to the yield stress, and is calculated as:

$$y_c \cdot (S_G + S_L \cdot \varphi) \quad (1)$$

y_c	=	amplifying coefficient	=	1.17
φ	=	Dynamic factor	=	1.2
S_G	=	Dead load		
S_L	=	Working load	=	820 kN

The extreme load has a safety factor of 1.1 to the yield stress. This load is calculated as:

$$(S_G + S_L \cdot \varphi) \quad (2)$$

S_L = Snag load = S_{snag}

Equation 1 and 2 can now be combined, together with the safety factors on the yield stress.

$$S_{snag} < \frac{1.5}{1.1} \cdot y_c \cdot (S_G + S_L \cdot \varphi) - S_G \quad (3)$$

All variables part from the dead load, are fixed for a single type of crane. The allowable snag load therefore depends linearly on the dead load.

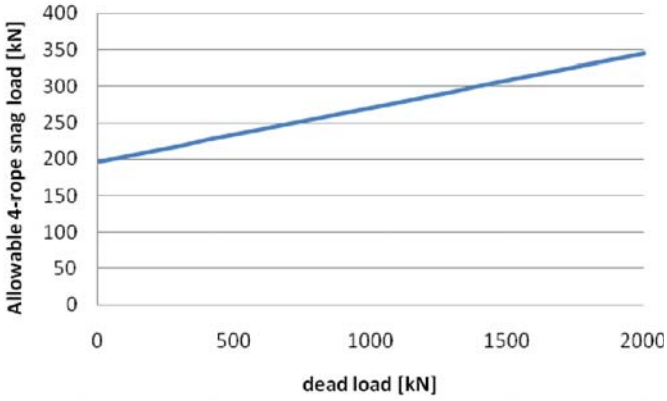

Fig 13: Relation of the maximum 4-rope snag load with the dead load acting on a part of the construction

1) 4-rope snag

Depending on what part of the crane is being analysed, the dead load varies. For example the dead load acting on the boom girder of the crane is equal to the trolley weight of 300 kN, which results in an allowable snag load of 1749 kN, which equals 219 kN of rope tension.

The forestay is subjected to a dead load equal to the boom weight: 1500 kN, which results in a maximum allowable rope tension of 308 kN.

2) 2-rope snag

The 2-rope snag limit for the construction depends on the type of bridge girder. A double box girder has a limit of 251 kN while a Monobox girder has a limit of 279 kN, due to its higher torsion stiffness.

B. *Mechanical components*

1) Tension loaded components: The tension loaded components of the crane are:

- Sheave bearings
- Rope drum
- Rope bearings
- Drum shaft
- Drum coupling

From analysis, is found that the critical component is the rope drum, which can sustain a maximum rope tension on every rope of 265 kN.

2) Torque loaded components: The torque loaded mechanical components are listed in the table below.

TABLE I
LOAD LIMITS VALID FOR THE SPRC CRANE

Limit	Value	
Construction, 2-rope snag	250	kN
Tension loaded components	265	kN
Construction, 4-rope snag	219	kN
Motor coupling	22.1	kNm
Drum coupling	660	kNm
Gearbox	760	kNm

X. CASE STUDY: 180 M/MIN WITHOUT AN ANTI-SNAG DEVICE

The design improvements mentioned in the previous paragraphs will now be implemented in a crane currently under construction. This super-post Panamax crane has a Monobox construction.

TABLE II
MAIN CHARACTERISTICS OF THE SPRC CRANE

Outreach		61	m
		22	containers
Duty points	Nominal load: 82 ton, 90 m/min		
	Empty spreader: 17 ton, 180 m/min		
Hoisting power		1460	kW
Nominal speed		1000	rpm
Wire rope length		177	m
Wire rope diameter		28	mm
Total winch inertia		54	kgm^2

With the original configuration, this crane is exposed to a 4-rope snag load of 326 kN of rope tension.

The following improvements are introduced to the design:

- Bypass PLC
- Variable rope tension limit
- Smaller brake discs
- Fast closing brakes
- Smaller motors with high overload factor

This reduced the 4-rope snag rope tension to 234 kN, which is still more than the maximum allowable snag load. Also, the torque on the motor coupling is 44 kNm, which is twice the maximum allowable torque. This torque load can be reduced by deactivating the operating brakes. These barely influence the rope tension from snag load, since they are activated very late.

To reduce the rope tension, the hoisting speed inside the ship cell will have to be reduced to 160 m/min, to reduce all loads below limits.

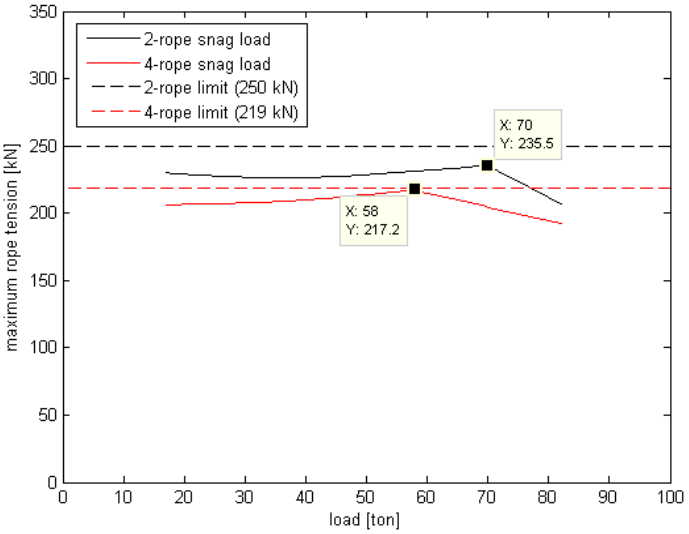

Fig 14: Resulting rope tension for a 2-rope and a 4-rope snag load. Dotted lines are the tension limits for both types of snag

The implementation of the reduced hoisting speed inside the ship cell will lead to an increase in hoisting time of almost 1 second. Assuming 40 moves per hour, this is an increase of 1%.

XI. CONCLUSIONS

With the improvements discussed in this paper, the snag loads on a crane can be reduced to acceptable levels. This way, a snag protection device can be left out, saving costs and maintenance.

To be able to sustain the snag loads, the hoisting speed inside the ship cell is limited to 160 m/min. This leads to an increase in cycle time of only 1 second.

The allowable snag load was based on supplier's information. The suppliers will also use safety factors, and the ultimate strength will be higher than the limit currently used. To find the real limit of the components, suppliers should be consulted.

The data used during calculation, i.e. the response times of the components, have a significant influence on the results. Measurements should therefore be performed to validate the data.

REFERENCES

[1] J. Erb, W. Jones, and R. Philips, "Coping with snags," *Cargo systems*, Jan. 1993.

[2] R. Philips and W. Jones, "Don't get caught out by snag," *Worldcargo News*, Jul. 1995.

[3] J. I. Suh and S. P. Chang, "Experimental study on the fatigue behaviour of wire ropes," *International journal of fatigue*, vol. 22, pp. 339-347, 2000.

Appendix B Existing anti-snag systems

There are several designs of anti-snag systems currently in use in STS-cranes, which will be described in this paragraph. These systems can be divided on their principle of operation, being either hydraulic or mechanical. Also some patents on anti-snag systems will be examined.

B.1 Hydraulic systems

Hydraulic anti-snag systems consist of a hydraulic cylinder, which acts as a buffer for the wire rope. In case of a snag situation the cylinder retracts, releasing the stored rope length. This way the tension in the rope does not rise too high, while the winch is slowing down during the emergency stop.

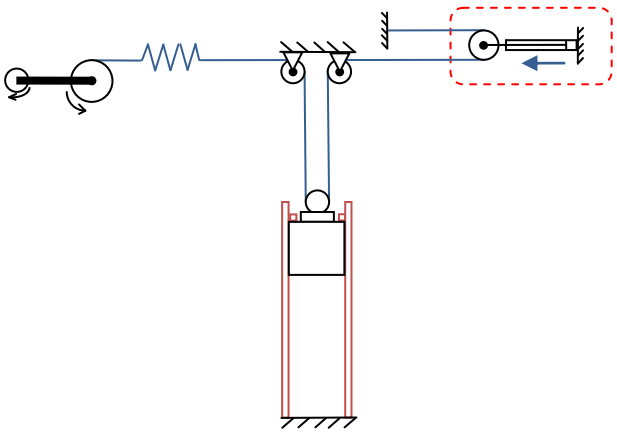

Figure B.1: simplified model of a hydraulic anti-snag device

B.1.1 Rima TLS anti-snag system

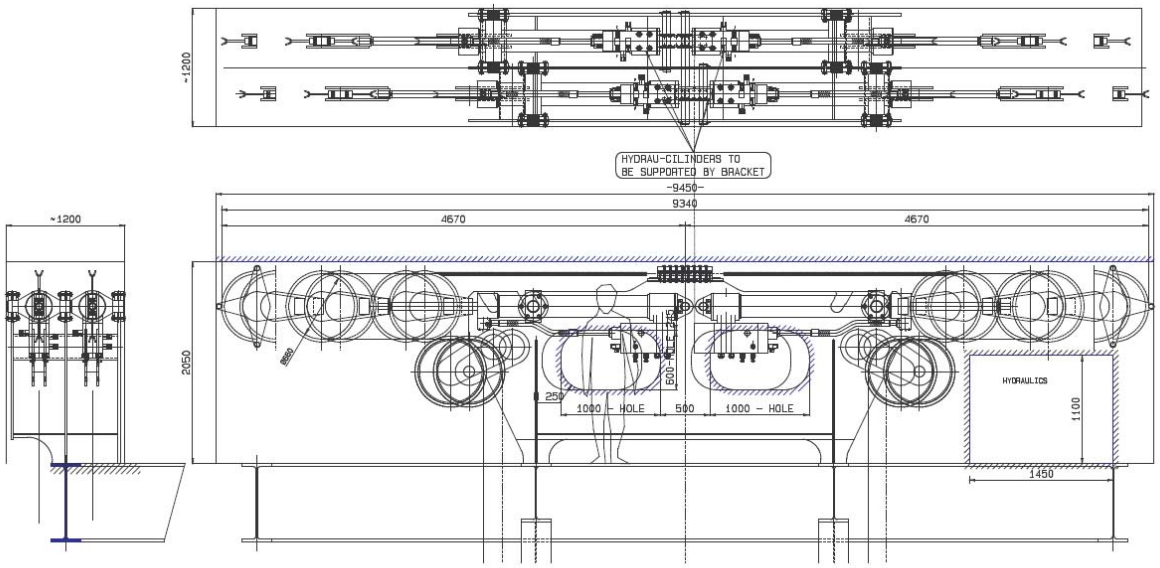

Figure B.2:Technical drawing of a hydraulic anti-snag device used by Kalmar (source: Cargotec)

This anti-snag system designed by Rima consists of 4 hydraulic cylinders, one for each of the 4 hoisting ropes. It is currently applied in a number of cranes designed by Kalmar, i.e. in the port of Antwerp at the MSC Home terminal and the Duerganck terminal.

During normal operation the cylinders are partially extended, which can then be used for trim and list adjustments to the load, for angles up to 5 degrees.

In case of a snag load an overpressure will develop in the hydraulic cylinders, which will trigger a pressure release valve. This will short-circuit hydraulic piping to the reservoir, causing the cylinders to retract. The valve will also cut the power to the complete hoist drive, causing the emergency brakes and service brakes to close. By letting the pressure switch cut the power to the complete hoist drive, the normal monitoring system is bypassed, reducing the response time of the system.

The tension in the hoisting ropes is measured in the cable sheaves located below the cylinders. These load cells monitor for cases of general overload, underload or uneven load distribution. In these cases, the service brakes are used.

The snag release happens at a hydraulic force of 390 kN, which corresponds to a maximum rope force of 195 kN due to the mechanical advantage. The response time of this pressure release valve is 4.3 ms according to manufacturer specifications.

In operation	350 kN, dynamically
Snag release at	390 kN, statically
Peakforce cylinders at snag	450 kN, statically
Cylinder speed at snag	3 m/s

Figure B.3: operating pressures of the hydraulic cylinders

Figure B.4: picture of the anti-snag device installed in an STS-crane at the MSC Delwaidedok terminal in Antwerp (source: Cargotec)

B.1.2 ZPMC

Figure B.5 shows an anti-snag device which is installed on STS-cranes located on the Euromax terminal in Rotterdam, which were constructed by ZPMC. It uses the same principle as the previously described system. The difference is that this system is installed on the back of the main girder, exposed to the environment, whereas the Kalmar system is installed in the machinery house. The benefit of the ZPMC configuration is that no additional adjustments need to be made to the reeving system, compared to an STS crane without anti-snag device.

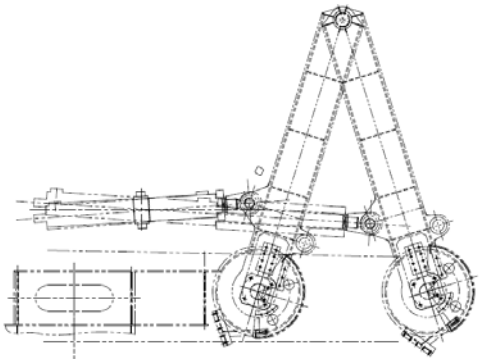

Figure B.5: side view of a ZPMC anti-snag device (source: Cargotec)

An alternative used by ZPMC is the anti snag device installed in several dual hoist-single trolley STS-cranes at the HHLA terminal of Hamburg. Because it is a dual hoist crane, 8 hoisting ropes are present in the crane, resulting in 8 anti-snag cylinders. In Figure B.7, 6 of these anti-snag devices are visible.

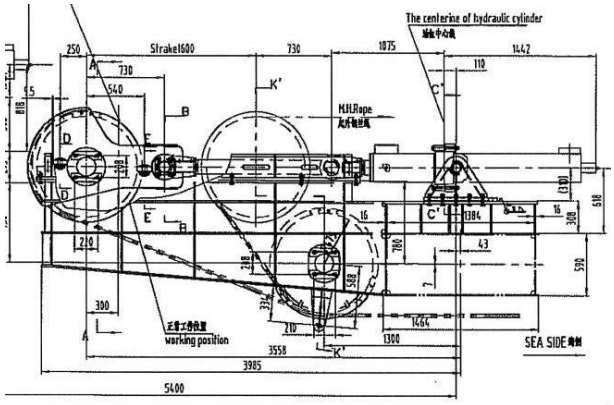

Figure B.6: Drawing of the side view of a ZPMC anti-snag device (source: Cargotec)
Figure B.7: Picture of the backreach of a dual hoist STS crane in operation in Hamburg. 6 of 8 anti-snag devices are visible (source: Cargotec)

B.2 Mechanical systems

There is a variety of mechanical anti-snag systems available. The systems are either based on friction or on couplings which can break away at a set torque limit.

B.2.1 Pintsch Bubenzer-Malmedie SOS-system

This system consists of Malmedie safety couplings (MSC) which break away at a certain torque limit, combined with a brake system provided by Bubenzer. It was developed in cooperation with Casper, Philips & Associates, a crane consultancy company.

The couplings are installed in between the motors and the service brakes, as is shown in Figure B.8. When a snag occurs, the couplings disconnect the motors from the service brakes and gearbox, greatly reducing the inertia connected to hoisting ropes. Sensors detect the tripping of the MSC, after which a plc will activate the service and emergency brakes, stopping the output shaft and preventing

the drums from reversing. The brakes are quick setting brakes, resulting in a total stopping time of 100 to 200 ms.

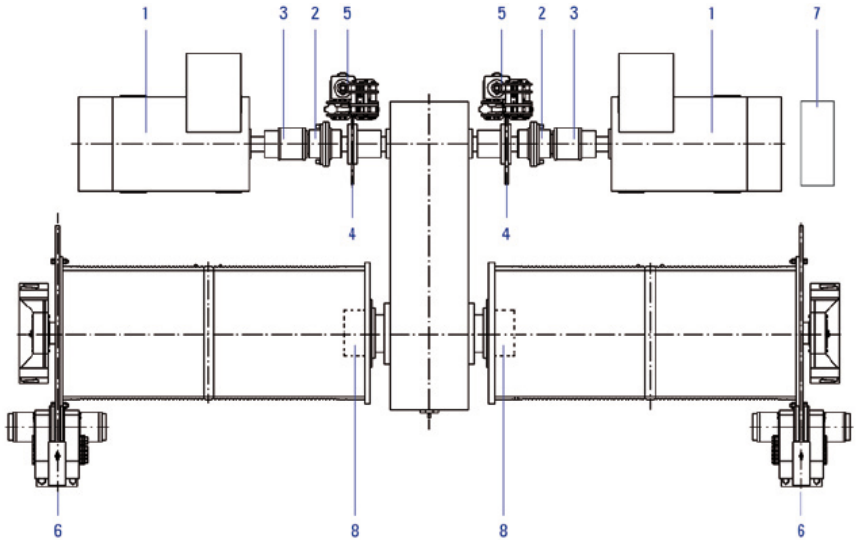

Figure B.8: Configuration of the Bubenzer-Malmedie system. The safety couplings are indicated by number 2.

The MSC itself consists of two disks, connected by balls which are nested in ball sockets. These balls transfer the torque from the input to the output disk. When the torque exceeds the torque limit, the balls release out of their sockets, no longer transferring the torque. After a snag situation, the balls can be reset manually within 5 minutes. Automatic reset is also an option, but is not recommended for safety reasons.

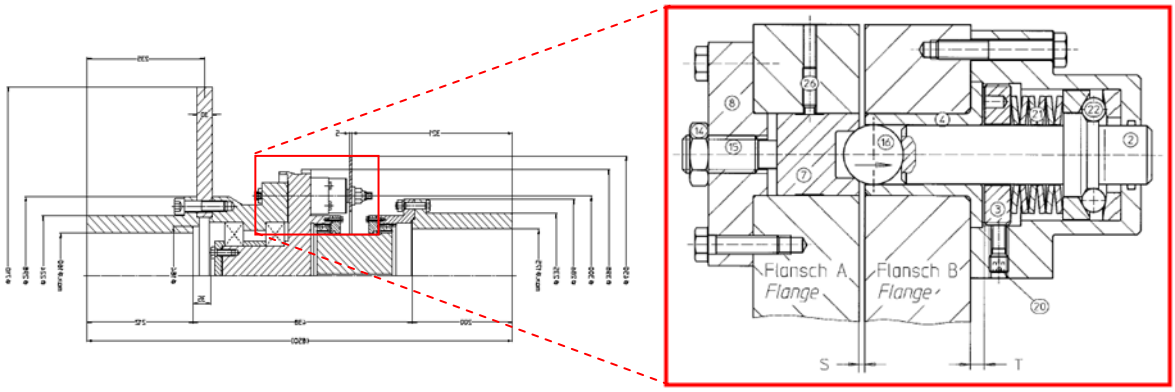

Figure B.9: cross section of the Malmedie Safety Coupling, with a detail of the ball and socket assembly

The total system has a mass of 500 kg, and requires about 3 hours of maintenance per year.
With this system, an emergency stop can also be initiated by surpassing a variable load limit, as was described in 8.1.3. This is required to be able to respond to single rope overloads as well. The safety coupling would be too slow to respond, since the torque will be increasing slowly during a single rope overload. The load monitoring is performed by Tecsis load cells located in the hoisting sheaves. The delay between a rope tension exceeding the tension limit and the signal being sent to the emergency brakes is 12 ms. Depending on the hoist drum speed, setting of the emergency brakes might trip the safety couplings. [9] [29] [30]

B.2.2 Friction based anti-snag system

The mechanism described in US patent no. 6,145,680 operates in the same way as the ones described in paragraph B.1.2. The only difference being that this mechanism operates on friction instead of hydraulic pressure. Since 1990, the system has been successfully installed in 40 cranes manufactured by Konecranes. [31]

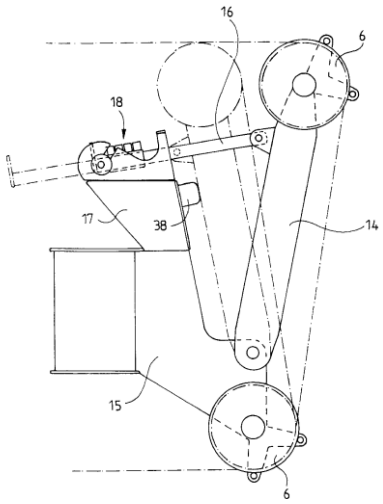

Figure B.10: Schematic drawing of the friction based anti snag system used by Konecranes. The friction part is indicated by nr. 18

B.2.3 Friction coupling

US Patent no. 0136752, dating july 2003, describes a system where the end of the hoisting ropes is connected to a small drum. This drum is than connected to a small electric mtoor through a friction coupling. During normal operation, these small motors are used for trim and list adjustments.

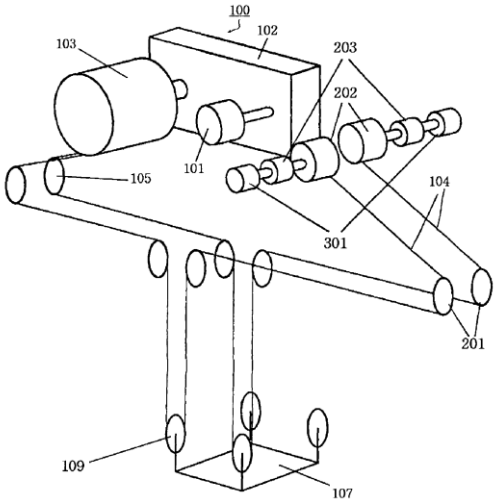

Figure B.11: Overview of the reeving system, with the friction couplings indicated by 203

In case of a snag situation, the friction couplings will start slipping because of the increased torque. This will result in extra rope length being released from the drums, which prevents the rope tension from rising too high.

B.2.4 Trim, list, skew and snag protection system with dual diameter drum

This system, patented in 2009 [32] utilizes a dual diameter drum as a buffer for the wire rope.

The working principal of this mechanism can be explained using Figure B.12.

The hoisting rope runs over a sheave (20) that's connected to a second sheave (26). The distance x between this second sheave (26) and the dual diameter drum (44) can be varied by rotation of the drum. The wire connecting the second sheave and the drum is wrapped around the drum at the smaller diameter and at the larger diameter in opposite directions.

The torque T acting on the drum is determined by:

$$T = \mathrm{F_{rope}}\,\frac{\mathrm{D}}{2} - \mathrm{F_{rope}}\,\frac{\mathrm{d}}{2} = \frac{\mathrm{T}}{2}(\mathrm{D} - \mathrm{d}) \qquad \text{(B.1)}$$

F_{rope} = Rope tension

D = Larger Diameter

d = smaller diameter

Δx is determined by:

$$\Delta x = \alpha\frac{D}{2} - \alpha\frac{d}{2} = \frac{\alpha}{2}(D - d) \qquad \text{(B.2)}$$

The drum is driven by an electric motor, which is connected to the drum through a friction coupling. During normal operation, the electric motor can be used to adjust distance x. This way the trim, list and skew of the spreader can be adjusted.

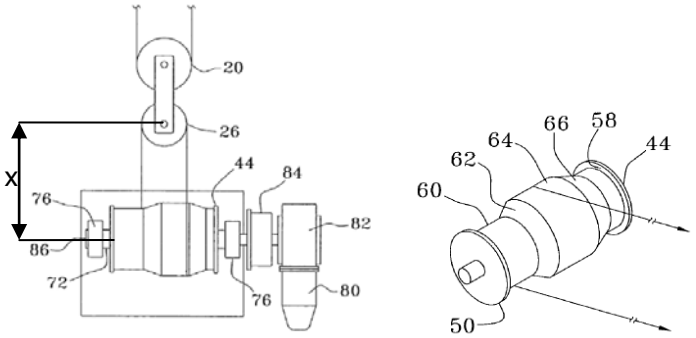

Figure B.12: Assembly of one of a total of four TLSS systems installed in a crane

In case of a snag load, the tension of the hoisting rope will rise, which causes the torque acting on the drum to rise as well. The torque will cause the friction clutch to start slipping. As indicated in Figure B.13, the rope on the drum will spool up at the smaller diameter, and spool off at the larger diameter. Because of the rotation of the drum, the distance x increases, which allows the main hoisting drums time to stop without stretching the main hoisting ropes too far.

At instance b, the rope will start to climb up the slope of the drum at the smaller diameter, while it will start to climb down the slope at the larger diameter. This causes the ratio between the diameters to decrease, which decreases the torque on this drum, which is equal to the torque on the friction clutch. The friction clutch will have to be dimensioned in such a way, that it will not slip during normal operation, while it will slip in case of a snag load.

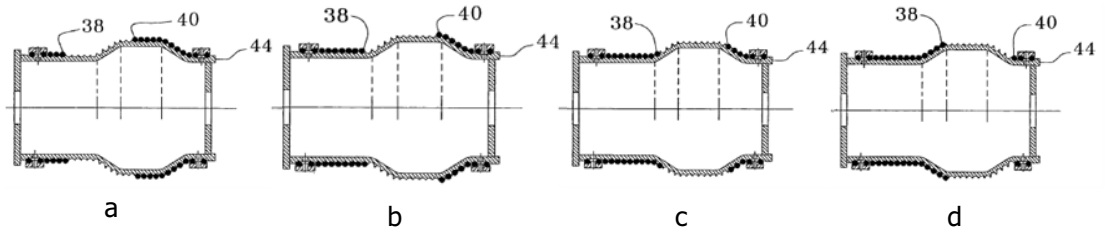

Figure B.13: travel of the rope on the dual diameter drum during a snag event

B.2.5 Stinis split headblock

This headblock is designed by Stinis for tandem lift operation of two 40' containers. It has rope sheave frames which are mounted on a joint, allowing them to rotate during a snag. This prevents the hoisting ropes from being damaged due to a too large fleet angle during a 2-rope snag. According to Stinis, a rotation of the spreader as small as 7-10° can destroy a wire rope and severely damage the rope sheave. These angles can be easily surpassed during a snag event, as can be seen in Figure 1.6.

The rotating sheave mounting has another advantage: it allows for detection of a 2-rope snag by detecting spreader rotation.

These measurements can also be used to measure trim caused by eccentric loading. When lifting eccentric loads deep inside a ship with a large STS crane, the difference between the PS and SB rope elongation could cause a snag event, due to skewing of the container. By monitoring this angle, the container can be levelled before hoisting. [33]

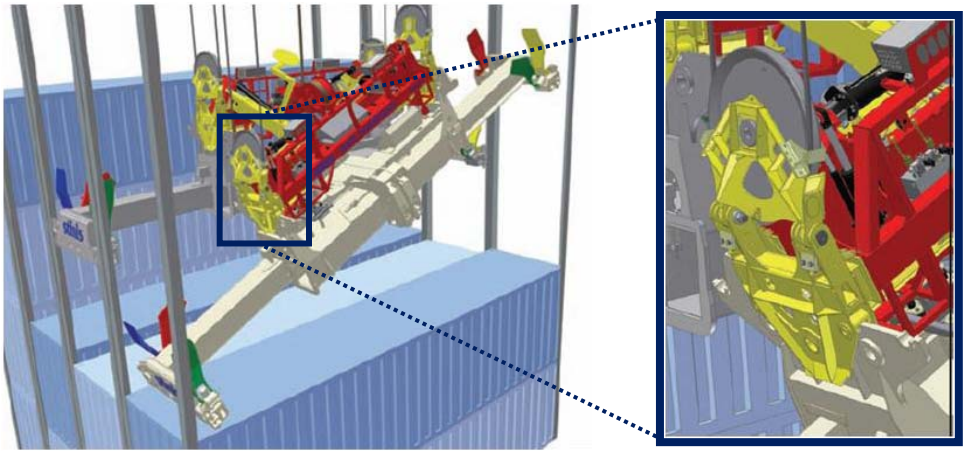

Figure B.14: Artist impression of a snagged Stinis split headblock with rotating hoist sheave mounting [33]

Appendix C Variable speed AC motor characteristics

A squirrel cage AC motor consists of a rotor and a stator, which is fed by the three phase AC source. The stator produces a rotating magnetic field. The rotor will rotate slower than this field, creating a speed difference. Because of the speed difference, a current will flow through the rotor. Due to the construction of the rotor, this current will create a magnetic field. The rotating field of the stator will therefore produce a torque on the rotor, causing it to rotate.

This speed difference between the rotor and stator is called the slip of the rotor, which usually has a value of 2-4%. If the load increases the slip will increase, causing a larger current to flow through the rotor, which will result in a higher output torque. The speed at 0% slip will be the synchronous speed. This cannot be reached, since slip is required to produce torque.

The nominal speed of an AC motor can be expressed as:

$$n_0[rpm] = \frac{f[Hz] \cdot 60}{p/2} \tag{C.1}$$

f=supply frequency

p=number of poles

The full-load torque (also known as nominal or continuous torque) is the torque which the motor is able to produce constantly at nominal speed without overheating.

The produced torque can increase until it surpasses the stall torque, typically around 350% of nominal torque for the hoist motors. At that point the required torque will be too high for the motor, causing the motor to stall, as shown in Figure C.1. Reaching this point can be very dangerous for hoist drives, since this will cause the load to drop. Therefore, a maximum allowable torque will be set at:

$$T_{max} = f_a \cdot T_{nom} \tag{C.2}$$

The factor f_a for the hoist motors will usually range from 1.6 up to 2.5.

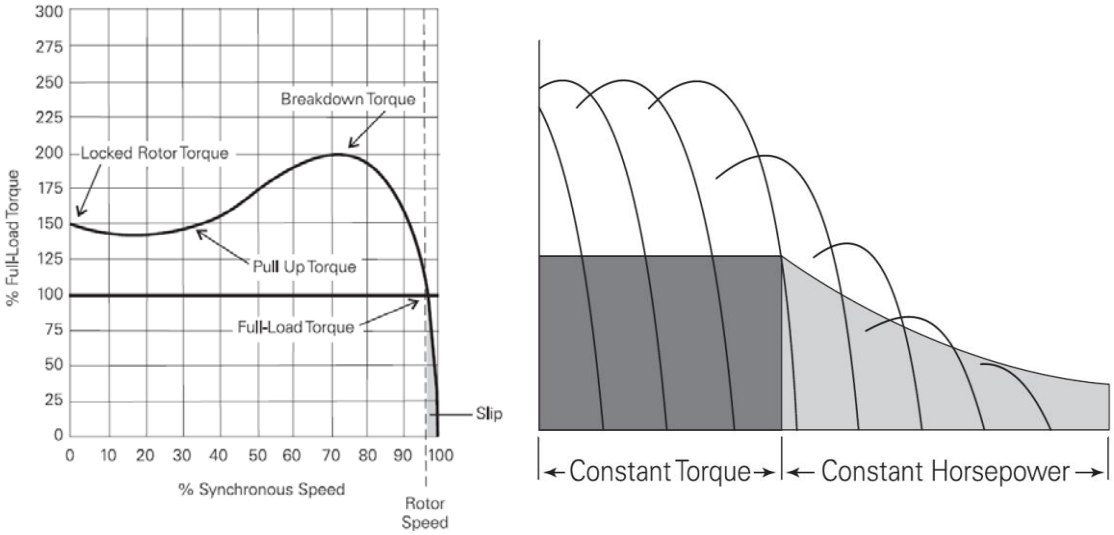

Figure C.1: Speed-torque diagram of a 3-phase asynchronous motor at a single supply frequency. Full load torque=nominal torque, breakdown torque=stall torque.
Figure C.2: Speed torque curves of a single AC motor at different supply frequencies. Dark part is below nominal speed, light grey part above nominal speed (field weakening range)

The frequency controllers allow for stepless speed control of the electric motors, by adjusting the supply frequency of the electric motor. By changing the supply frequency of the motor, the characteristics of the motor can be shifted throughout its speed range. Up to the nominal speed of the motor (usually at 50 Hz), the produced torque remains constant, as is shown in Figure C.2.

To make the motor run at higher speeds than nominal speed, the frequency can be increased over the nominal frequency. The nominal torque will decrease along the line of constant power (P=T·n). However the stall torque is proportional to the square of the magnetic flux. Therefore it is inversely proportional to the square of the supply frequency [34]:

$$T_{max} \sim \left(\frac{f_{nominal}}{f_{supply}}\right)^2 \quad \text{(C.3)}$$

This characteristic is shown in Figure C.2, where the Torque-speed graphs for different supply frequencies scale down faster than nominal torque.
For safety purposes, the maximum allowable torque will scale down in the same fashion. This means that at some point, the maximum allowable torque will be higher than nominal torque.

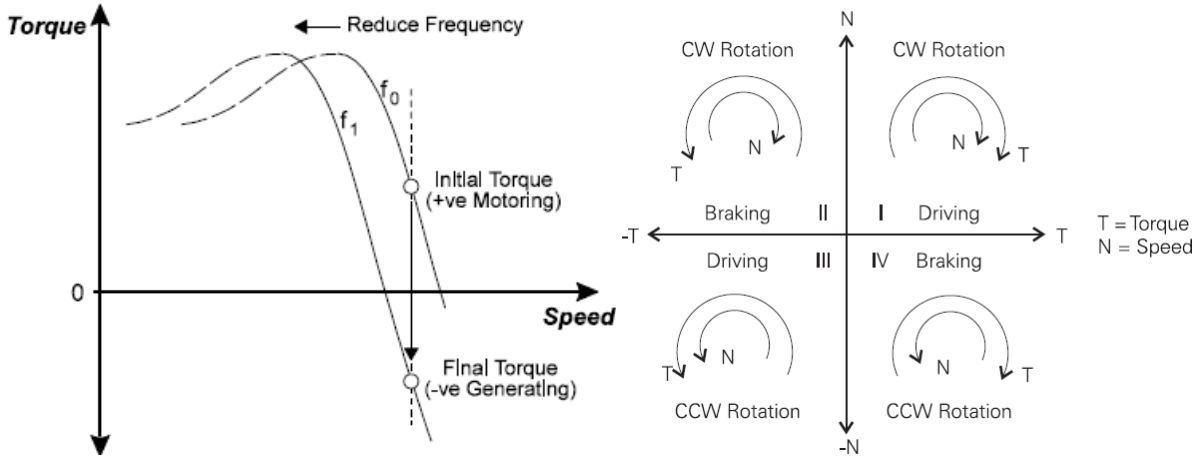

Figure C.3: The effect of dynamic braking, by changing the supply frequency
Figure C.4: The four possible quadrants of operation

The motor can be used for braking as well, by reducing the supply frequency. If the speed of the rotating magnetic field of the AC motor is reduced below the rotational speed of the rotor, the magnetic field of the rotor will reverse. Therefore the motor will start braking, and current direction in the stator is reversed. Figure C.4 shows the four possible combinations of torque and speed direction of the motor. A hoist motor will usually only operate in quadrant I or IV, because the load direction will always be the same due to gravity. In case of an emergency stop during hoisting, it is possible to operate in quadrant II, because the inertia of the motor needs to be stopped. This is also the case in a snag situation. [13] [15]

Appendix D Ideas for anti-snag solutions

This thesis focused on improving the current hoist system of a crane in such a way that the snag load is reduced as much as possible. Depending on the parameters of the crane, an anti-snag device is or is not required to keep the rope tension below the limits.

During this master assignment, some ideas for anti-snag solutions were developed, which could decrease the rope tension during snag events. These ideas were not worked out into detail, since this was not the focal point of the project, however, the ideas will be described briefly in this appendix.

D.1 Addition of wire rope falls

D.1.1 Principle

By adding an additional rope sheave at the headblock to the reeving, the amount of rope falls is doubled. That way, the maximum load during normal operation will be halved, which allows for a smaller hoisting rope to be used. A smaller hoisting rope has a higher elasticity, which will result in a lower resulting rope tension caused by snag. The sheave diameter can also be reduced, due to the smaller wire rope diameter.

There are also disadvantages to this change in the reeving system. First, four additional rope sheaves will have to be added to the headblock, increasing its weight and complexity. The second disadvantage is the introduction of additional bending of the wire rope and doubling the wire rope speed, which both reduce the fatigue life of the rope.

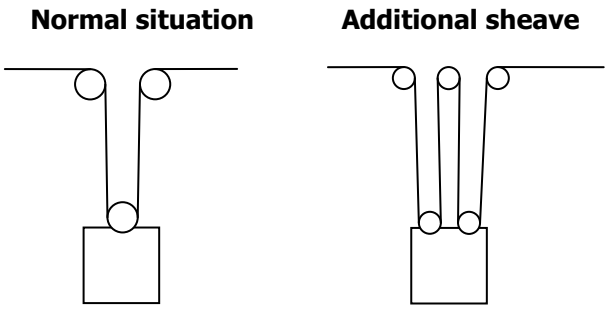

Figure D.1: wire rope reeving change for one rope corner
Figure D.2: Picture from an advert of SweFrame, showing a headblock with additional rope parts [35]

D.1.2 Example

The HNN MSC crane, which was used previously in section 5.3, will be investigated to see what the influence of this change on the snag load will be.

The new wire rope will be selected in such a way that it will have the same safety factor on the nominal centric load as the current wire rope.

The safety factor of the current wire rope on nominal centric load is:

$$\frac{640\ kN}{\frac{80\ ton \cdot 9.81}{8\ rope\ parts}} = 6.5$$

The rope tension on the doubled wire rope reeving with nominal centric load is:

$$\frac{80\ ton \cdot 9.81}{16\ rope\ parts} = 49kN$$

This results in a required minimum breaking load of 49 x 6.5 = 319 kN. A 22 mm diameter wire rope can now be selected, which has a minimum breaking load of 313 kN for 1960 N/mm^2 quality.

Due to the extra rope length of the rope falls, the stiffness of the wire rope will be decreased even more.

	Rope type	Diameter	Area	Minimum breaking load	stiffness
Current wire rope	6x36 WS + IWRC	30 mm	414 mm^2	640 kN	142 kN/m
New wire rope	6x36 WS + IWRC	22 mm	223 mm^2	313 kN	67 kN/m

Table D.1: data of the current wire rope and the selected wire rope with the improved reeving system

The original wire rope leads to a total snag load of 376 kN for a 2-rope snag of an empty spreader at 180 m/min. The improved wire rope reeving reduced the rope tension during snag to 235 kN. This is a reduction of 38%. The loads on some of the tension load components of the crane will therefore decrease by 38%. However, because of the doubled reeving, the total load on the crane will increase by 25%.

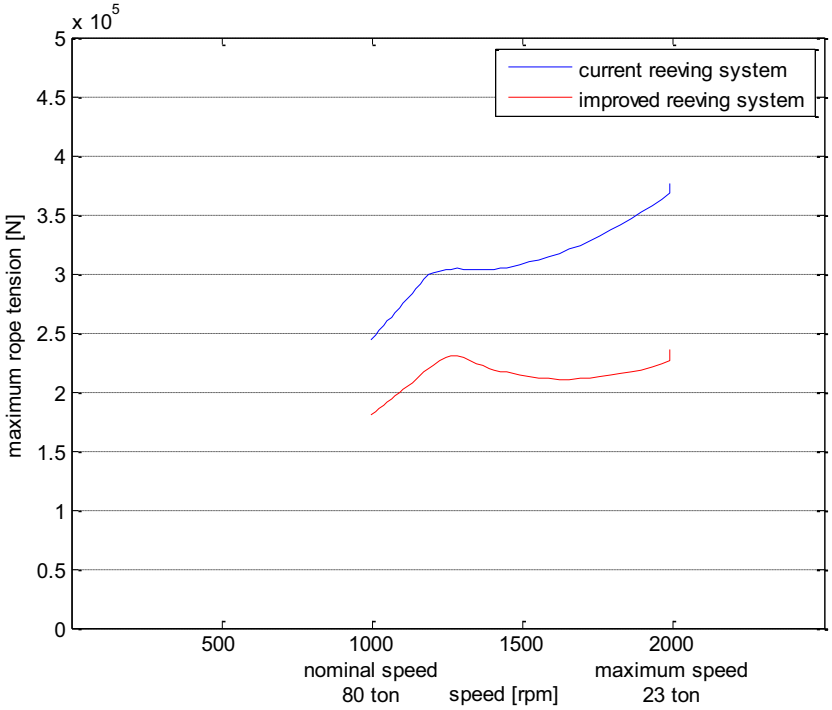

Also, the safety factor on the snag load has decreased. For the current wire rope the safety factor on snag is 1.7. With the changes in the reeving system, the safety factor has reduced to 1.33.

D.1.3 Conclusion

The addition of rope parts in the reeving to the trolley is not a good solution in reducing the snag load. Although the rope tension has decreased, the total load on the crane structure will increase and the safety factor on the wire rope decreases.

D.2 Mass to limit the maximum rope tension

By introducing a mass in the reeving system, supported by the structure of the crane, the rope tension can be limited. When the load tension exceeds the tension limit in case of a snag, the mass will be lifted from its base, preventing the rope from being stretched even more. While the winch is being stopped, the mass moves upwards.

The mass will have to be determined at the value at which it is in balance with the maximum allowable rope tension. The examples below show estimates of the required mass, but these values neglect the inertia effect when accelerating the buffer mass.

Normal operation **Snag**

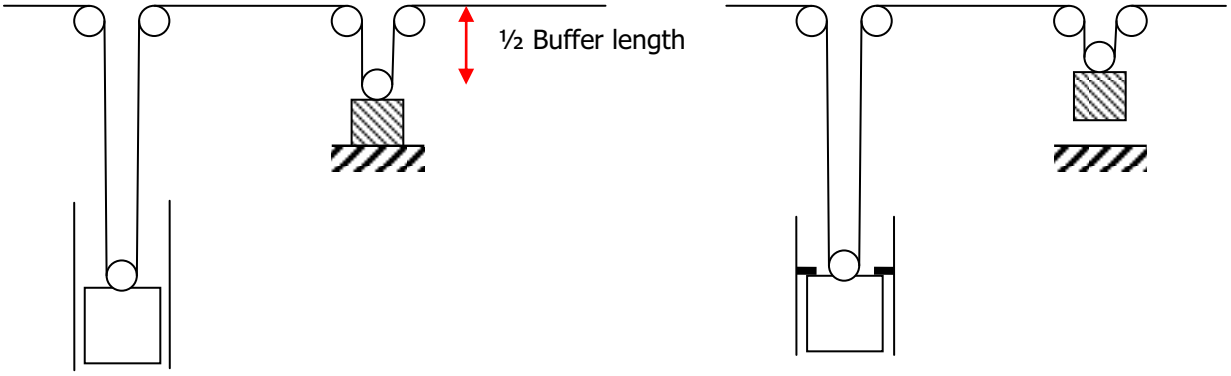

$$m = 2 \cdot \frac{F_{rope\ max}}{g}$$

$$required\ stroke = 0.5 \cdot required\ buffer$$

The solution described above requires a lot of mass to be added to the crane. With a maximum rope tension of 200 kN, it will be required to install four masses of 40 tons each, somewhere in the crane.

It would be beneficial if the masses can be installed at the landside legs, since a lot of cranes add counterweight at this location. If this is not possible, the weight has to be reduced. Two ways to reduce this weight are displayed below.

Normal operation **Snag**

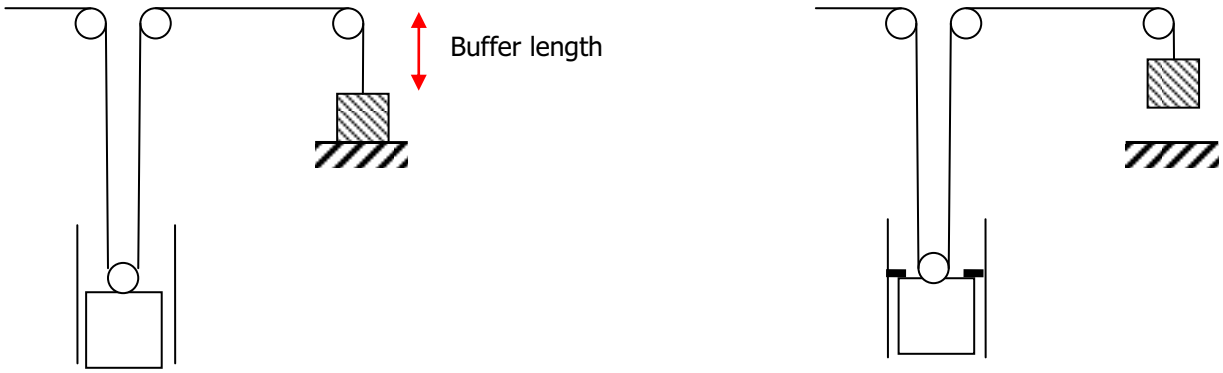

$$m = \frac{F_{rope\ max}}{g}$$

$$required\ stroke = required\ buffer$$

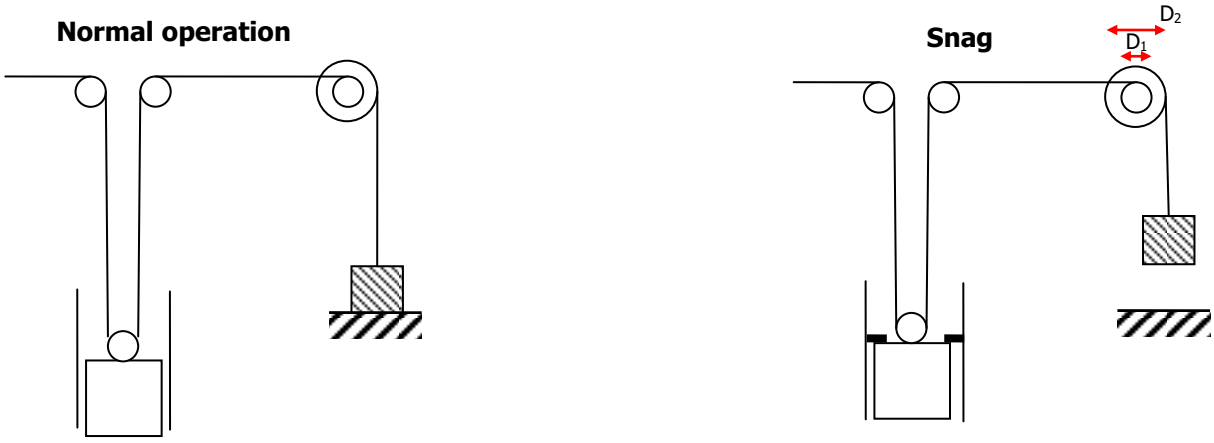

$$m = \frac{D_1}{D_2} \cdot \frac{F_{rope\ max}}{g}$$

$$required\ stroke = \frac{D_2}{D_1} \cdot required\ buffer$$

D.2.1 Pulley solution

By adding pulley's to the buffer mass rope, the required mass can be reduced even further. It does however introduce other difficulties, like the maintenance of these pulleys.

A benefit of this configuration is that a spindle could be attached to the secondary rope, so that the trim and list movements of the container can be controlled from this position.

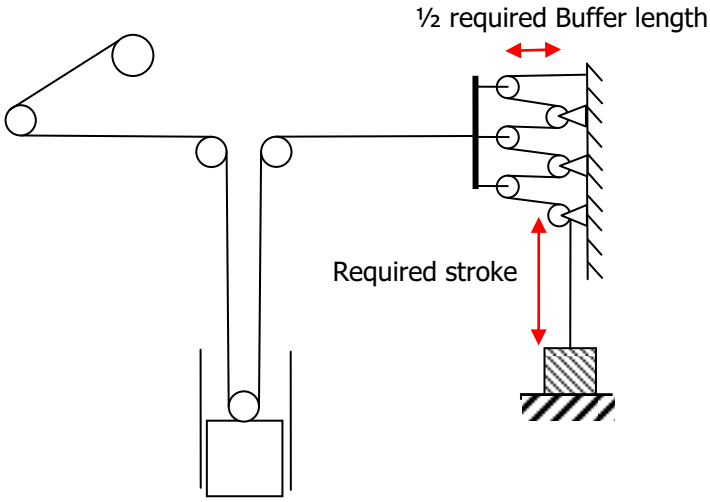

$$m = \frac{F_{rope\ max}}{g \cdot n_{rope\ falls}}$$

$$required\ stroke = required\ buffer\ length \cdot n_{rope\ falls}$$

A better location for the buffer mass will be somewhere on the backreach, since this is creates a more preferable loading of the crane regarding balance.

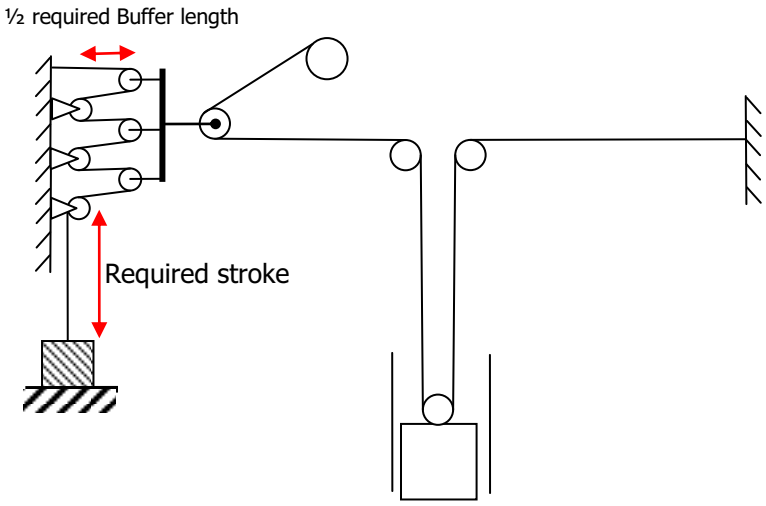

D.2.2 Conclusion

This concept has the possibility to limit the rope tension to a certain limit, depending on the mass. It does require four of these mechanisms to protect all the hoisting ropes, so a lot of mass will have to be added to the crane. Using pulleys, this mass can be reduced, but the dynamic effect of the added friction should then be investigated.

Besides, it can be questioned if a pulley mechanism can function when it only moves a few times in a year, when a snag occurs.

D.3 Spring based rope buffer

D.3.1 Increasing wire rope elasticity

By introducing more elasticity into the reeving system, the rope tension will rise less quickly during a snag event. Also, more energy will be absorbed by the ropes. This will result in a lower rope tension caused by snag, as was indicated in section 8.6.

Elasticity could be added by adding a spring to reduce wire rope stiffness:

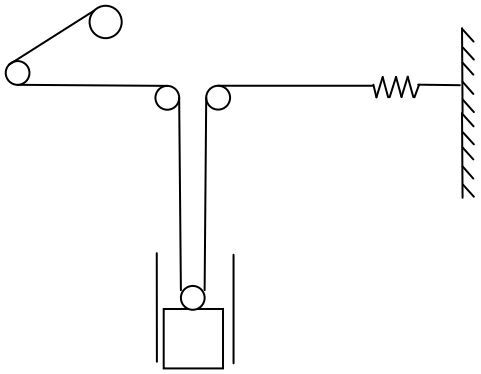

Figure D.3: adding elasticity to wire rope reeving

D.3.2 Spring based non-linear snag system

This mechanism is based on a principle of buckling. During normal operation, the mechanism allows very little movement, due to its dimensions. When the rope tension exceeds a certain limit, the mechanism 'collapses', allowing rope to be taken in at the winch without increasing the tension.

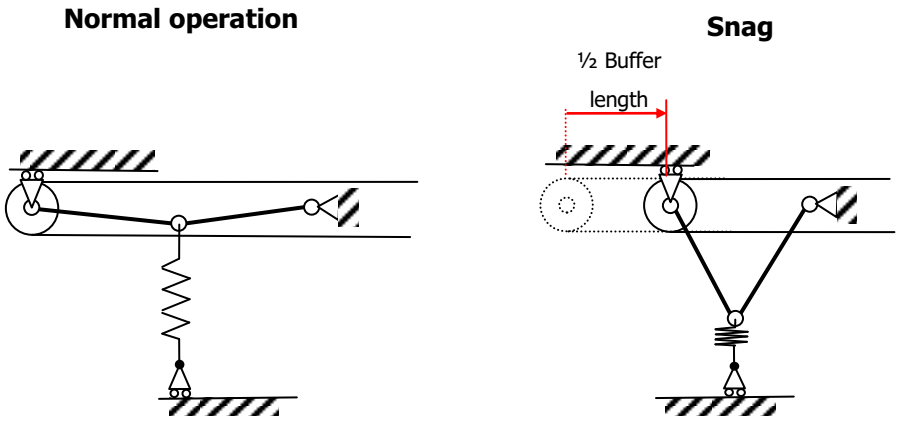

D.3.2.1 Analysis of the mechanism using principle of potential energy

The buckling of the mechanism can be analyzed using the principle of potential energy. The point of buckling can be determined, as well as post-buckling behaviour.

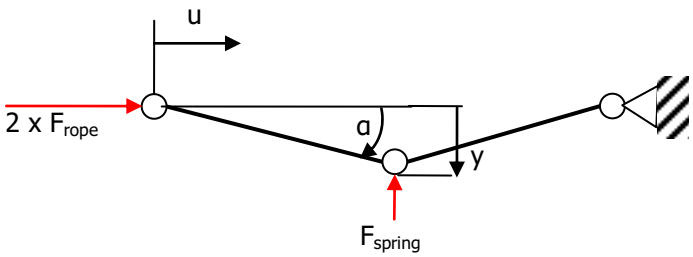

Kinematics:

$$y = L \cdot \sin\alpha$$
$$u = 2L \cdot (1 - \cos\alpha)$$

Potential energy:

$$P = E + B$$
$$E = \frac{1}{2} k \cdot y^2$$
$$B = -2 \cdot F_{rope} \cdot u$$
$$P(\alpha) = \frac{1}{2} k \cdot L^2 \cdot \sin^2\alpha - 4F_{rope} L \cdot (1 - \cos\alpha)$$

Static equilibrium:

$$\frac{\partial P}{\partial \alpha} = 0 = kL^2 \cdot \cos^2\alpha \cdot \sin^2\alpha - 4LF \cdot \sin\alpha$$

This is only valid for α=0.
The critical buckling load can be found using:

$$\frac{\partial^2 P}{\partial \alpha^2} = kL^2 \cdot (\cos^2\alpha - \sin^2\alpha) - 4LF \cdot \cos\alpha$$

Inserting the point of equilibrium returns:

$$F_{cr} = \frac{kL}{4}$$

I.e. if the load limit is set at 200 kN, and dimension L of 1 m, the spring constant k is equal to 50 kN/m.

To check for symmetry of the buckling:

$$\frac{\partial^3 P}{\partial \alpha^3} = -4kL^2 \cdot \cos^2 \alpha \cdot \sin^2 \alpha + 4LF \cdot \sin \alpha$$

Inserting α=0 and F_{cr} into the equation yields:

$$\frac{\partial^3 P}{\partial \alpha^3} = 0$$

So the buckling is symmetrical.

To see if the post-buckling behaviour is stable, the 4th derivative is used:

$$\frac{\partial^4 P}{\partial \alpha^4} = 4kL^2 \cdot (\sin^2 \alpha - \cos^2 \alpha) + 4LF \cdot \cos \alpha$$

Inserting α=0 and F_{cr} into the equation yields:

$$\frac{\partial^4 P}{\partial \alpha^4} = -3kL^2$$

Because the 4th derivative is negative, the post-buckling behaviour is unstable. This implies that once the mechanism buckles, it will not stop moving until the entire stroke is travelled.

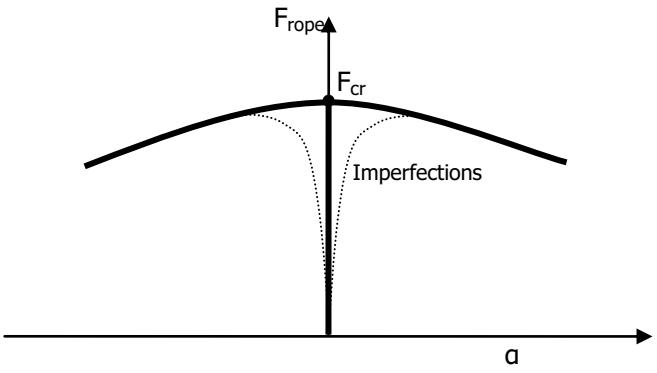

The mechanism is unstable. This means that once the critical load has been exceeded, the mechanism will collapse and suddenly travel its entire stroke. Therefore a buffer should be added to catch the travelling sheave and prevent shock loads.

By inserting an initial angle α into the mechanism, the buckling point can be set accurately, reducing the influence of imperfections.

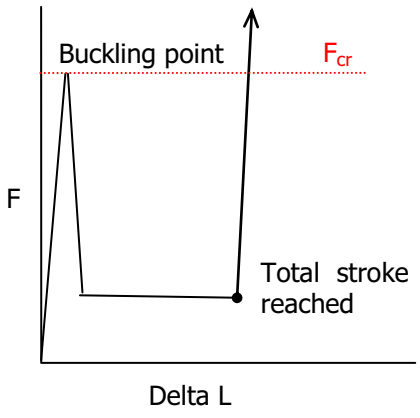

Figure D.4: Estimated behaviour of the buckling mechanism

D.3.2.2 Conclusion

This mechanism could be used to insert a rope buffer into the wire rope reeving. It can quickly become expensive, because four mechanisms are required to protect all four ropes. It is the question whether this pays off, since the mechanism will require maintenance as well.

D.4 Conclusion

In this chapter several concepts to reduce the snag load were discussed, which arose during the period of this project.

The concepts can reduce the snag load, but it is the question if this can compensate the extra costs the mechanisms add to the crane. Besides the extra costs, the new mechanisms will add weight and complexity to the crane, especially since most mechanisms will have to be added to the crane four times, because of the four separate hoisting ropes.

Appendix E Simulink model and code

E.1 Global model

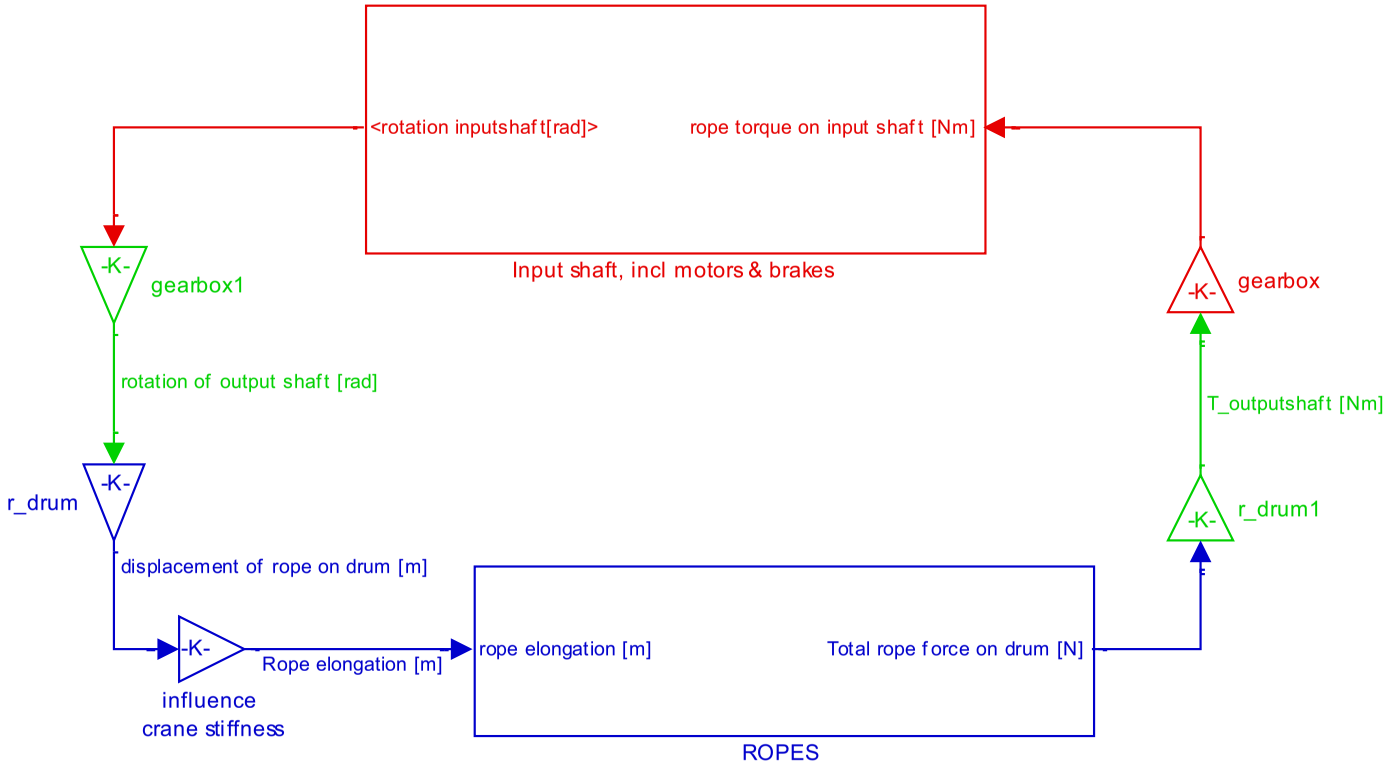

The global model consists of two sub-models, the rotating parts and the wire ropes, which are modelled as linear springs. The rotation of the input shaft determines the displacement of the rope on the drum. Using the relative stiffness of the crane, the wire rope deformation can be determined.

E.2 Input shaft + motors & brakes

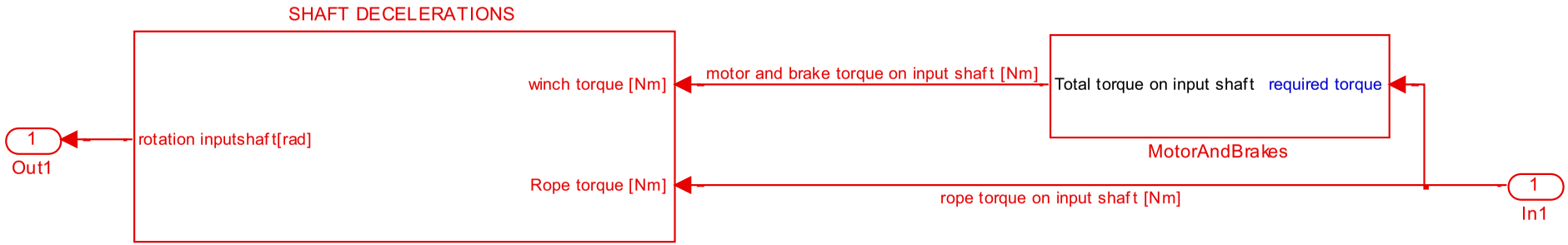

Depending on the wire rope tension, the motors and brakes deliver a different amount of torque. This torque, together with the torque generated by the wire rope determines the deceleration of the input shaft. This is determined in the sub-model of "Shaft decelerations".

E.3 Brakes & motors

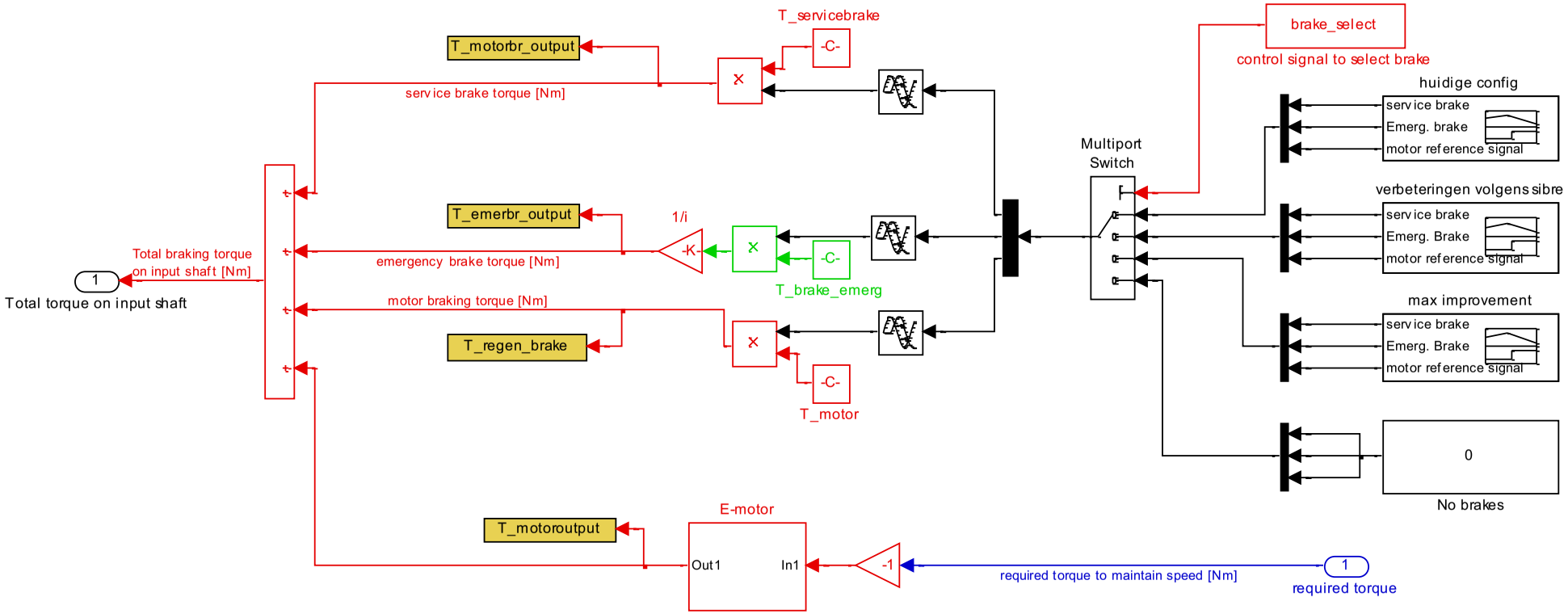

This part of the model operates from right to left, to coincide with the part described in the previous section. At the start of the simulation, the delay time due to monitoring is calculated. The blocks on the right contain the behaviour of the brakes and the electric motor braking.

The bottom part of this model contains the electric motor block.

E.4 AC-motor

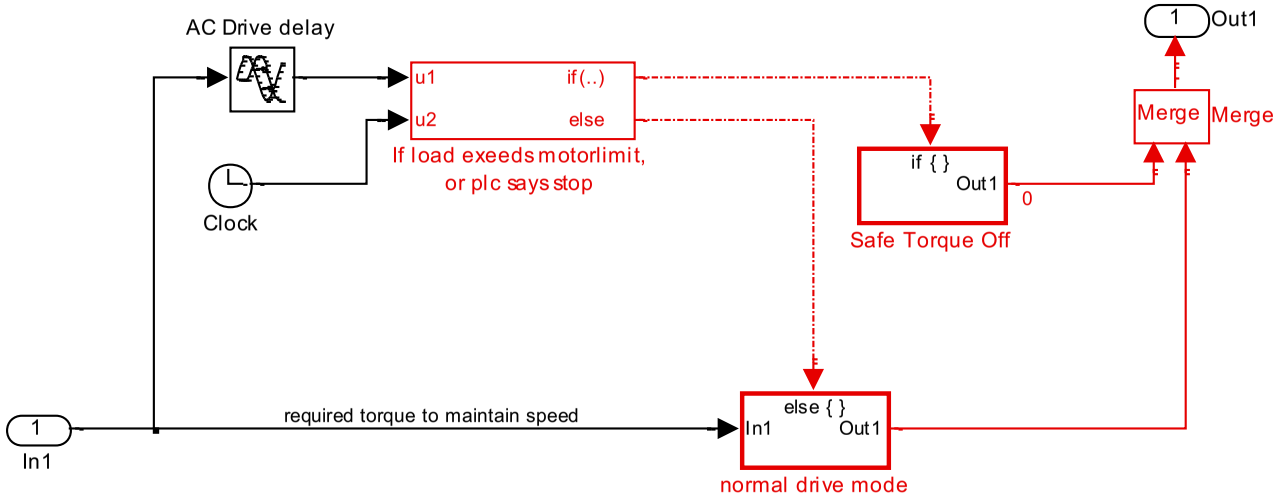

The AC motor will try to maintain the same torque as that is generated by the wire rope torque. That way a constant motor speed is maintained. The slip of the motor is neglected in the model.

When the motor limit is exceeded, the motor switched off, after the AC drive delay has passed. The motor can also be shut down when the delay time from the wire rope monitoring has passed.

E.5 Shaft decelerations

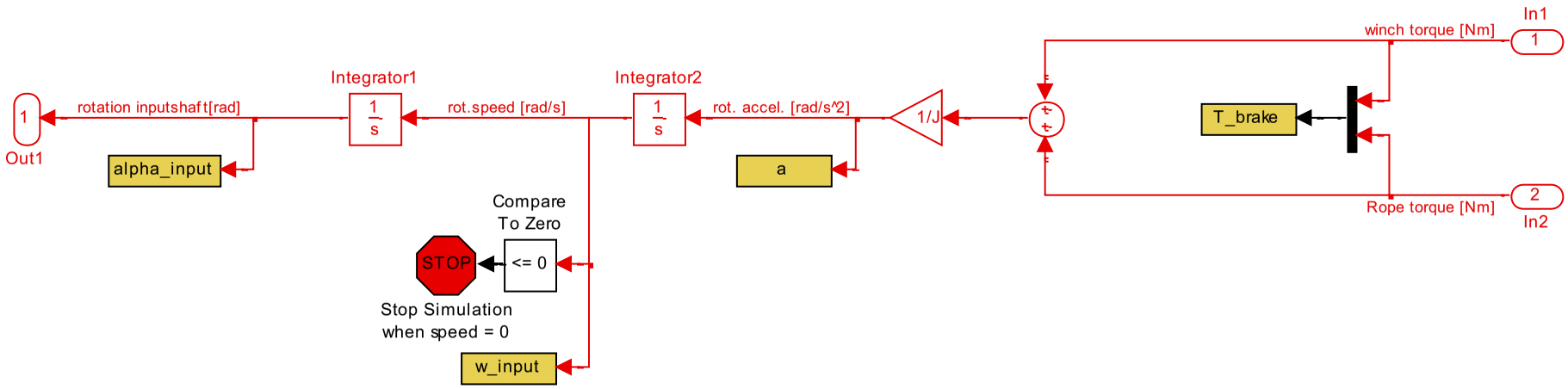

The shaft decelerations are integrated twice to determine the speed and rotation of the shaft. When the speed of the shaft has reached 0, the model is stopped. The initial condition of the shaft speed is entered in integrator1.

The rotation of the input shaft is used to determine wire rope elongation.

E.6 Ropes

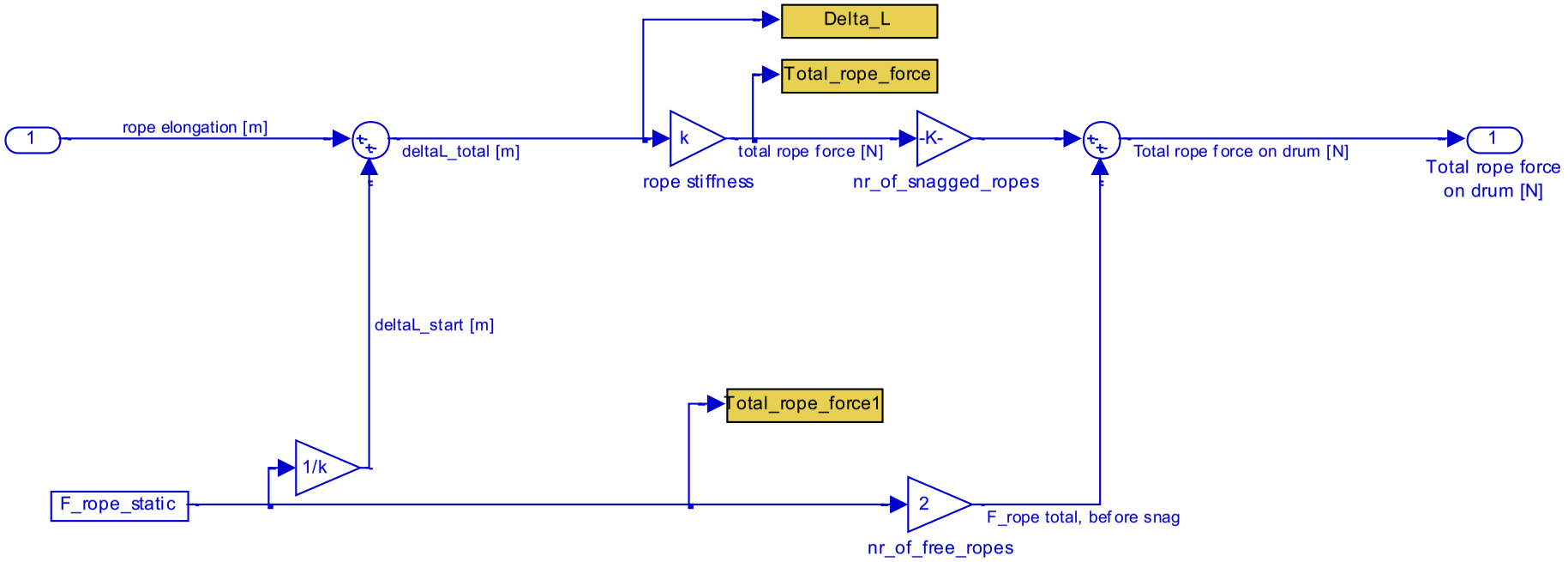

The wire rope elongation determines the wire rope tension of the snagged ropes. Together with the tension of the free ropes the total force on the rope drum is determined.

E.7 Code

The code consists of two parts:

- Main code
- Calc_resp_time.m

E.7.1 Main code

Below the total Matlab code is listed. Green text is commented, and is not executed. By commenting and uncommenting this text, different parts of the code can be executed. Comments are included in the code for clarification.

The first part of the code consists of the loading of a memory file. These files contain the data described in Appendix F.

```
clc;    %clear screen
clear;  %clear memory
%%%%%%%%%%%%%%%%%%%%%%%%%%%%%%%%%%%%%%%%%%%%%%%%%%%%%%%%%%%%%%%%%%%%%%%%%%%%
%        load variables of certain crane, uncomment one file to load       %
%%%%%%%%%%%%%%%%%%%%%%%%%%%%%%%%%%%%%%%%%%%%%%%%%%%%%%%%%%%%%%%%%%%%%%%%%%%%
% variables_HNN1989;
% variables_dubai;

% variables_ecthome;
% variables_rst1;
% variables_noordnatie;
% variables_eurogate;
% variables_havre;
% variables_finnsteve;
% variables_evyap;

% variables_HNN;
% variables_HNN_overload;
% variables_HNN_synchr;
% variables_HNN_4pole;

variables_sprc;
% variables_sprc_4pole;
% variables_sprc_overload;


%%%%%%%%%%%%%%%%%%%%%%%%%%%%%%%%%%%%%%%%%%%%%%%%%%%%%%%%%%%%%%%%%%%%%%%%%%%%
% CALCULATE VARIABLES                                                      %
%%%%%%%%%%%%%%%%%%%%%%%%%%%%%%%%%%%%%%%%%%%%%%%%%%%%%%%%%%%%%%%%%%%%%%%%%%%%
%determine all duty points using linear interpolation
    loads  = ( min(load_speed_curve_interp(:,1)) : 1 : max(load_speed_curve_interp(:,1)));
    speeds = interp1(load_speed_curve_interp(:,1),load_speed_curve_interp(:,2)   ,  loads , []
);

    v_start=interp1(load_speed_curve_interp(:,1),load_speed_curve_interp(:,2)   ,  load , [] );

%type of snag
    nr_of_snag_ropes=4;                   %[-] nr of cables affected by the snag
    nr_of_free_ropes=4-nr_of_snag_ropes;  %[-] nr of cables NOT affected by the snag

%winch properties
    J               = J+(2*950+nr_of_snag_ropes*101)/i_gb^2;
%[kgm^2]  add inertia of hoisting sheaves and the two rope drums %950 for r=0.45, 1340 for r =
0.55, 1811 for r=.65m
    J=J+0.55; % brake improvement
    motor_speed     = v_start*i_gb/(r_drum);
%[rad/s]  motor speed at start of snag
    T_motor_limit   = T_motor*interp1(T_n_curve(:,1),T_n_curve(:,2),motor_speed,[],'extrap');
%[Nm]     total torque the winch is allowed to produce at certain speed
    T_brake_motor   = T_motor_limit;
%[Nm]     maximum braking torque of the motor at current speed
```

```
%stiffness
    k               = E*A/(L);       %[N/m]
    k_crane         = 2.34e4*1000;   %[N/m] total stiffness of crane structure
    k_reduction     = k_crane/(4*nr_of_snag_ropes*k+k_crane); % [-] reduction factor due to
crane deformation

%monitoring system
    t_delay_plc     = 0.08;          %[s]    PLC (siemens 319f)
    plc_in_circuit = 0;              %[-]    als plc bypassed wordt voor rope tension
monitoring, op 0 zetten
    t_delay_pk      = 0.02;          %[s]    Pat-Kruger + tension wave speed
    t_delay_eb      = 0.01;          %[s]    emergency brake delay time
    t_delay_sb      = 0.01;          %[s]    service brake delay time
    brake_select    = 2;             %1=current config, 2 = improvements by sibre, 3= instant
application of brakes 4=no brakes
    t_delay_em      = 0.05;          %[s]    AC drive delay time
    t_delay_wave    = 0.05;          %[s]    tension wave propagation speed
    overloadfactor = 1.53;           %[-]    fraction of the tension at which e-stop is
triggered, set at 999 or higher when no dyn limit is used

%%%%%%%%%%%%%%%%%%%%%%%%%%%%%%%%%%%%%%%%%%%%%%%%%%%%%%%%%%%%%%%%%%%%%%%%%%%%%%%%%%%%%%%%%%%%%%%%
% RUN SIMULATION                                                                                 %
%%%%%%%%%%%%%%%%%%%%%%%%%%%%%%%%%%%%%%%%%%%%%%%%%%%%%%%%%%%%%%%%%%%%%%%%%%%%%%%%%%%%%%%%%%%%%%%%

% calculate the correct time for activating the brakes, depends on whether
% rope tension or motor torque exceeds its limit first

    calc_resp_time; %run calc_resp_time.m, to calculate response times of the system

%single run
    sim('snag_v3',10); %preventing errors when all other runs below are not applied

% ____________________________________________________________________________%
%  % variation of loads and speeds using interpolation                        %
% ____________________________________________________________________________%
%
%
%     figure;
% plot(loads,speeds);
% axis([0 100 0 7]);
% %create data collection matrix
% record=zeros(length(loads),7); %create data collection matrix
%
% for j=1:length(loads)
%     load=loads(j);
%     F_rope_static    = load*10*1000/8; %[N]
%     v_start=speeds(j);
%     motor_speed      = v_start*i_gb/r_drum; %[rad/s]
%     T_motor_limit    =
T_motor*interp1(T_n_curve(:,1),T_n_curve(:,2),motor_speed,[],'extrap'); %[Nm]
%     T_brake_motor    = T_motor_limit;  %braking torque of the motor
%
%     calc_resp_time; %run calc_resp_time.m, to calculate response times of the system
%
%
% %simulate
%     sim('snag_v3',10);
%
% %record results
%     record(j,1) = motor_speed*60/(2*pi);
%     record(j,2) = max(Total_rope_force);
%     record(j,3) = t_overload_motor;
%     record(j,4) = t_overload_rope;
%     record(j,5) = t_delay;
%     record(j,6) = 1+(T_motor_limit-T_motor_load)/T_motor_load;
%     record(j,7) = load;
%
% end
% %output results
%   max(record(:,2))
%     % figure;
%     plot(record(:,1),record(:,2)/1e3,'k-','linewidth',1);
%     xlabel('speed [rpm]');
%     ylabel('maximum rope tension [kN]');
```

```
%     axis([0 2500 0 500]);
%     my_xticklabels([500 1000 1500 2000],{'500',{'1000','nominal speed','80
ton'},'1500',{'2000','maximum speed','23 ton'}});
%
% % % figure;
% %     plot(record(:,7),record(:,2)/1e3,'r-');
% %     line([0 100],[219 219],'Color','r','LineStyle','--','linewidth',1);
% %     line([0 100],[250 250],'Color','k','LineStyle','--','linewidth',1);
% %     xlabel('load [ton]');
% %     ylabel('maximum rope tension [kN]');
% %     axis([0 100 0 5e2]);
% %
%
% % %%%%%%%%%%%%%%    response times of motor and rope overload  %%%%%%%%%%%%%
% % figure;
% % plot(record(:,7),record(:,3),'b-',record(:,7),record(:,4),'r-',record(:,7),record(:,5),'k-
');
% % xlabel('input shaft speed [rpm]');
% % ylabel('response time [s]');
% % legend('time until motor overload','time until rope overload','time until plc response');
% % axis([0 2500 0 1]);
% %
% % figure;
% % plot(record(:,1),record(:,6),'b-');
% % xlabel('input shaft speed [rpm]');
% % ylabel('motor reserve [-]');
% % axis([0 2500 0 3]);

%_____________________________________________________________________%
% variation of loads and speeds
% %_____________________________________________________________________%
% record=zeros(length(load_speed_curve),7); %create data collection matrix
%
% for j=1:length(load_speed_curve)
%
%     load             = load_speed_curve(j,1);
%     F_rope_static    = load*10*1000/8; %[N]
%     v_start          = load_speed_curve(j,2); %[m/s]
%     motor_speed      = v_start*i_gb/r_drum; %[rad/s]
%     T_motor_limit    =
T_motor*interp1(T_n_curve(:,1),T_n_curve(:,2),motor_speed,[],'extrap'); %[Nm]
%     T_brake_motor    = T_motor_limit;  %braking torque of the motor      00000
!!!!!!!!!!!!
%
%  calc_resp_time; %run calc_resp_time.m, to calculate response times of the system
%
% %simulate
%     sim('snag_v3',10);
%
% %record results
%     record(j,1) = motor_speed*60/(2*pi);
%     record(j,2) = max(Total_rope_force);
%     record(j,3) = t_overload_motor;
%     record(j,4) = t_overload_rope;
%     record(j,5) = t_delay;
%     record(j,6) = 1+(T_motor_limit-T_motor_load)/T_motor_load;
%     record(j,7) = load;
%
% end
% %output results
%     max(record(:,2))
% %     %  figure;
% %     plot(record(:,1),record(:,2),'b');
% %     xlabel('speed [rpm]');
% %     ylabel('maximum rope tension [N]');
% %     axis([0 2500 0 5e5]);
% %     my_xticklabels([500 1000 1500 2000],{'500',{'1000','nominal speed','80
ton'},'1500',{'2000','maximum speed','23 ton'}});
%
%    % figure
%        plot(record(:,7),record(:,2),'b-');
%     xlabel('load [ton]');
%     ylabel('maximum rope tension [N]');
%     axis([0 100 0 5e5]);
%
% % % % %%%%%%%%%%%%%%    response times of motor and rope overload  %%%%%%%%%%%%%
```

```
% %     figure;
% %     plot(record(:,1),record(:,3),'b-',record(:,1),record(:,4),'r-
',record(:,1),record(:,5),'k-');
% %     xlabel('input shaft speed [rpm]');
% %     ylabel('response time [s]');
% %     legend('time until motor overload','time until rope overload','time until plc
response');
% %     axis([0 2500 0 1]);
%
% % %%%%%%%%%%%%%%%% motor reserve %%%%%%%%%%%%%%%
%     % figure;
%     % plot(record(:,1),record(:,6),'bx-');
%     % xlabel('input shaft speed [rpm]');
%     % ylabel('motor reserve [-]');
%     % axis([0 2500 0 3]);
% %_____________________________________________________________________________%
% % J vs max rope force
%_____________________________________________________________________________%
% record=zeros(20,2);
% R_step=0.05*J:0.05*J:2*J;
% for R=1:length(R_step)
%         J=R_step(R);
%         sim('snag_v3',10);
%         record(R,1)=J;
%         record(R,2)=max(Total_rope_force);
% end
% % figure;
% plot(record(:,1),record(:,2)/1e3,'b','linewidth',1);
% xlabel('J [kgm^2]');
% ylabel('maximum rope force [N]');
% axis([0 J 0 7e2]);
% %
%_____________________________________________________________________________%
% % % electrical delay time vs max rope force
%_____________________________________________________________________________%
% % record=zeros(21,2);
% R_step=0 : 0.01 : 0.2;
%
% for R=1:length(R_step)
%
% %vary plc response time
%     t_delay_plc=R_step(R);
%
% % calculate the correct time for activating the brakes, depends on whether
% % rope tension or motor torque exceeds its limit first
%
% %  calc_resp_time; %run calc_resp_time.m, to calculate response times of the system
%
% %simulate and record results
%     sim('snag_v3',10);
%     record(R,1)=t_delay_plc;
%     record(R,2)=max(Total_rope_force);
% end
% % figure;
% plot(record(:,1),record(:,2)/1e3,'linewidth',1);
% xlabel('time delay [s]');
% ylabel('maximum rope force [kN]');
% axis([0 t_delay_plc 0 7e2]);

%_____________________________________________________________________________%
% % component delay time vs max rope force
%_____________________________________________________________________________%
% record=zeros(21,2); %create data collection matrix
% t_delay_step=0 : 0.01 : 0.5; %create input set for delay time
% for R=1:length(t_delay_step)
%         t_delay_em=t_delay_step(R); %set time delay
% %         t_delay_sb=t_delay_eb;
%         sim('snag_v3',10);          %run simulation
%         record(R,1)=t_delay_em;     %collect results
%         record(R,2)=max(Total_rope_force);
% end
% %plot result
% % figure;
% plot(record(:,1),record(:,2));
% xlabel('time delay [s]');
% ylabel('maximum rope force [N]');
% axis([0 t_delay_em 0 7e5]);
```

```
%_____________________________________________________________________%
% %Torque emergency brakes vs max rope force
%_____________________________________________________________________%
% record=zeros(20,2); %create data collection matrix
% R_step=T_brake_service/10;
% for R=1:20
%         T_brake_service=R_step*R;
%         sim('snag_v3',10);
%         record(R,1)=T_brake_service;
%         record(R,2)=max(Total_rope_force);
% end
% figure;
% plot(record(:,1),record(:,2));
% xlabel('emergency brake torque [Nm]');
% ylabel('maximum rope force [N]');
% axis([0 T_brake_service 0 7e5]);

%_____________________________________________________________________%
% % wire rope stiffness
%_____________________________________________________________________%
% record=zeros(20,2); %create data collection matrix
% R_step=0.1*k:0.1*k:2*k;
% for R=1:length(R_step)
%         k=R_step(R);
%         sim('snag_v3',10);
%         record(R,1)=k/1e3;
%         record(R,2)=max(Total_rope_force)/1e3;
% end
% figure;
% plot(record(:,1),record(:,2),'b');
% xlabel('rope stiffness [kN/m]');
% ylabel('maximum rope force [kN]');
% axis([0 max(R_step)/1e3 0 7e2]);
% %
% %_____________________________________________________________________%
% %hoisting speed
%_____________________________________________________________________%
% record=zeros(15,2); %create data collection matrix
% R_step=0.1*v_start : 0.1*v_start : 1.5*v_start;
% for R=1:length(R_step)
%         v_start=R_step(R);
%         sim('snag_v3',10);
%         record(R,1)=v_start*60/2;
%         record(R,2)=max(Total_rope_force);
% end
% figure;
% plot(record(:,1),record(:,2));
% xlabel('hoisting speed [m/min]');
% ylabel('maximum rope force [N]');
% axis([0 max(R_step*60/2) 0 5e5]);

%_____________________________________________________________________%
% % J vs reaction time vs max rope force
%_____________________________________________________________________%
% result=zeros(0,0); %create data collection matrix
% time_step=0 : 0.05 : 1;
% R_step=0.1*J:0.1*J:2*J;
% record=zeros(length(R_step),length(time_step));
% for R=1:length(R_step)
%     for S=1:length(time_step)
%         t_delay=time_step(S);
%         J=R_step(R);
%         sim('snag_v3',10);
% %         record(R,S)=max(Total_rope_force);
%         record(20*R+S,1)=J;
%         record(20*R+S,2)=t_delay;
%         record(20*R+S,3)=max(Total_rope_force);
%         result(S,R)=max(Total_rope_force);
%         record(20*R+S,5)=S;
%     end
% % end
%
```

```
% %%%%%%%%%%%%%%%%%%%%%%%%%%%%%%%%%%%%%%%%%%%%%%%%%%%%%%%%%%%%%%%%%%%%%%%%%%%%%%%
% % PLOT RESULTS                                                                   %
% %%%%%%%%%%%%%%%%%%%%%%%%%%%%%%%%%%%%%%%%%%%%%%%%%%%%%%%%%%%%%%%%%%%%%%%%%%%%%%%
%   determine time at which plc receives signal
t_delay=min(t_overload_rope,t_overload_motor);
t_delay_index=find(tout>t_delay, 1 );

figure;

   % rpm
   graph(1)=subplot(4,1,1);
   plot(tout,w_input*60/(2*pi),'linewidth',1);
   hold;
%    plot(t_delay,(w_input(t_delay_index)*60/(2*pi)),'rx');
   legend('rot. speed input shaft','location','Northeast');
   set(gca,'XTick',[0.2 0.4 0.6 0.8]);
   hold;
   grid;
   axis([0 0.8 0 1.1*n_max]);%max(tout)+0.1
   xlabel('time[s]');
   ylabel('speed [rpm]');

   % Total deformation
   graph(2)=subplot(4,1,2);
   plot(tout,Delta_L,'linewidth',1);
   hold;
%    plot(t_delay,Delta_L(t_delay_index),'rx');
   legend('Total rope elongation','location','Southeast');
   set(gca,'XTick',[0.2 0.4 0.6 0.8]);
   hold;
   grid;
   axis([0 0.8 0 4]);
   xlabel('time[s]');
   ylabel('elongation [m]');

   % Total Rope Force
   graph(3)=subplot(4,1,3);
   plot(tout,Total_rope_force/1e3,'linewidth',1);%,tout,Total_rope_force1);
   hold;
%    plot(t_delay,Total_rope_force(t_delay_index),'rx');
   legend('snagged rope tension','location','Northwest');%'free rope tension',
   set(gca,'XTick',[0.2 0.4 0.6 0.8]);
   hold;
   grid;
   axis([0 0.8 0 500]);
   xlabel('time[s]');
   ylabel('Tension [kN]');

   % braking torque
   graph(4)=subplot(4,1,4);
   plot(tout,T_brake/1e3,'linewidth',1);
   hold;
%    plot(t_delay,T_brake(t_delay_index),'rx');
   legend('Motor + Brakes','Wire rope','location','Northeast');
   set(gca,'XTick',[0.2 0.4 0.6 0.8]);
   hold;
   grid;
   axis([0 0.8 -80 80]);
   xlabel('time[s]');
   ylabel('Torque [kNm]');

   linkaxes(graph,'x');
% %%%%%%%%%%%%%%%3d plot of motor torque%%%%%%%%%%%%%%%%%%%%%%%%%
%
% figure;
% %3d plot time,speed,torque
% subplot(2,2,2),plot3(tout,w_input*30/pi,T_motoroutput);
% grid on;
% xlabel('time[s]');
% ylabel('n');
% zlabel('T');
% axis square;
% view(30,20);
%
% subplot(2,2,3),plot(tout,T_motoroutput);
% grid on;
```

```
% xlabel('time[s]');
% ylabel('T');
%
% subplot(2,2,1),plot(tout,w_input*30/pi);
% grid on;
% xlabel('time[s]');
% ylabel('n');
%
% subplot(2,2,4),plot(w_input*30/pi,T_motoroutput);
% grid on;
% xlabel('n');
% ylabel('T');
%
% %ac1_example (Ac motor library simulink)
% %
% %motor torque detailed
% % figure;
% % plot(w_input*60/(2*pi()),T_motoroutput,'r-','LineWidth',2);
% % hold;
% % plot(T_n_curve(:,1)*60/(2*pi()),-T_motor*T_n_curve(:,2));
% % plot(T_n_curve(:,1)*60/(2*pi()),T_motor*T_n_curve(:,2));
% % xlabel('speed [rad/s]')
% % ylabel('Torque [Nm]')
% %
% % % % %%%%%%%%%%%% plot torques on input and output shaft %%%%%%%%%%%%%%%%%%%%%
figure;

coupling_limit=22;%kNm
drum_limit = 660; %kNm
gb_limit=760; %kNm

% input shaft, between motor and disc brake
subplot(3,1,1),plot(tout,( T_emerbr_output/n_motors +T_motorbr_output/n_motors
+T_brake(:,2)/n_motors ) / 1e3,'linewidth',1);
line([0 max(tout)],[-coupling_limit -coupling_limit],'Color','r','LineStyle','--');
legend('input shaft','location','Southwest');
grid;
% axis([0 1 0 n_max]);
xlabel('Time[s]');
ylabel('Torque [kNm]');

subplot(3,1,2),plot(tout,(T_emerbr_output*i_gb/2-Total_rope_force*r_drum*2) /
1e3,'linewidth',1); %2 = 2 ropes per drum, 2 rope drums
line([0 max(tout)],[-drum_limit -drum_limit],'Color','r','LineStyle','--');
legend('drum coupling','location','Southwest');
grid;
% axis([0 1 0 n_max]);
xlabel('Time[s]');
ylabel('Torque [kNm]');

subplot(3,1,3),plot(tout,(T_brake(:,2)*i_gb+T_emerbr_output*i_gb) / 1e3,'linewidth',1);
line([0 max(tout)],[-gb_limit -gb_limit],'Color','r','LineStyle','--');
legend('output shaft of gearbox','location','Southwest');
grid;
% axis([0 1 0 n_max]);
xlabel('Time[s]');
ylabel('Torque [kNm]');
```

E.7.2 calc_resp_time.m

This m-file calculates the response time to a snag.

```
%calculate response times

% rope tension monitoring
    rope_limit         = min([ (1.1*(max(load_speed_curve(:,1)))*9.81e3 -
2*nr_of_free_ropes*F_rope_static) / (2*nr_of_snag_ropes)  ...
                               overloadfactor * F_rope_static      ...
                               265000                              ]); %[N]

   t_overload_rope     = (rope_limit-F_rope_static)/(v_start*k)+t_delay_pk
+t_delay_wave;% [s] %time until plc knows rope limit is exceeded
```

```
% motor torque overload
    Tpsec               = nr_of_snag_ropes * v_start*k * r_drum/i_gb; % [Nm/s]
torque increase per second
    T_motor_load        = load * 10*1000/2 * r_drum/i_gb;             % [Nm]
    t_overload_motor    = (T_motor_limit-T_motor_load) / Tpsec+t_delay_em
+t_delay_wave; % [s] +t_delay_plc*plc_in_circuit;
%resulting time delay
    t_delay             = min(t_overload_rope+t_delay_plc*plc_in_circuit+t_delay_em
, t_overload_motor+t_delay_plc); %[s]
```

E.8 Model used for container movement

This model was used in chapter 4, to analyze the container movement.

E.8.1 Model

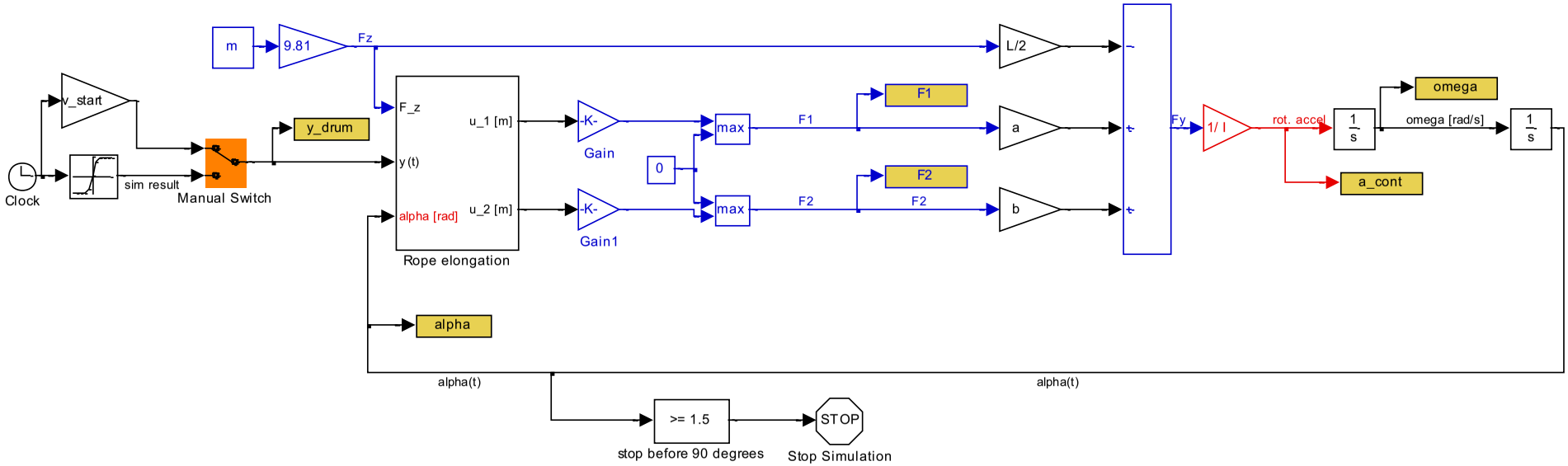

Rope elongation calculation submodel:

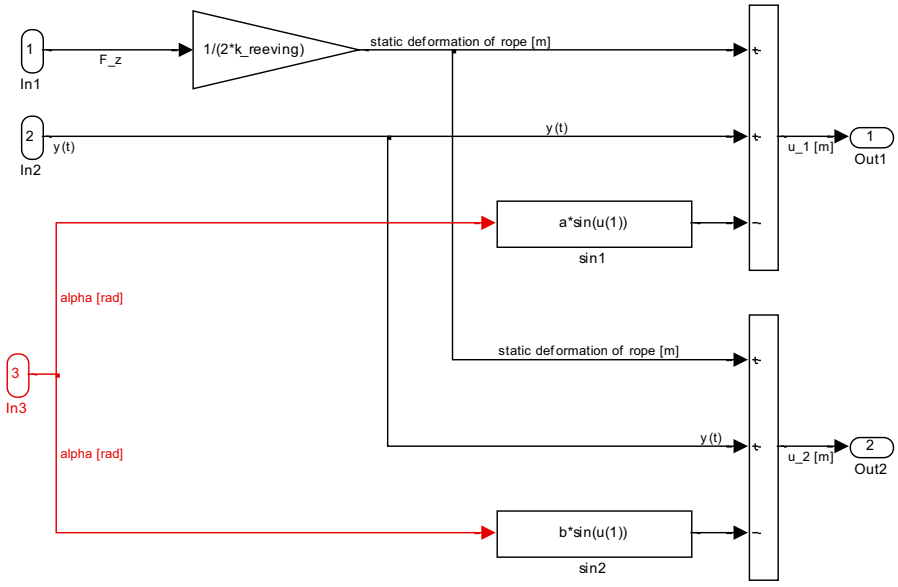

E.8.2 Code

```
%Note:
% Because simulink calculates in a certain variabel timestep, two
% consecutive derivative blocks did not work correctly, it created a lot of
% noise. Therefore the manaul derivative block was constructed
% the deriv_constant is used to power the manual derivative block.

%Switch in model switches between  rope displacement result from simulation
% and a constant rope displacement

    clc;
    clear;
%%%%%%%%%%%%%%%%%%%%%%% load variables %%%%%%%%%%%%%%%%%%%%%%%%%%%%%%%%%%
%     variables_HNN;
    variables_sprc;
    % variables_evyap;

    a               =   0.1;        %[m] %20' =0.4, 40' =3.55, or 0.1
    b               =   5.1+a;       %[m]
    L               =   a+b;         %[m]
    k               =    145e3;      %[N/m] rope stiffness
    k_reeving       =   1160e3;      %[N/m] reeving stiffness
    v_start         =   3;           %[m/s] 2.3 voor 20 foot
    m               =   17e3;        %[kg] 47.5e3 voor 20 foot
    c               =   (b-a)/2;     %[m]
    deriv_constant  =   0.01;        %[s]
    I               =   m*L^2/3;
    overloadfactor  =   200;
    loadlimit       =   min(1.1*9.81*1e3*max(load_speed_curve_interp(:,1)),
overloadfactor*10*m);
    y=open('Y_t.mat'); %y(t) = hoisting speed as a function of time

    nr_of_snag_ropes=2;                 %[-] nr of cables affected by the snag load
    nr_of_free_ropes=4-nr_of_snag_ropes; %[-] nr of cables not affected by snag

    w_start=(v_start)/((L/2)+L/1.5);

%%%%%%%%%%%%%%%%%%%%%%%%%% start simulation %%%%%%%%%%%%%%%%%%%%%%%%%%%%%%

    sim('cont_rotation14' ,12);

% calculate linear approximation of the load development through time
    lin_approx=(m*9.81 + tout*v_start*2*k*2*nr_of_snag_ropes)/1e3;

% %time at which rope tension is 0:
    zero_indexnr=find(F2<0.01,1,'first');
    tout(zero_indexnr)
```

```
%time at which load limit is reached
    limit_indexnr=find((F1+F2)>loadlimit,1,'first');
    tout(limit_indexnr)

%%%%%%%%%%%%%%%%%%%%%%%%%%%% plot results %%%%%%%%%%%%%%%%%%%%%%%%%%%%%%%%

% figure;
% graph(1)=subplot(3,1,1); %displacement of rope on drum
% plot(tout,y_drum);
% xlabel('time [s]');
% ylabel('displacement of rope on drum [m]');
% axis([0 1 0 4]);
%
% graph(2)=subplot(3,1,2); %rotation of container
% plot(tout,alpha*360/(2*pi));
% xlabel('time [s]');
% ylabel('containe rotation [degrees]');
% axis([0 1 0 100]);
%
% graph(3)=subplot(3,1,3); %rope tensions
%      plot(tout,F1/1e3, ...
%      tout,F2/1e3,      ...
%      tout,(F1+F2)/1e3, ...
%      tout,(m*9.81 + tout*v_start*2*k*2*nr_of_snag_ropes)/1e3,'k');%approximation of rope
tension
% xlabel('time [s]');
% ylabel('reeving force [kN]');
% legend('F_1 (Portside)','F_2 (Starboard)','F_{total}','linear
approximation','location','Southeast');%'-F_{ship}',
% axis([0 1 0 4e3]);
%
% linkaxes(graph,'x');

%seperate plot of rotation angle
    figure;
    plot(tout,alpha*360/(2*pi));
    xlabel('time [s]');
    ylabel('containe rotation [degrees]');
    axis([0 1 0 100]);

% seperate plot of rope tension
    figure;
    plot(tout,F1/1e3, ...
         tout,F2/1e3,      ...
         tout,(F1+F2)/1e3, ...
         tout,lin_approx,'k')%,...

    xlabel('time [s]');
    ylabel('reeving force [kN]');
    legend('F_1 (Portside)','F_2 (Starboard)','F_{total}','linear
approximation','location','Southeast');%'-F_{ship}',
    axis([0 1 0 4e3]);
%_____________________________________________________________________%
%            variation of loads and speeds using interpolation        %
%_____________________________________________________________________%
%
datapoints=50;
record=zeros(datapoints,5); %create data collection matrix

for j=1:datapoints+1
    F1      = 0; %empty result vector to prevent bugs
    F2      = 0; %empty result vector to prevent bugs
    load    = max(load_speed_curve_interp(:,1)) - (j-1)* (max(load_speed_curve_interp(:,1))-
min(load_speed_curve_interp(:,1))) /datapoints;
    v_rope  =
interp1(load_speed_curve_interp(:,1),load_speed_curve_interp(:,2),load,[],'extrap'); %[m/s]
    m       = 1e3*load; %[kg]

    F_rope_static = m*9.81/8;
    loadlimit     = min(1.1*9.81e3*max(load_speed_curve_interp(:,1)),
8*overloadfactor*F_rope_static);

    loadlimit_static = 1.1*9.81*1e3*max(load_speed_curve_interp(:,1));
    loadlimit_dyn    = overloadfactor*10*m/2; %variable load limit

    v_start=v_rope/2;
```

```
    w_start=(v_start)/((L/2)+L/1.5);

%simulate
    sim('cont_rotation14',8);

%_____________________________________________________________________%
% %        Find response time from the results of the simulation      %
%_____________________________________________________________________%
%
%%%%% time until free ropes slack      %%%%%%%%
    zero_indexnr=find(F2<0.01,1,'first');
    if isempty(zero_indexnr)
        zero_time=NaN; %als tension niet 0 wordt
    else
        zero_time=tout(zero_indexnr); %time until rope tension is 0
    end

%%%%% time until static limit is reached %%%%
    limit_static_indexnr=find((F1+F2)>loadlimit_static,1,'first');
    if isempty(limit_static_indexnr)
        limit_time_static=NaN;
    else
        limit_time_static=tout(limit_static_indexnr); %time until load limit is reached
    end

%%%%% time until dynamic limit is reached %%%%
    limit_dyn_indexnr=find((F1)>loadlimit_dyn,1,'first');
    if isempty(limit_dyn_indexnr)
        limit_time_dyn=NaN;
    else
        limit_time_dyn=tout(limit_dyn_indexnr); %time until load limit is reached
    end
%******** resulting response time of rope **********%
    limit_time=min(limit_time_static,limit_time_dyn);

%%%%%%  response time of the motor     %%%%%%
    motor_speed=v_start*2*i_gb/r_drum;
    T_motor_limit  = T_motor*interp1(T_n_curve(:,1),T_n_curve(:,2),motor_speed,[],'extrap');
%[Nm]total torque the winch is allowed to produce at certain speed

    limit_motor_indexnr=find(( (F1+F2)/2*r_drum/i_gb)>T_motor_limit,1,'first');
    if isempty(limit_motor_indexnr)
        motor_time=NaN;
    else
        motor_time=tout(limit_motor_indexnr); %time until load limit is reached
    end


%_____________________________________________________________________%
% %                  Estimation of response times                     %
%_____________________________________________________________________%
%
    rope_limit_total       =(1.1*(max(load_speed_curve(:,1)))*9.81e3 -
2*nr_of_free_ropes*F_rope_static) / (2*nr_of_snag_ropes); %[N]

    t_overload_rope_total  = (rope_limit_total-F_rope_static)/(v_rope*k);% [s]

    rope_limit_single      =  min(overloadfactor*F_rope_static , 265000); %[N]
    t_overload_rope_single = (rope_limit_single-F_rope_static)/(v_rope*k);% [s]

    t_overload_rope        = min(t_overload_rope_total,t_overload_rope_single);


    Tpsec              = nr_of_snag_ropes * v_rope*k * r_drum/i_gb;
    t_overload_motor   = (T_motor_limit-m/2*9.81*r_drum/i_gb) / Tpsec;
%_____________________________________________________________________%
% %                            Record results                         %
%_____________________________________________________________________%
    record(j,1) = m/1e3;
    record(j,2) = v_start;
    record(j,3) = zero_time;
    record(j,4) = limit_time;
    record(j,5) = t_overload_rope;
    record(j,6) = motor_time;
    record(j,7) = t_overload_motor;
end
%_____________________________________________________________________%
% %                            Plot results                           %
```

```
%_____________________________________________________________________%
figure;
plot(record(:,1),record(:,4),'r-
',record(:,1),record(:,5),'k',record(:,1),record(:,6),'r:',record(:,1),record(:,7),'k:'); %40'
result
% plot(record(27:51,1),record(27:51,4),'r-
',record(27:51,1),record(27:51,5),'k',record(27:51,1),record(27:51,6),'r:',record(27:51,1),rec
ord(27:51,7),'k:');%20' result
xlabel('load on ropes [tons]');
ylabel('time [s]');
axis([0 80 0 1]);
legend('time until tension limit is reached','approximation of rope response time','time until
motor limit is reached','approximation of motor resp time')

% % max error
max(abs((record(:,4)-record(:,5))./record(:,4)))
```

Appendix F Data of existing cranes

		unit	HNN	Dubai	ECT Home	Noordnatie	RST	Le Havre
	Kalmar order nr.	-	52370	52395	52508	52445	52535	52610
General information	year	-	1989	1995	1997	1998	1998	2000
	Duty points	-	63 ton, 60 m/min 48 ton, 90 m/min 19 ton, 118 m/min	65 ton, 46 m/min 53 ton, 60 m/min 19 ton, 120 m/min	77 ton, 30 m/min 55 ton, 48 m/min 45 ton, 72 m/min 20 ton, 120 m/min	80 ton, 40 m/min 66 ton, 60 m/min 25 ton, 140 m/min	52.5 ton, 40 m/min 19 ton, 100 m/min	98 ton, 40 m/min 78 ton, 60 m/min 50 ton, 90 m/min 18 ton, 120 m/min
	i	-	24.2	24.5	27.4	24.63	92.114	20.26
	Drum diameter	m	1.2	1	0.84	1.2	1.465	0.86
	Total Inertia of winch	kgm^2	54	27.2	18.1	48.4	21.06	42.9
Motor information	# of motors	-	2	2	2	2	1	2
	type	-	GE-motor, CD4463	Siemens 1GH312-J83 6735	Siemens 1LL8 317-4, size 315	Siemens 1GG5-352	-	Alstom
	Power	kW	2 x 420	2 x 290	2 x 300	2 x 360	400	430
	AC / DC	-	DC	DC	DC	DC	AC	AC
	nominal speed	rpm	1150	900	1500	784	1000	1000
	maximum speed	rpm	-	1800	2400	1830	-	2000
	f_a (overload factor)	-	1.6	1.6	1.6	1.6	1.6	1.6
	Inertia of 1 motor	kgm^2	20	6.8	3.6	Unknown	10.8	16
Operational brakes	# of brakes	-	2	2	2	2	2	2
	Type	-	Unknown	Bubenzer 14.21 201/6	Bubenzer SB28 630x30	Unknown	Bubenzer SB28 630x30	Bubenzer SB28 630x30
	Torque	Nm	2 x 10 000	2 x 10 000	2 x 9700	2 x 12300	2 x 9700	2 x 12500
Emergency brakes	# of brakes	-	0	0	0	0	0	4
	Type	-	-	-	-	-	-	Bubenzer SF15
	T	Nm	-	-	-	-	-	4 x 84360
Wire rope	Type	-	Unknown	Unknown	8 x 25 WS + IWRC	6 x 36 WS + IWRC	Casar Turboplast	Casar Turboplast
	diameter	mm	28	28	28	30	26	28
	Length[1]	m	214	171.25	203	240	20	210
	Area	mm^2	311	361	311	414	352.4	405
	Young's module	N/mm^2	1.05e5	1.05e5	1.05e5	1.05e5	1.05e5	1.05e5
	Minimum breaking load	kN	500	494	500	600	538.1	683
	Strength class	N/mm^2	1770	1770	1770	1770	1960	1960
	Wire rope stiffness	kN/m	153	221	161	181	1850	203
	Anti-snag system	-	no	no	no	no	no	no
	Remarks						Machinery on trolley, Johnnie Walker rope reeving	

[1] = Length is calculated with snag located 20 meters below the trolley. Shorter distance is not possible since there are no objects that close to the crane

		unit	Eurogate	HNN MSC	Finnsteve	Evyap	SPRC
	Kalmar order nr.	-	52669	52673	52717	52731	52735
General information	year	-	2003	2007	2008	2010	2011
	Duty points	-	55 ton, 80 m/min 27.5 ton, 160 m/min	80 ton, 90 m/min 61 ton, 108 m/min 42 ton, 135 m/min 23 to 15 ton, 180 m/min	101.8 ton, 50 m/min 87.4 ton, 75 m/min 27 ton, 150 m/min	82 ton, 60 m/min 17 ton, 120 m/min	82 ton, 90 m/min 17 ton, 180 m/min
	i	-	26.698	15.3	18.84	23.57	19.2
	Drum diameter	m	1.34	0.9	0.9	0.9	1.1
	Total Inertia of winch	kgm^2	31.4	59.2	32.012	25	43.5
Motor information	# of motors	-	2	2	2	2	2
	type	-	Wölffer DRKF355L-6bT	Wölffer ODRKF 400L-6T	Wölffer ODRKF 315X-6	Wölffer ODRKF 315L-6bT	Wölffer ODRKF 355X-6T
	Nominal power	kW	2 x 400	2 x 700	2 x 500	2 x 375	2 x 730
	AC / DC	-	AC	AC	AC	AC	AC
	nominal speed	rpm	1000	1000	1000	1000	1000
	maximum speed	rpm	2000	2000	2000	2000	2000
	f_a (overload factor)	-	1.8	1.6	2.6	2.2	2.2
	Inertia of 1 motor	kgm^2	10.25	20.4	7.9	6.96	13.6
Operational brakes	# of brakes	-	2	2	2	2	2
	Type	-	Bubenzer SB28 630x30	Sibre TEXU 710 301/6	Sibre TEXU 710 301/6	Sibre USB 3-III-630x30-201/6	Bubenzer SB28 710x30-301/10 BB
	Torque	Nm	2 x 9700	2 x 10700	2 x 10400	2 x 8000	2 x 10700
Emergency brakes	# of brakes	-	4	2	2	0	2
	Type	-	Bubenzer SF15	Sibre SHI 252	Sibre SHI 252	-	Bubenzer SF15, fast setting
	T	Nm	4 x 110 000	2 x 160 000	2 x 150 000	-	2 x 162 000
Wire rope	Type	-	Casar Stratoplast	6 x 36WS + IWRC	8 x 25 Filler + IWRC	8 x 25 Filler + IWRC	8 x 25 Filler + IWRC
	diameter	mm	28	30	30	28	28
	Length	m	40	307	280	171	185
	Area	mm^2	405	414	414	311	311
	Young's module	N/mm^2	1.05e5	1.05e5	1.05e5	1.05e5	1.05e5
	Minimum breaking load	kN	616.3	640	626	547	547
	Strength class	N/mm^2	1770	1960	1960	1960	1960
	Wire rope stiffness	kN/m	1060	142	155	190	177
	Anti-snag system	-	Yes, Hydraulic	Yes, Hydraulic	Yes, Hydraulic	no	Yes, Bubenzer-Malmedie mechanical SOS
	Remarks		Machinery On Trolley				Under construction Electric motors dimensioned for S1-100%